Fuel xxx (xxxx) xxx

Contents lists available at ScienceDirect

Fuel

journal homepage: www.elsevier.com/locate/fuel

Full Length Article

Exploring the potential of ammonia as a fuel: Advances in combustion understanding and large-scale furnace applications☆

Sven Eckart [a,b,*], Ernesto Salzano [b,c], Andreas Richter [d], Mohammad Alnajideen [e], Agustin Valera-Medina [e], Krishna Prasad Shrestha [f], Ahmed Yasiry [g,h], Jinhua Wang [h], Florian Bauer [i], Chunkan Yu [j], Hartmut Krause [a], Gianmaria Pio [c]

[a] Professorship for Gas and Heat Technology, Institute of Thermal Engineering, TU Bergakademie Freiberg, Germany
[b] VSB – Technical University of Ostrava, Faculty of Safety Engineering, Centre of Excellence for Safety Research, Czech Republic
[c] Department of Civil, Chemical, Environmental and Materials Engineering, Alma Mater Studiorum - University of Bologna, Italy
[d] Professorship for Modeling of Thermochemical Conversion Processes, TU Bergakademie Freiberg, Germany
[e] Centre of Excellence on Ammonia Technologies, Cardiff University, Cardiff, United Kingdom
[f] Department of Mechanical Engineering, College of Engineering, University of Louisiana at Lafayette, LA, USA
[g] Automotive Engineering Department, College of Engineering-Musaib, University of Babylon, Iraq
[h] State Key Laboratory of Multiphase Flow in Power Engineering, Xi'an Jiaotong University, Xi'an, China
[i] Institute of Engineering Thermodynamics, Friedrich-Alexander-University, Erlangen, Germany
[j] Institute of Technical Thermodynamics, Karlsruhe Institute of Technology, Karlsruhe, Germany

A B S T R A C T

From an environmental standpoint, carbon-free energy carriers such as ammonia and hydrogen are essential for future energy systems. However, their high-temperature chemical behavior remains insufficiently understood, posing challenges for the development and optimization of advanced combustion technologies. Ammonia, in particular, is globally available and cost-effective, especially for energy-intensive industries. The addition of ammonia or hydrogen to methane significantly reduces the accuracy of existing predictive models. Therefore, validated and detailed data are urgently needed to enable reliable design and performance predictions. This review highlights the compatibility of ammonia with existing combustion infrastructure, facilitating a smoother transition to more sustainable heating methods without the need for entirely new systems. Applications in high-temperature heating processes, such as metal processing, ceramics and glass production, and power generation, are of particular interest.

This review focuses on the systematic assessment of alternative fuel mixtures comprising ammonia and hydrogen, as well as natural gas, with particular consideration of existing safety-related parameters and combustion characteristics. Fundamental quantities such as the laminar burning velocity are discussed in the context of their relevance for fuel mixtures and their scalability toward turbulent flame propagation, which is of critical importance for industrial burner and reactor design. The influence of fuel composition on ignition limits is examined, as these are essential parameters for safety margin definitions and operational boundary conditions. Furthermore, flame stability in mixed-fuel systems is addressed to evaluate the practical feasibility and robustness of combustion under varying process conditions. A detailed overview of current diagnostic and analysis methods follows, encompassing both pollutant measurement techniques and the detection of key radical species. These diagnostics form the experimental basis for reaction kinetics modeling and mechanism validation. Given the importance of emission formation in combustion systems, a dedicated subsection summarizes major emission trends, even though a comprehensive treatment would exceed the scope of this review. Thermal radiation effects, which are highly relevant for heat transfer and system efficiency in large-scale applications, are then reviewed. In parallel, current developments in numerical simulation approaches for industrial-scale combustion systems are presented, including aspects of model accuracy, boundary conditions, and computational efficiency. The review also incorporates insights from materials engineering, particularly regarding high-temperature material performance, corrosion resistance, and compatibility with combustion products. Based on these interdisciplinary findings, operational strategies for high-temperature furnaces are outlined, and selected industrial reference systems are briefly presented. This integrated approach aims to support the design, optimization, and safe operation of next-generation combustion technologies utilizing carbon-free or low-carbon fuels.

☆ This article is part of a special issue entitled: 'INFUB14' published in Fuel.

* Corresponding author.
E-mail address: sven.eckart@iwtt.tu-freiberg.de (S. Eckart).

https://doi.org/10.1016/j.fuel.2025.136746
Received 22 December 2024; Received in revised form 30 July 2025; Accepted 3 September 2025

1. Introduction

As global demand for sustainable energy and lower carbon emissions increases, hydrogen and ammonia have emerged as preferred carbon-neutral fuels for clean and efficient power and heat production. [1,2]. As with other scientific and technological endeavors, effectively utilizing these non-carbon species necessitates a comprehensive understanding of their chemical dynamics across various applications. The pursuit of sustainable energy has propelled research into advanced combustion systems, where hydrogen, bio-methane, and ammonia play crucial roles. For instance, adding hydrogen to flammable mixtures significantly affects the reliability of widely used predictive models and correlations. However, these gases' interactions and synergistic effects in different combustion scenarios remain poorly understood, presenting a critical research gap. Furthermore, the expanding use of hydrogen and ammonia in diverse energy applications highlights the urgent need for robust and validated kinetic frameworks to accurately model their behaviors [3].

This review primarily focuses on the comprehensive gathering and organization of existing knowledge about ammonia combustion as well as binary and ternary fuel mixtures from methane, hydrogen and ammonia. It aims to delve deeper into properties that play a crucial role in specific applications related to large-scale combustion facilities such as ovens and furnaces. The main aim is to extract valuable insights and essential knowledge necessary for retrofitting high-temperature processes that involve ammonia and hydrogen mixtures. Moreover, this investigation seeks to derive practical implications and guidelines for implementing ammonia and hydrogen mixtures in retrofitting scenarios. The goal is to distil practical recommendations while considering the particular intricacies and challenges associated with integrating these mixtures into current systems [2,4].

Additionally, this investigation delves into the chemical processes within composite mixtures, providing new insights into the combined effects of hydrogen and ammonia in methane/air combustion flames. These findings are crucial for everyday combustion practices and in scenarios involving unexpected releases of gaseous fuels in various configurations. The push for renewable energy generation using carbon–neutral fuels has been initiated by numerous international institutions. Hydrogen, ammonia, and bio-methane are recognized as viable and promising solutions for this energy transition. However, technologies for their reliable storage and optimized combustion are still in the developmental or prototype stages. Combining hydrogen and ammonia with methane or natural gas is seen as a practical short- and medium-term solution [5]. In binary mixtures, hydrogen has demonstrated an ability to heighten the reactivity of the mixture [6], while ammonia tends to decrease it. In most cases, the addition of hydrogen to pure methane has been primarily considered, thereby limiting its positive environmental effects. Utilizing biologically produced methane could potentially extend these beneficial aspects. Nonetheless, the impacts of the initial composition on chemical and thermal aspects are not yet comprehensively understood. In this context, characterizing overall reactivity and severity, particularly in terms of flammability and laminar burning velocity in the event of accidental release, offers an appealing solution.

Ammonia, in its gaseous state, is rather impractical for grid systems but can be stored and combined locally in industrial facilities. As a result, it can act as a carrier substance for renewable hydrogen and aid in the decarbonization of large-scale industrial applications. Presently, only a limited number of studies exist on mixtures encompassing all three components. Therefore, this study will present a detailed analysis and investigation to achieve a deeper understanding of the phenomena involved in tertiary mixtures of hydrogen, ammonia, and methane. This consists of evaluating gas mixtures' total reactivity, considering potential mixing scenarios for the lower flammability limit (LFL) and upper flammability limit (UFL). The primary effects of operational conditions on flammability phenomena were determined and discussed numerically. The findings gathered herein establish a robust foundation for the comprehensive assessment of both normal operation and accidental release scenarios involving fuels containing hydrogen, ammonia, and methane.

Looking at Table 1, it is evident that the properties of ammonia differ significantly in many areas. These properties have already been categorized by Chai et al. [7] and will not be reiterated here. Besides these points, many other properties, such as the quenching distance during the flame-wall interaction and the flame stability against extinction (e.g., the extinction strain rate), also present a similar tendency that the ammonia has a significant difference compared with other conventional fuels. Specifically for high-temperature systems in the basic materials industry, two points can be emphasized. Firstly, the relatively high ignition temperature leads to incomplete combustion in colder areas, and secondly, the low burning velocity results in generally reduced reactivity that can cause stability issues in industrial burners. In Fig. 1, a comparison illustrates the general conditions during combustion concerning methane as a reference point. Assuming equal performance levels between furnaces and referencing 1 mol of methane, it becomes apparent that both hydrogen and ammonia require larger amounts of fuel due to their lower calorific values. Consequently, this necessitates adjustments in burner design, potentially requiring adaptations to achieve similar mixing ranges. Additionally, modifications to supply lines might be necessary. Both hydrogen and ammonia also possess lower air–fuel ratios (AFR) than methane, resulting in a reduced total air volume flow at comparable power levels in both cases. This suggests that the components on the inlet side for the air might be adequately sized for retrofitting facilities. The overall volume flow directed through the burner, which comprises fuel and air, is also higher for hydrogen and ammonia compared to methane. Adapting mixing plates, swirl bodies, or nozzles could potentially address this, as similar conversions have been feasible from L- to H-gas and from town gas to natural gas. Examining the exhaust gas side of the combustion chamber reveals that the exhaust quantity decreases with hydrogen but increases with ammonia. Thus, in a purely theoretical scenario utilizing ammonia as the sole fuel, adjustments on the flue gas side might be necessary to handle the exhaust quantities. Conversely, mixtures of hydrogen and ammonia might potentially produce equivalent exhaust volume flows (assuming equal temperatures), reducing the necessity for modifications.

In addition to the general properties and the retrofitting with ammonia mixtures, several key areas can be compiled from the current literature, which are summarized in Fig. 2. Some of these points are further elaborated in this review. The focal aspect pertains to the utilization of furnaces fuelled by ammonia, hydrogen and methane mixtures. These ammonia mixtures-based furnaces can find application in various industrial processes such as kilns, cement production, power generation through steam, chemical reactions, and other industrial domains demanding elevated temperatures [9].

Ammonia is playing an increasingly important role in the energy transition, particularly for hard-to-abate sectors such as cement and steel manufacturing. Compared to hydrogen, ammonia offers advantages in storage, transport, and scalability, serving as an efficient

Table 1
Properties of ammonia compared to common fuels [7].

	Hydrogen	Methane	Propane	Ammonia
Density (g/L, 25 °C, 1 atm)	0.082	0.657	493	0.703
Lower heating value (MJ/kg)	~120.1	~50	~46.4	~18.8
Lower heating value (MJ/m^3)	~12	~35.8	~93.1	~13.72
Minimum ignition energy (mJ)	~0.011	~0.28	~0.25	~8
Auto-ignition temperature (°C)	~571	~537	~450	~651
Flammability limit (Equivalence ratio)	0.1–7.1	0.5–1.7	0.55–2.9	0.63–1.4
Maximum laminar burning velocity (m/s)	~2.9	~0.37	~0.43	~0.07

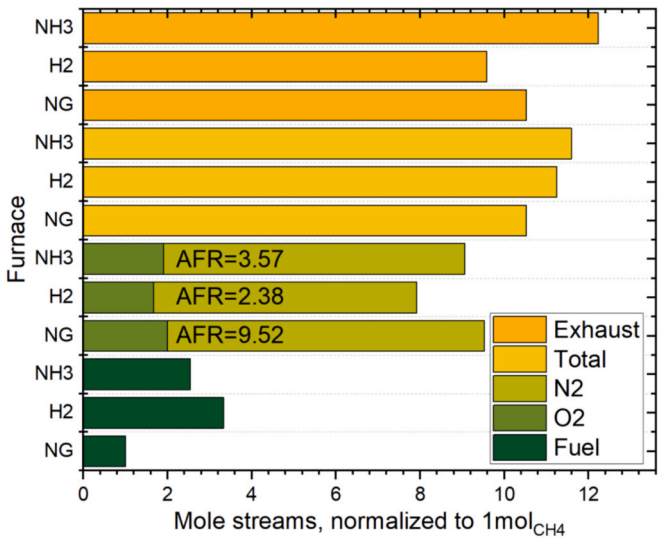

Fig. 1. Overall conditions during combustion, using methane (1 mol) as a benchmark at reference for the same power level

hydrogen carrier. Pilot projects, such as those by Heidelberg Materials [10] in the UK and UBE Mitsubishi Cement in Japan [11], demonstrate its use as a fuel or hydrogen source in cement kilns to reduce CO_2 emissions [12]. In the steel industry, ammonia is also being explored as a direct reducing agent for iron ore [13]. With a global production volume of approximately 200 million tonnes in 2023 [11], ammonia could present a viable and scalable solution for industrial decarbonization.

2. Safety of Ammonia-containing mixtures

Once released into the atmosphere, ammonia presents flammable and toxic behaviour. More specifically, a lower flammability limit (LFL) and an upper flammability limit (UFL) of ~ 16.5 %v and 29.0 %v can be retrieved in the literature at atmospheric conditions [14].

Nevertheless, it is worth noting that ammonia is characterized by a slower and less intense reaction tendency in comparison with most of the conventional and alternative fuels, as indicated by the data previously reported in Table 1. Indeed, ammonia shows the highest auto-ignition temperature, the lowest maximum laminar burning velocity, and the narrowest range of equivalence ratios for the flammability limits among the reported solutions. As for the toxicity, ammonia itself is a corrosive gas that can irritate the respiratory system, eyes, and skin, or be significantly toxic to aquatic life [15]. Besides, the combustion of ammonia can generate a significant amount of nitrogen oxides, potentially responsible for acid rain (e.g., NO and NO_2) or greenhouse gas (e.g., N_2O), as well as hydrogen cyanide (HCN) under specific combustion conditions [16]. As a way of example, the coexistence of ammonia and hydrocarbon-based species has been identified as a possible cause of enhanced production of HCN during the pyrolysis and oxidation processes [17]. Therefore, several factors and equipment should be analysed for the evaluation of the safety aspects of ammonia-based power plants. Considering the scope of this review and section, a specific focus on the acute exposure is given because of the characterization of the consequences of accidental releases of hazardous materials.

In this light, it is worth mentioning that ammonia has a short-term exposure limit (STEL) and the immediately harmful to life or health (IDLH) values, respectively, of 35 ppm and 300 ppm [18]. These values are commonly considered for the evaluation of consequences related to accidental releases of toxic species, and they are ~ one order of magnitude lower than the vast majority of fuels [19], indicating the strong toxicity of ammonia. In addition, in the presence of impurities or an oxidative environment, ammonia and some derived species can pose issues to the durability of industrial facilities due to their corrosive tendency, as discussed in detail in a dedicated review available in the current literature [20]. In this case, the safety characterization of hazardous materials can be focused on the dispersion in the atmosphere or a closed environment (e.g., engine room) for what concerns the toxicity aspects and on the thermal dose or fuel concentration in the proximity of the releasing point for what concerns the flammability aspects. Besides, in the latter case, specific considerations are recommended to evaluate the possibility of domino effects, based on the consequence analysis and given threshold values [21]. A recent study even shows that ammonia can be used as an inhibitor in the hydrogen combustion system, which

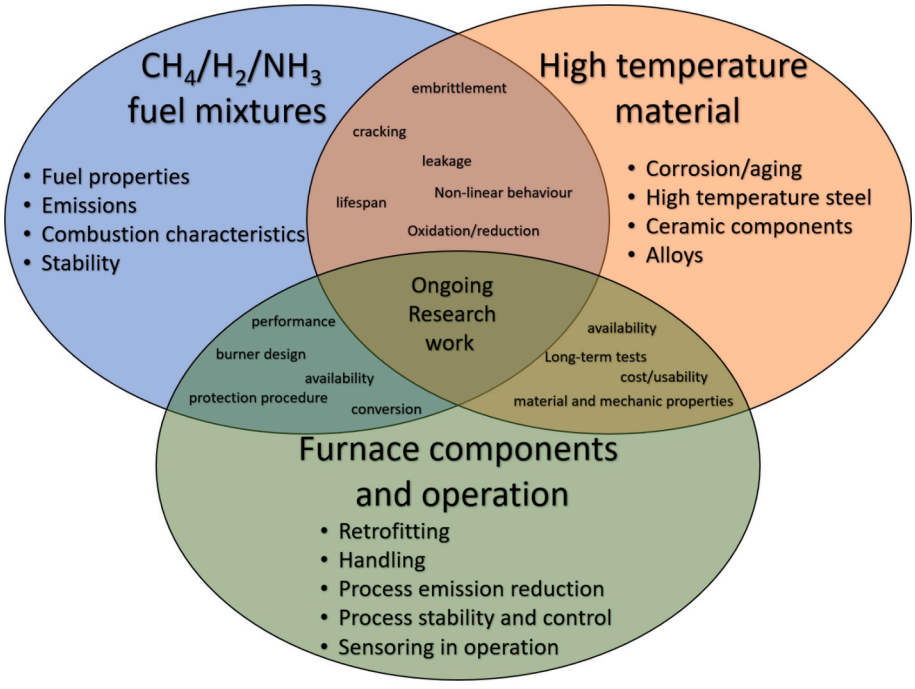

Fig. 2. Several key areas for use of the ammonia in furnaces

suppresses the high reactivity and explosive properties of hydrogen [22].

The flame-related case is composed of different scenarios, which are determined by the releasing conditions and the possible presence of effective ignition sources in the proximity of the release. Based on the investigated system (e.g., equipment item), different losses of containment and corresponding credit factors can be considered [23]. Typically, particular emphasis is given to the storage systems because of the larger amount of hazardous materials handled. Therefore, it is necessary to distinguish the possible storage and handling systems suitable for the ammonia case. Regardless of the process considered for the production of ammonia, this compound can be conveniently stored in a liquid phase to guarantee a larger density. Taking into account the physical properties of ammonia, a liquid storage system can be either based on moderate pressure (e.g., ~ 10 bar) or low temperature (e.g., ~ − 20 °C) [24]. Currently, the former is mostly adopted on an industrial scale, although the utilization of the latter strategy is gaining momentum due to the possible combination with cryogenic systems for the storage of light energy vectors, such as Liquefied Natural Gas (LNG) and Liquid Hydrogen (LH2) [25].

Considering the low reactive nature of ammonia (please refer to Table 1 for ignitability and flame velocity), the likelihood of the occurrence of a vapour cloud explosion is very low, unless a strongly congested area is considered. Indeed, significantly larger burning velocities are required to generate a non-negligible over-pressure [26]. Similarly, the comparison between critical and operating conditions indicates that the boiling liquid expanding vapour explosion (BLEVE) can be neglected [27]. Fireballs are possible only in the case of an abrupt release of large amounts of ammonia in the atmosphere, typically associated with catastrophic ruptures of storage tanks. Large consequences are associated with this scenario. However, the credit factor of this scenario is about 2 orders of magnitude smaller than the corresponding value associated with a small continuous leak, leading to comparable risks to scenarios generated by a continuous leak [23]. In this case, jet fire, flash fire, and pool fire can be observed based on the releasing conditions as well as the presence of an ignition source in the proximity of the flammable cloud. More specifically, in the case of accidental release, different chains of events and scenarios can be observed. If the release is generated by a compressed system, leakage of ammonia generates an under-expanded jet. It should be considered that the expansion of compressed ammonia affects the fluid temperature in the proximity of the releasing point, leading to partial evaporation, droplet formation, and rainout. Therefore, the isentropic expansion produces intense turbulence, entrainment of liquid droplets, and – thus – a two-phase choked flow. The characterization of fluid dynamic regimes remains one of the main challenges for the evaluation of these scenarios because of the elevated computational requirements [28]. Different models can be considered for the calculation of the critical flow accounting for the vapor quality (e.g., Homogeneous Equilibrium Model, HEM, Homogeneous Frozen Model, HFM, or Homogeneous Non-Equilibrium Model, HNEM [29]). As the consequence analysis is concerned, the scenarios deriving from the two phases are evaluated separately. To cope with the issue related to the vapor phase, theories like the Mach Disk approximation have been produced to account for the near-field supersonic regime under simplifying assumptions [30]. These correlations have been developed and largely adopted for the evaluation of the release of methane, hydrogen, and their mixtures in the atmosphere. However, there is no actual constraint limiting their applicability to the case of mixtures containing ammonia. In the case of an immediate ignition, a jet fire is produced, requiring the quantification of flame length and thermal profiles. Different techniques can be used for this scope, including empirical correlations and computational fluid dynamics, as described in detail elsewhere [31]. The fraction of liquid released in the two-phase flow can accumulate and form a pool which produces flammable vapours. The possible scenarios deriving from this branch overlap with the case of accidental release from a low-temperature system dealing with liquid ammonia. If the release is caused by a low-temperature system, a leakage of liquid ammonia is followed by an initial flash and a pool formation, followed by a pool spread on the ground and vapour mixing with the surrounding air. The presence of a sufficient and immediate ignition source in the proximity of the flammable cloud will lead to pool fire. Alternatively, a flash fire can be observed if the ignition source is delayed with respect to the release.

The characterization of a pool fire aims at the quantification of the flame geometry (e.g., flame diameter, length, and tilt angle) and the spatial distribution of the thermal radiation. These results are obtained starting from the flame properties of the involved species, including the mass burning rate. The mass burning rate represents the overall reactivity of the fuel per unit of area, and it can be affected by the size of the pool [32]. Several experimental approaches are available for the quantification of the overall reactivity of pool fires as well as the flame structure, including bench-scale equipment (e.g., cone calorimeter), diagnostic systems (e.g., thermocameras) [33]. The gathered information can also be used for the validation and identification of the most suitable models to be considered for advanced numerical analyses (e.g., implementation of kinetic mechanisms in computational fluid dynamics) [34]. A detailed description and a comprehensive list of the existing models and assumptions for the evaluation of these scenarios can be found in the dedicated literature [35]. From a consequence analysis point of view, the characterization of flash fire is intended as the assessment of the area potentially involved by a flammable cloud. More specifically, the safety distance is defined on the basis of the lower flammability limit and fuel distribution in the surrounding atmosphere. The former is strictly related to the initial composition of the releasing fuel, whereas the latter can be affected by the case-specific boundary conditions, including the geometry of the releasing area, the presence of obstacles, and the atmospheric conditions. Computational fluid dynamics and Gaussian dispersion models are largely adopted for this scope. The occurrence of a flash fire can turn into a pool fire, as well. Regardless of the releasing condition, in the absence of an ignition source, toxic release into the atmosphere and soil contamination are the main scenarios. For details on the possible consequences on human health and environmental contamination together with the corresponding relevant concentrations, readers can refer to specific reviews and sources available in the literature (e.g., [36]). For the sake of clarity, possible event trees deriving from the accidental release of compressed ammonia (Fig. 3) and cryogenic ammonia (Fig. 4) systems, both starting from a liquid phase, are reported below.

Different mitigation strategies can be adopted based on the location of release (i.e., indoor or outdoor) or initial conditions [37]. To suppress vapour cloud dispersion, the use of a water curtain is recommended [38]. Besides, the effectiveness of this mitigation system can be greater for the case of ammonia release than for other substances since ammonia dissolves in water. In addition, because of the limited evaporation rate, providing water in the proximity of an accidental release has been recently suggested as a possible mitigation strategy to significantly limit the duration and the consequences of scenarios related to the formation of an ammonia liquid pool [39]. Therefore, the effects of the initial composition of the releasing fluid shall be carefully evaluated, especially in the case of process units and outdoor installations where water and moisture can be present.

The comparison of flame-related properties of ammonia with alternative fuels [3] suggests its possible use as a component of a mixture. In the view of possible utilization of flammable mixtures containing significant quantities of ammonia, hydrogen, and methane, it is evident that the existence of an accurate and robust database of the flammability limits and overall reactivity is paramount to guarantee meaningful results. Although several empirical correlations have been developed for the estimation of safety parameters of gaseous mixtures starting from properties and parameters of the pure species [40], none of them has been proven to be accurate when dealing with non-hydrocarbon species,

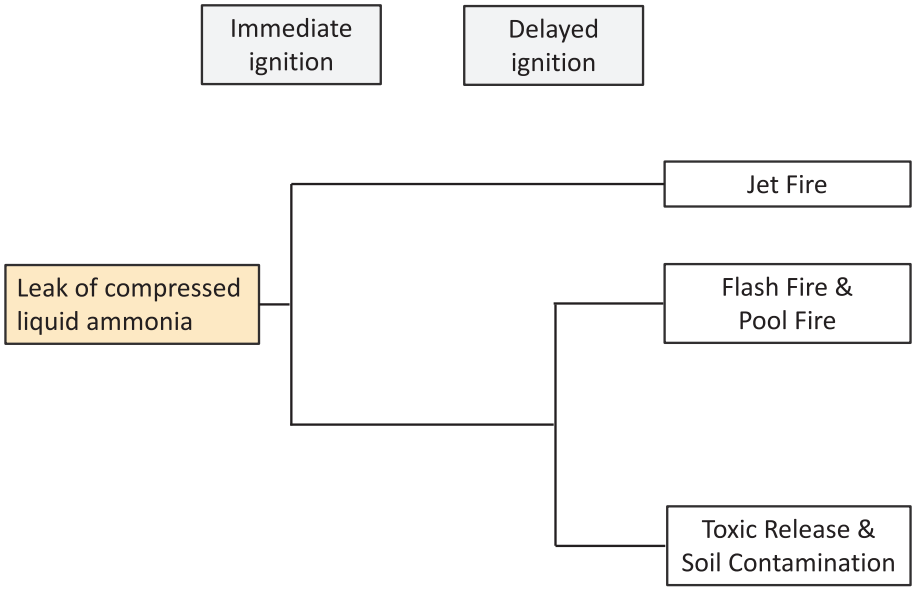

Fig. 3. An event tree deriving from a continuous release of liquid ammonia at an initial compressed condition.

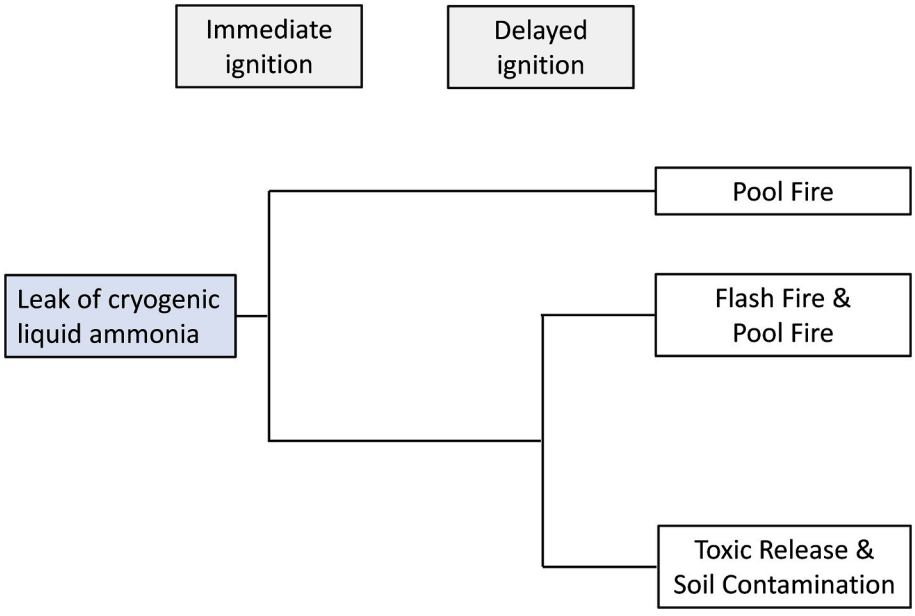

Fig. 4. Event tree deriving from a continuous release of liquid ammonia at an initial cryogenic condition.

and in particular with hydrogen [41]. As an alternative option, the experimental approach or the use of detailed kinetic mechanisms is recommended. In this sense, the evaluation of the laminar burning velocity represents a paramount step either for the direct measurement of the target parameters or for the validation of suitable kinetic models. Several experimental systems can be used in this scope, including a spherical bomb, heat flux burner, and counter flow flame, as reported in a dedicated review [42]. Similarly, many approaches have been proposed for the development of kinetic mechanisms, such as automated generation and manual selection, as well as for the evaluation of thermodynamic and kinetic properties to be included within the mechanisms (e.g., group additivity and quantum mechanics calculations) [43]. The availability of robust and validated mechanisms enables the assessment of safety and phenomenological aspects also under conditions and geometry representative of real large-scale industrial systems [44], including furnaces and storage systems.

Distribution systems also need to be properly analysed to guarantee elevated standards in terms of safety for the whole supply chain, including delivery systems of ammonia. Although the chemical has been employed for more than 150 years, issues related to the rupture of pipelines or leaks from nursing tanks can be found from time to time in the literature and the news. Lately, some large complexes have been re-evaluated to ensure their safety is still within national standards. One case would be the Magallan's Line in the USA. Although promising, the line has suffered from safety incidents over the years. On the 27th October 2004, a 20 cm diameter pipeline of the network ruptured in Kansas, releasing approximately 4,858 barrels of anhydrous ammonia [45]. Fortunately, no human casualty was recorded due to the quick answer from the emergency services (sheriff and firefighters), although the release was in a farming zone where endangered species of fish and wildlife lived. Therefore, more than 25,000 fish were killed, including some threatened specimens. During the event, the operator was

monitoring the pressure of the lines. He finally managed to close the delivery system whilst contacting his manager and contractors. During the incident, it was recognised that more training was needed for the controller (i.e., use the information in the board to recognise a leak, estimate released product, further review of risk assessment, and constant contact with the National Response Centre). Another example occurred in the Russian/Ukrainian line that runs from Togliatti to Odessa (which at the time of the incident was the longest in operation). Although no large incidents had been documented or were public, in 2015, an incident in Ternovo made the news. The event occurred in the evening, allowing people to be warned by the mayor, house by house, and evacuated [46].

Although the likelihood of BLEVEs is low, these can still occur. Explosions from the sudden release of ammonia have been documented [47]. Pressure starts building up when cylinders or gas-containing components are exposed to a heat source. The increase in pressure reaches a point when the structural integrity of the component is compromised, resulting in damage and sudden release of the contained gas. The problem aggravates if the heat source or a spark comes in contact with the boiling, uncontained ammonia. If this happens, the probability of explosion increases with the likelihood of catastrophic scenarios. Ammonia explosions have only been documented for large-scale facilities and large tankers [47]. However, precaution needs to be taken to avoid similar incidents in incipient technologies.

Quite obviously, the evaluation of real-case industrial applications requires more specific inputs related to the layout and ancillary equipment items involved within the analysed configurations. Nevertheless, some general and common aspects can also be highlighted also in this case. As a way of example, the combustion of ammonia-containing mixtures leads to the production of intermediates and oxidized species showing a corrosive behaviour also with materials typically constituting boiler and furnace systems, as reported in specific investigations available in the current literature [48,49]. Recently, the corrosion of air preheaters was found to be significantly increased by the addition of ammonia as a reactant at low boiler loads. However, the impacts of increased costs can be mostly mitigated by the introduction of reasonable carbon tax rates [50]. Moreover, the utilization of non-corrosive compounds together with ammonia within the fuel mixture is encouraged to reduce the corrosiveness of the exhaust gases as well as the raw materials, thus inherently requiring less demanding materials. Considering the operative conditions required, the use of hydrogen and methane together with ammonia is recommended [51]. In this sense, it is worth mentioning that the differences in the overall reactivity of the adopted fuels can cause significant fluctuations in ignitability, the occurrence of blow-off and flashback phenomena, making the position of the flame inconsistent during the burning process and thus making the retrofitting of the existing technologies challenging as recently extensively investigated in the literature [52,53].

Another important parameter to consider when using these blends is also the potential of hydrogen embrittlement, which could reduce the lifespan and therefore cause unexpected failure of system components. Recent studies [54–56] show that the use of ammonia in furnaces, boilers, or combustors leads to the production of high hydrogen content at the post-flame zone. The hydrogen content can reach measurable values up to 7 % in volume of the total flue gases, making it possible to ignite the chemical in staged combustion zones for further energy production. However, this phenomenon also leads to the contact between materials and hydrogen molecules, which, due to their high diffusivity, permeate the materials and embrittle them, reducing ductility and potentially leading to fractures or failure.

The phenomenon has been observed in high-temperature resistant alloys, but it has also been documented in stainless steels directly exposed to ammonia flames [57,58]. Wang et al. [8] showed, by exposing various plates to an ammonia flame, that the impacts of ammonia on industrially used steel at higher temperatures can produce nitration effects that directly affect the material's crystallography, Fig. 5. This effect leads also to significant increase in surface hardness, a potential problem for the final use of the molecule. Simultaneously, the combustion of ammonia under rich fuel conditions has demonstrated to deliver large hydrogen quantities, as exposed in previous paragraphs. The work from Kovaleva et al. [58] shows the impact of these flames on gas turbine-based materials (Inconel designed for high temperature resistance). The findings denote how the exposure to ammonia-based flames leads to hydrogen embrittlement not only at the surface but also within interstitial layers, another problem that can also lead to the weakening of mechanical properties in the materials of interest. It must be remembered that ammonia combustion can also lead to slip ammonia traces and large NO emissions. The combustion of the chemical also generates large water quantities, thus potentially leading to the formation of nitric acid and ammonium, an acid and a base, respectively, that can degrade structural components. Some of these analyses have been encapsulated in the work done by Alnajideen et al. [59]. Finally, although coatings have been proposed for their use in combustion-based ammonia systems, current results show that we are still in the infancy of such an area of research. AIST (one of Japan's main institutes) has evaluated the use of Co/Ni-based coating for gas turbine systems. Although less relevant to furnaces, the materials can still be used to reduce the impact of nitration, particularly under atmospheres $> 500\ ^{\circ}C$, as previously explained. However, the finding from the group showed that although Co/Ni-based alloys can retard the nitration process, they still suffer from the impact of the molecule, reducing their ductility and causing cracks that potentially lead to failure modes. It was recognised that Fe-based coatings need further studies before conclusive statements can be made, thus showing that further research is required in the area.

Under this impulse, it is possible to conclude that new insights promoted by the need for accurate safety analysis can have beneficial effects

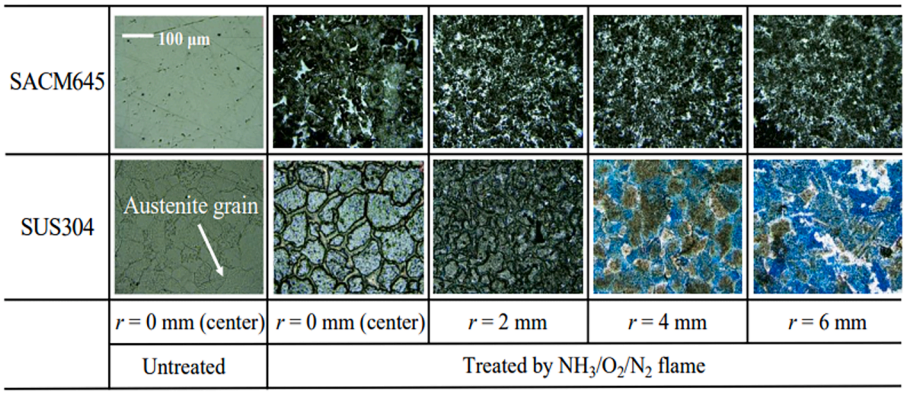

Fig. 5. Optical micrographs of the SACM645 and SUS304 test plate surfaces after being exposed to the NH3/O2/N2 flame at 550 °C for 5h [8]

also on the identification of optimized conditions during normal operation of industrial processes, pursuing more sustainable and lean production and conversion systems.

3. Flame characteristics

This chapter summarizes some fundamental combustion properties, specifically focusing on blends of7 ammonia, methane, and hydrogen. These properties are categorized according to their interdependencies.

Laminar burning velocity (LBV).

The laminar burning velocity is one of the key parameters globally used to compare fuels regarding their reactivity. Moreover, it has long been one of the primary validation targets for chemical reaction kinetics. However, when considering the combustion of ammonia, these mechanisms must additionally account for nitrogen (N) chemistry, besides carbon (C), hydrogen (H), and oxygen (O) chemistry. Therefore, these mechanisms rely on new, unambiguous, and reliable validation data for these mixtures. While advancements in measurement techniques have led to increased research on ammonia's LBV in the past decade, discrepancies, especially in fuel-rich mixtures, still persist, with disparities of up to 25 % between various determination methods. The existing mechanisms do, however, provide a reasonable reflection of the observed trends (refer to Fig. 6). The maximum burning velocity for ammonia air was found around 7 cm/s, while methane/air combustion is around 37 cm/s [60]. The following sections will summarize these findings concerning temperature and pressure dependencies and mixtures. In the final stages of this review, a highly comprehensive study by Szanthoffer et al. was published, which specifically addresses NH_3/air mechanisms [61].

It is evident from the experiments (only a few shown) that there is considerable scatter. However, it's also apparent that despite significant efforts in this field in recent years, several mechanisms can predict the trend but fail to accurately represent this global parameter in its absolute values. Szanthoffer et al. [62] recently demonstrated this in an extensive comparison of 18 mechanisms involving ammonia and ammonia-hydrogen mixtures, encompassing a database of over 3700 data points. Through sensitivity analyses, they notably emphasized the influence of chain branching steps and highlighted the coupling between carbon and nitrogen chemistry. Improvements in these effects are expected to impact emission predictions, which will be further addressed later.

In Fig. 7, data from the literature for laminar burning velocity are systematically collected. The main purpose is to illustrate the trends observed in binary mixtures. As there are only a few measurements available for ternary mixtures [63], it is observed that the relationship between methane and ammonia follows a predominantly linear trend. Methane shows approximately 8 times the velocity of ammonia, and it's worth noting that the maximum velocity occurs at roughly similar equivalence ratios. The scenario differs with hydrogen, where the maximum occurs at about 1.7 in the significantly rich region. Also, mixtures with hydrogen do not display linear relationships, but around 50 % in the mixture, there is a sharp increase in burning velocity, indicating a predominant regime of hydrogen chemistry. For CH_4-H_2 mixtures, these combinations have already been measured in laboratory [64–66] and predicted using neural networks [67].

Furthermore, for the complete dataset, dependencies on temperature and pressure were examined for the two mixtures involving ammonia, see Fig. 8. It is evident that, especially at higher temperatures, significant gaps exist in the data, with no available data points beyond 490 K. Additionally, there is a lack of data in the range above 10 bar, possibly due to the further reduction in burning velocity under increased pressure. This reduction can lead to significant challenges in mixtures with high ammonia contents, including buoyancy, cellularity, and flame extinction. For ovens and furnaces, atmospheric conditions are usually of utmost interest. It can be observed that there is sufficient data available for binary mixtures concerning these conditions. However, due to the limitation of preheating temperatures, due to pre-cracking, some conclusions cannot be drawn regarding recuperators and regenerators for industrial burners. It would be highly beneficial to expand the fundamental understanding to higher temperatures for these systems with non-premixed systems.

Correlation between laminar and turbulent burning velocity.

Combustion is invariably observed within a turbulent flow regime as a result of two contributing influences. The first is that turbulence

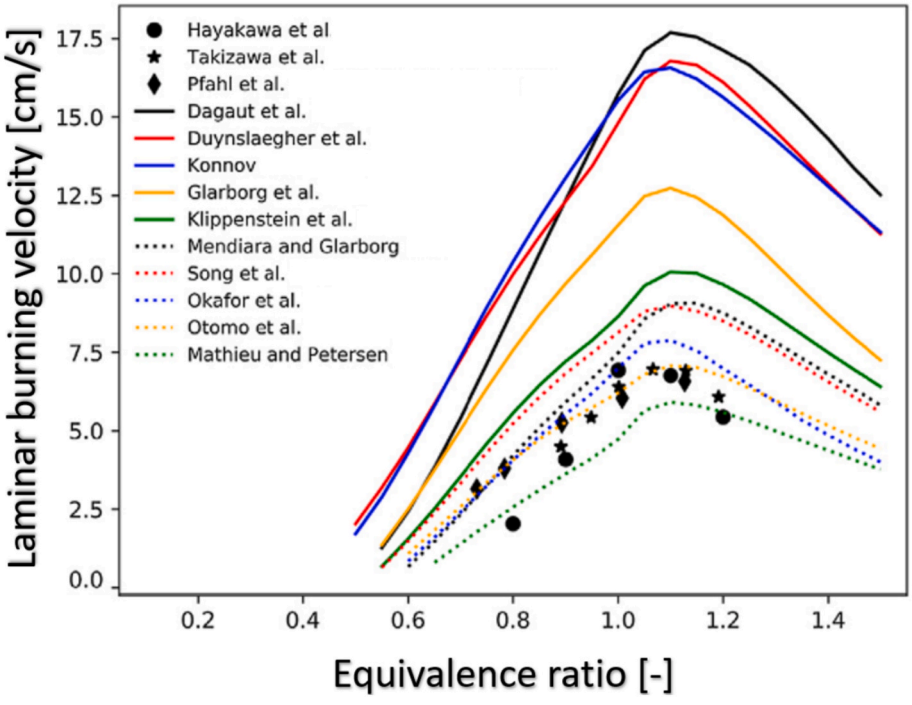

Fig. 6. Laminar burning velocity of ammonia (T_{gas}=298K, p_{gas}=1bar) in air. Figure adapted from Da Rocha et al. [68]; Hayakawa et al. [69] (spherical chamber), Takizawa et al. [70] (spherical chamber), Pfahl et al. [71] (spherical chamber)

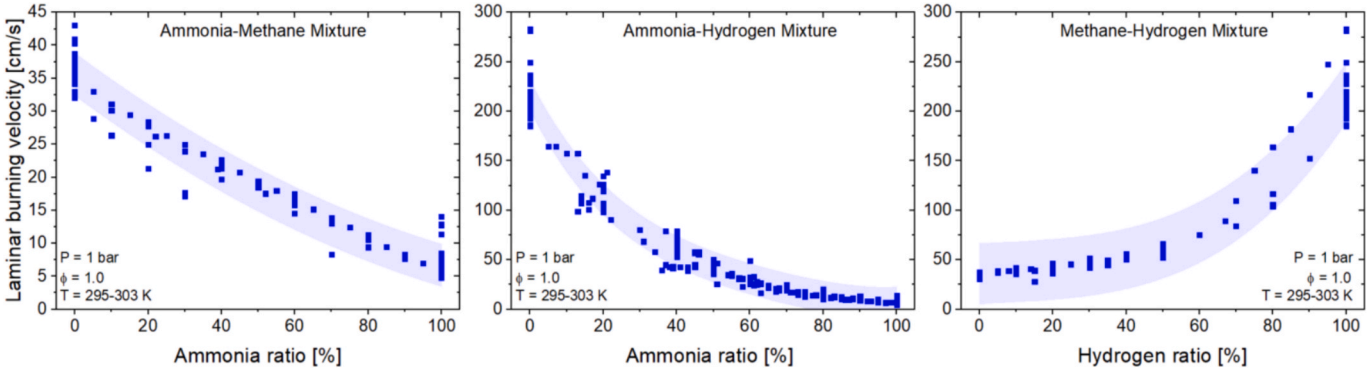

Fig. 7. Laminar burning velocity of ammonia-methane, ammonia-hydrogen, and methane-hydrogen mixtures (T_{gas}=295-303K, p_{gas}=1bar) in the air. Original data (points) from several publications from 2005-2023, summarized in [60,67]

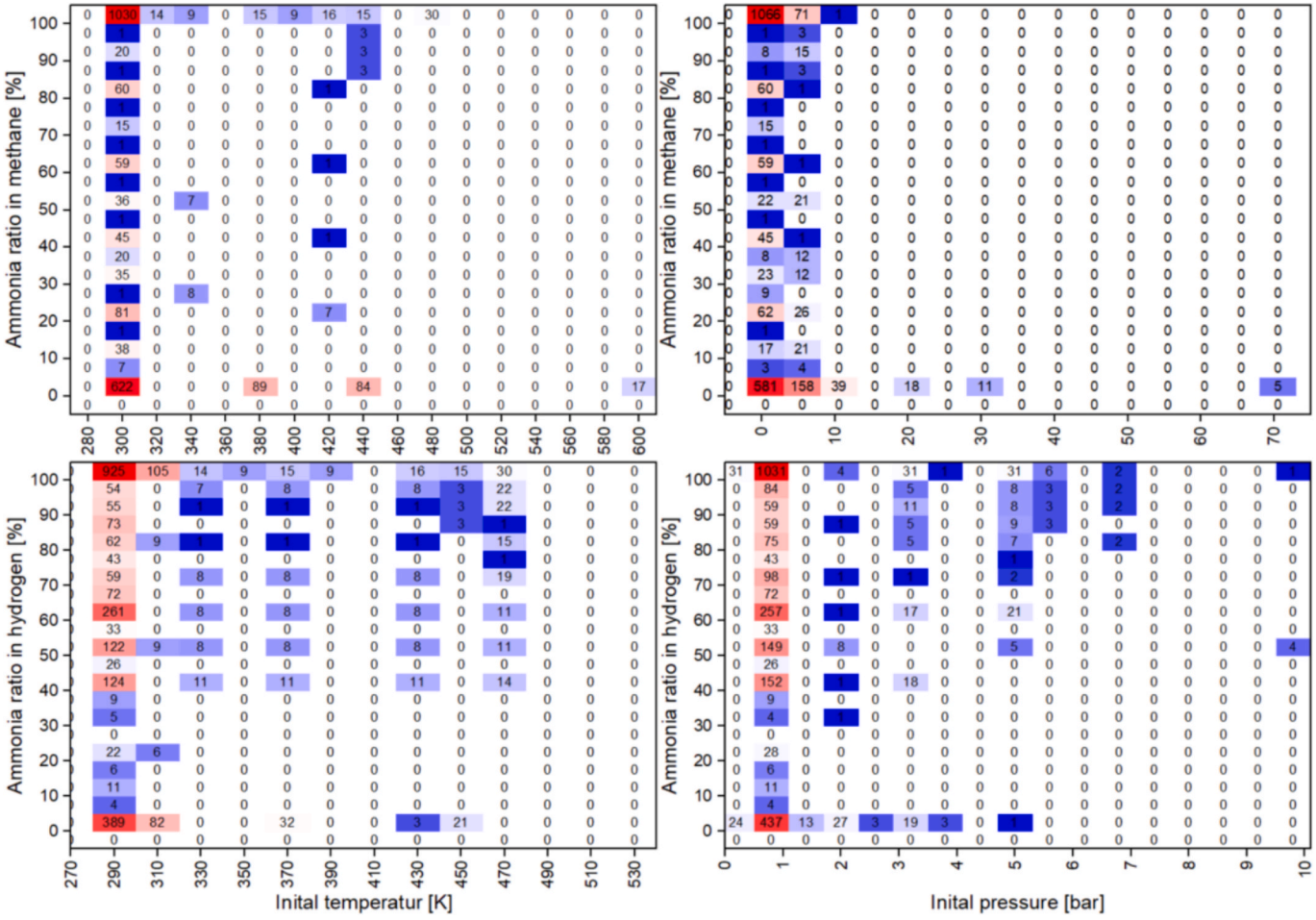

Fig. 8. Count of data points for the laminar burning velocity of ammonia-methane, ammonia-hydrogen, and methane-hydrogen mixtures at different pressures and different temperatures. Original data from several publications from 2005-2023, summarized in [60,67]

promotes enhanced mixing and increases combustion efficiency. However, the second factor revolves around generating heat during combustion, which introduces flow instability through gas expansion and buoyancy, consequently playing a pivotal role in the transition toward turbulence [72]. Recently, researchers within the combustion field appear to have been mainly motivated by the persistent unresolved issues pertaining to turbulent combustion. Turbulence, a phenomenon not yet comprehensively elucidated, is arguably the most prominent outstanding problem within traditional physics. Given that turbulent flows are prevalent across various engineering contexts, the pressing necessity to address engineering challenges has prompted the development of provisional resolutions known as turbulence models. There are three modes, including premixed, non-premixed, and partially premixed combustion; each mode has its characteristics and is important in different combustion processes [73].

Turbulent or laminar premixed flames can be achieved across different configurations for both stationary and nonstationary flames. When the speed of the mixture reaches a certain value, turbulence develops within the Bunsen tube. In a constant volume chamber, turbulence can be induced by employing four high-speed fans positioned in

opposition, resulting in an almost uniform and isotropic turbulent field [74–76]. This arrangement proves highly conducive to investigating flames' transient evolution during their growing stages.

Various researchers [77–80] have proposed diagrams delineating the different regimes of premixed turbulent combustion based on length scale and velocity ratios. Fig. 9 shows that the boundary lines $Re = 1$ and $Ka = 1$ demarcate the transitions between distinct combustion regimes. Additionally, the boundary line $u'/SL = 1$ distinguishes between corrugated and wrinkled flamelets, while the line indicated by $Ka = 1$ breaks thin reaction zones from broken reaction zones. The line $Re = 1$ acts as a separator, differentiating turbulent flame regimes with $Re > 1$ from the laminar flame regime $Re < 1$, which occupies the bottom-left quadrant of the diagram.

Damköhler was the pioneer in formulating theoretical equations for the turbulent burning velocity. He categorized premixed turbulent combustion into two distinct regimes: the large-scale regime, also known as the corrugated flamelets regime, and the small-scale turbulence regime, referred to as the thin reaction zones regime [73]. The characteristics of the turbulent combustion of hydrogen (H_2), ammonia (NH_3), and methane (CH_4) are crucial to comprehension of the progressively more worrying "green fuel" used in engines and marine combustors. Natural gas containing CH_4 and H_2 is frequently utilized to improve ignition and combustion performance. Understanding $H_2/NH_3/CH_4$ combustion in engine-related turbulence conditions is thus critical for evaluating turbulent flame speed in turbulent spherical premixed expanding flames with elevated temperature (T_i), pressure (P_i), and turbulent intensities (u'). Turbulent combustion of ternary fuels has received less attention in the literature [81]. Because of the benefits of low-carbon generation, the diversity of flame speed, a broad range of flammability limits, and other storage and transportation advantages discussed earlier, H_2, NH_3, and CH_4 may be utilized to lower the carbon number and improve fuel oxidation. Thus, the fundamental data of unary, binary, and ternary fuel turbulence characteristics are essential topics for future study, and turbulent burning velocity (S_T) is considered a necessary parameter of the operational condition and knowledge for developing turbulent models [82,83].

Extensive research has examined the turbulence characteristics of a combustion chamber's turbulent field generated by fan rotation, which requires determining the turbulence intensity and integral length scale. The ultimate turbulent field for a combustion chamber is homogeneous and isotropic for a better understanding of fluid dynamics by simplifying the random characteristics of an applied turbulent field. The primary diagnostic methodologies employed for analyzing turbulent flow typically consist of hot wire anemometry (HWA), laser Doppler velocimetry (LDV), and particle image velocimetry (PIV). HWA and LDV techniques can primarily capture single-point measurements, whereas PIV enables the determination of instantaneous velocities within two-dimensional fields. Sick et al. [84]used PIV and discovered a linear relationship between the turbulence intensity and fan speed. PIV data is found to be smaller by 30 % compared with LDV [85]. The integral length scale is not significantly affected by the initial temperature and pressure [86] and elevated pressure [87]. Zhao et al. [88] reported the turbulence characteristics at elevated pressure with different combustion chamber impeller sizes and investigated the methanol/air turbulent expanding flames. They found that u′ is independent of P and proportional to ω.

Extensive research has been conducted on the relationship between turbulent burning velocity, yet a comprehensive model for turbulent burning velocity remains indefinable. Several researchers have conducted in-depth studies on the Spalding-Taylor correlation at unity Lewis number (Le) despite neglecting the impacts of molecular transport and thermal diffusion instability [73,89–91].

Karpov et al. [92] adeptly formulated a model for turbulent flame speed, which aligns with experimental data for H_2-air mixtures and established correlations under conditions of moderate turbulence, where both the Damköhler number (Da) and Reynolds number (Re) are less than one. The preferential diffusion into highly curved flamelets reduces the chemical time scale by 50 for lean hydrogen-air mixtures. This contrasts with the correlation proposed by Bradley et al. [93]. Wu

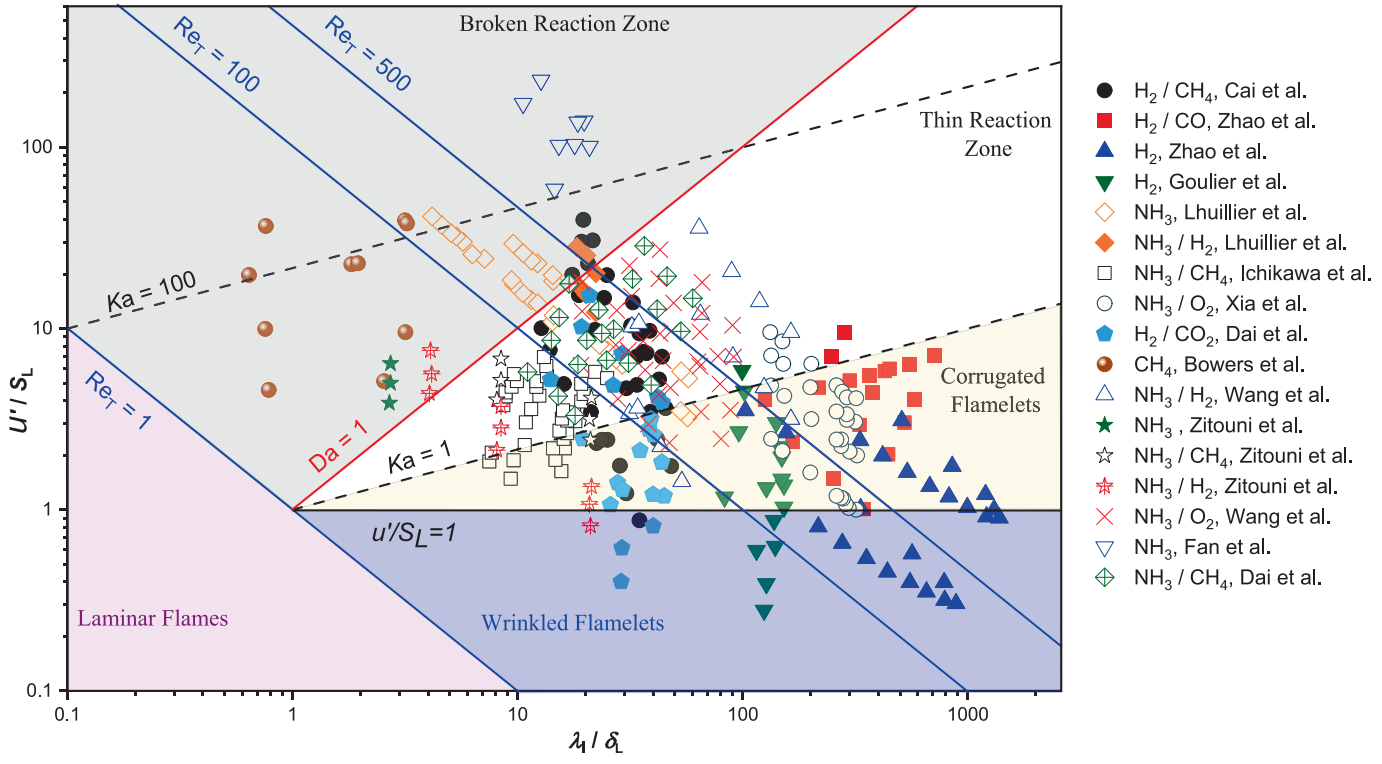

Fig. 9. Experimental conditions on the turbulent regime diagram [152] alongside literature H_2-NH_3-CH_4 based database of Cai et al. [153] (H_2/CH_4), Zhao et al. [96] (H_2 / CO), Zhao et al. [88](H2), Goulier et al. [98](H_2), Lhuillier et al. [143](NH_3), Xia et al. [102](NH_3/O_2), Dai et al. [150](H_2/CO_2), Bowers et al. [154](CH_4), Wang et al. [131](NH_3/H_2), Zitouni et al. [142](NH_3, NH_3/H_2, NH_3/CH_4), Wang et al. [78](NH_3/O_2), Fan et al. [155](NH_3), and Dai et al. [80]

et al. [94] observed that a lean H_2/air mixture exhibits a higher turbulent flame speed with increased wrinkling than a rich H_2/air flame, given the same laminar burning velocity. The Markstein length (L_b) in the turbulent Reynolds number equation has been replaced by the laminar flame thickness by Chaudhuri et al. [95].

Zhao et al. [96] investigated the turbulent burning velocity of H_2/air flames across a wide range of equivalence ratios, focusing on the impact of molecular transport on flame morphology and burning characteristics. The effects of molecular transport on flame stability and turbulent burning velocity were investigated, demonstrating how molecular transport influences the flames' shape and their propagation speed. Lean H_2/air flames have a higher ST than the rich side when LBV is the same due to many wrinkles [94]. Different general correlations in terms of Reynolds number and Lewis number were presented [96,97], while Goulier et al. [98] proposed a correlation containing the effects of integral length scale and S_T.

Numerous researchers conducted experiments on pure ammonia to study the turbulent propagation process of ammonia/air flames [99–101]. Ichimura et al. [99] indicated that the flame's maximum value of S_T can be achieved at u′=1.4 m/s and $\phi = 0.9$, and found the effect of Le and ϕ on the extinction of turbulent NH_3 flames. Furthermore, Fan et al. [79] explored the turbulent characteristics of NH_3/air flames using laser-based measurements to understand the structures and NO formation in a distributed reaction zone regime at higher values of *Ka* conditions. The measurements of the turbulent burning velocity of NH_3– O_2 enrichment (up to 40 %) have been conducted to analyze the effect of turbulent stretching and thermal diffusion, and at constant turbulent stretch on the lean fuel, the ratio of turbulent to laminar burning velocity increases because of the diffusional thermal instability [102,103–105]. Somarathne et al. investigated the combustion and emission characteristics of turbulent non-premixed Liquid NH_3 [101,106], NH_3, and CH_4 [107] /air swirl flames in a rich-lean gas turbine-like combustor under various wall thermal boundary conditions at high pressure. Yamashita et al. [108] compared the fundamental characteristics of liquid NH_3 spray and combustion with gaseous NH_3 combustion. They found that the stability limits of LNH_3 are narrower compared with GNH_3, and they extended due to H_2 and CH_4 blending.

Shy et al. [109] explored the turbulent burning velocity data of lean CH_4/air flames, found that turbulent burning velocities decrease with increasing pressure at constant Reynolds numbers [110–112], and suggested a new relationship based on *Da* at constant elevated pressures and *Re*. Previously, the discrepancies in the power law correlation of Da between lean CH_4 [111], which supports a distributed reaction zone model [113], and lean syngas [110], which supports the theory of homogeneous mixture at high Reynolds numbers [114]. Tamadonfar et al. [115] analyzed the flame brush characteristics and S_T of CH_4/air flames. It was noticed that increasing ϕ, total turbulence intensity, and longitudinal integral length scale decreases the normalized flame height. In contrast, it increased with increasing bulk flow velocity and verified the suggested correlations by [116–118]. Later, these equations were updated based on Da with non-unity Le to show the effect of molecular diffusion [95,97,119–122]. Wang et al. [123] examined the flame structure and turbulent burning velocities of CH_4/air flames at higher values of *Ka* and u'/S_L. They proposed that increased turbulent heat and mass transfer at high Karlovitz numbers predominantly enhances the combustion rate.

Ichikawa et al. [91] conducted NH_3/CH_4/air turbulent flames under elevated pressure in the corrugated flamelets and thin reaction zone regimes of turbulent premixed flames. They found that increasing the NH_3 blend decreased the burning velocity ratio. This suggests that the combustion oscillation in NH_3/CH_4/air flames can be managed similarly to CH_4/air flames.

Dai et al. [80] measured the turbulent burning velocity of methane-ammonia-air mixtures with unity Le, while Hashimoto et al. [104] showed that increases in the methane blending ratio widened the flammability limit of ammonia. Avila et al. [124] reported a stable operation on the micro gas turbine when fuelled by NH_3/CH_4 blends, which was possible until $X_{NH3} = 0.63$. However, increasing NH_3 blending decreased the combustion efficiency and, in turn, the thermal efficiency of CO_2 emission, while NOx N_2O emissions increased rapidly. Kurata et al. [125,126] examined the potential operation range, combustion and thermal efficiencies, exhaust gas analysis, and NO conversion ratio of the NH_3-air and NH_3/CH_4-air flame. They have also investigated various combustor configurations' effects on NOx, unburnt NH_3, and N_2O emissions.

Fairweather et al. [89] investigated the turbulent flame speed of spherically expanding turbulent CH_4-H_2 flames. They revealed that a minor addition of H_2 does not substantially alter the characteristics of pure methane flames. The 10 % H_2 blending ratio did not enhance the normalized turbulent burning velocity. At the same time, the increase can be noticed for 20 % H_2 blending at lean equivalence ratios, resulting in a doubling of S_T, but not for rich ones. Mandilas et al. [90] also examined the influence of H_2 on CH_4 on turbulent burning velocity and indicated that LBV was the principal factor in increasing the turbulent burning velocity.

Shy et al. [109] indicated that with the introduction of H_2 into the CH_4 fuel mixture, the effect of increased mixture reactivity predominates over the flame front broadening caused by rising turbulence intensity. The bending effect, described by Kobayashi et al. and Ichikawa et al. [127–129], refers to the flattening of the S_T/S_L curve, increasing the turbulence intensity [72].

In their study on the co-firing of ammonia with hydrogen, Dai et al. [130] examined the impact of the Lewis number (*Le*) on the morphology and propagation characteristics of a wide range of laminar and turbulent ammonia with hydrogen-air flames. Wang et al. [131,81] explained the inconsistency when considering the influences of the *Le* alone for self-similar propagation of H_2-NH_3/air flames. They suggested the necessity of characterizing it by both the Ka to show the effect of turbulent stretch and the *Le* or *Ma* to show the effect of the flame stretch. Regarding that, Cai et al. [132] explored the differential diffusion effect in high Karlovitz number NH_3/H_2/air flames, while Yang et al. [133] also studied a turbulent outwardly expanding spherical NH_3/H_2 flame employing Direct Numerical Simulation (DNS). Furthermore, Yu and Lipatnikov [134] discovered the differences between the optimum fits to DNS data on developed steady turbulent flame speeds. Chi et al. [135] investigated the influence of various molecular diffusions on S_T of ammonia/hydrogen-air flame mixtures, analyzing the interaction mechanisms between molecular diffusion and turbulence and emphasizing the importance of differential and molecular diffusion models.

Tang et al. [136,137] experimentally investigated the differential diffusion effects in the near field of non-premixed NH_3/H_2/N_2-air jet flames at elevated pressure, showing that strong differential diffusion effects in the near field up to 10 diameters downstream of the nozzle, which becomes negligible further downstream where turbulent mixing dominates. Furthermore, Wang et al. [138] also introduced two non-premixed NH_3/H_2/N_2-air turbulent jet flames that emulate the combustion of cracked ammonia at 5 bar and quantitatively measure NO, showing that increasing the NH_3 cracking ratio reduces the NO production. Valera-Medina et al. [139,140] discussed the potential use of rich (50/50 and 70/30) NH_3/H_2 blends as an alternative fuel for gas turbine combustion, focusing on the combustion characteristics, emissions, and potential for power generation. Katoch et al. [141] presented a novel dual-fuel, dual-swirl burner that can generate different levels of compositional inhomogeneities between NH_3/H_2 at the injection plane. The burner was characterized using non-reacting measurements, and the effects of these inhomogeneities on the flame morphology and acoustic signature were investigated.

Wang et al. [81] examined the influence of molecular diffusion on S_T of NH_3/H_2/CH_4/H_2O/air mixtures with subunity Le at higher pressure. Differential diffusion effects play a significant role in turbulent flame speed and morphology, especially at low *Le,* where flame acceleration occurs. Additionally, the water dilution generally improves flame speed

due to changes in chemical reactivity. It reduces the overall laminar flame speed due to increasing Ka and $Re_{T,flow}$, which leads to increased S_T/S_L. Zitouni et al. [142] concluded that adding NH_3 to CH_4 and H_2 utilizing Mie-scattering tomography, where the NH_3 blending ratio showed an enhancement of the wrinkling ratio due to low values of S_L and increased stretch effects. Wang et al. [81] analyzed the evolution of turbulent flame speed and NO emissions as a function of H_2/CH_4/air flames at elevated pressures.

Lhuillier et al. [143] investigated the impact of CH_4 or H_2 addition on the turbulent expanding premixed flame speed of NH_3/air mixtures. They found that increasing methane blending to lean ammonia /air flames led to a decrease in S_T/S_L and a decrease in CH_4 with an increase in H_2 enrichment due to the diversity of thermo-diffusive properties and stretch rate behaviour. This finding contrasts with the results of Ichikawa et al. [91] due to their contrasting influences on the Le and L_b.

Several scaling theories have been proposed to correlate S_T/S_L with turbulent characteristics like Lewis number (*Le*), Karlovitz number (*Ka*), Damköhler number (*Da*), or turbulent flame Reynolds number ($Re_{T,flame}$) with different fuels at different initial conditions, as shown in Table 2. These correlations can provide experimental support for developing turbulent combustion theory under lean premixed conditions. Additionally, the differential diffusion effects and the self-similar propagation should be considered to understand the propagation of these fuels. Furthermore, *Ka* is introduced to represent the effects of flame stretch rate induced by turbulence in the correlation of normalized turbulent burning velocity. These parameters were essential for understanding the role of the chemical term in turbulent combustion modeling equations. Bradley [93] identified that the burning velocity ratio is associated with the *Ka* and *Le*. Lipatnikov and Chomiak [144,145] provided a comprehensive review of empirical correlations for turbulent burning velocity. They noted that when the mass diffusivity of the deficient reactant surpasses the thermal diffusivity of the mixture or the mass diffusivity of the excess reactant, it enhances the chemical energy at the flame front.

However, extensive experiments observed that differential diffusion in the flamelets and TRZ regimes strongly influences ignition, propagation, and burning velocity. Different correlations were assumed to fit the experimental data of S_T, and the correlations for the S_T were also developed with the consideration of the differential diffusion effect in the flamelets and TRZ regimes. Dai et al. [131] investigated the H_2/n-heptane-air mixture. They correlated a new equation divided into two lines according to the value of Ka, regardless of the chamber size, H_2 blend, ϕ, P_i and u' for different fuels. This equation can be well correlated with different $NH_3/H_2/CH_4$ blends due to the combined effects of *Ka* and *Le*, which also show little deviation for high-pressure data due to instability and consistency with almost constant *Le*.

Table 2
Correlations of turbulent flame speed by different authors.

Authors [Ref.]	Equation	
Karpov et al. [92]	$S_T \sim u' Da^{1/4}$	(1)
Chaudhuri et al. [146]	$S_T/S_L \sim Re_{T,flame}^{0.5}$	(2)
	$S_T/u' \sim Da^{0.5}$	(3)
	$S_T/u' \sim (Re_{T,flame} Ma)^{0.5}$	(4)
Bradley et al. [93]	$S_T \sim u' (Ka \cdot Le)^{-0.3}$	(5)
Kobayashi et al. [147]	$S_T/S_L \sim [(u'/S_L)(p/p_0)]^{0.38}$	(6)
Nguyen et al. [119]	$S_{T,c=0.5}/S_L \sim [(u'/S_L)(p/p_0)]^a Le^{-b}$	(7)
	$S_T/S_L \sim (Re_{T,flame} Le^{-1})^{0.5}$	(8)
	$S_T/u' \sim (DaLe^{-1})^{0.5}$	(9)
Dai et al. [80]	$S_T/S_L \sim (l_l/l_0)^{0.5}[(u'/S_L)(p/p_0)]^{0.41}$	(10)
Shy et al. [148]	$(S_T - S_L)/u' \sim Da^{0.39-0.47}$	(11)
Venkateswaran et al. [149]	$S_D/S_{L,max} \leq 1 + u'_{LP}/S_{L,max}$	(12)
Kitagawa et al. [97]	$S_T/S_L \sim (Re_{T,flame} Le^{-2})^{0.54-0.6}$	(13)
Wang et al. [131]	$S_T/S_L \sim Da^{-0.4}(Re_{T,flame} Le^{-2})^{0.5}$	(14)
	$S_T/S_L Ka^{-1} \sim (Da/Le)^{0.86}$	(15)
Lhuillier et al. [143]	$S_T/S_L \sim Ka^{1.17} Da$	(16)
Dai et al. [150]	$S_{T,c=0.1}/S_L Ka^{0.2} \sim (u'/S_L) Le^{-1}$	(17)

Ka: Karlovitz number, $Ka = (u'/S_L)^{\frac{3}{2}}(l_l/\delta)^{\frac{-1}{2}}$.
Ma: Markstein number, $Ma = l_b/\delta$, L_b is the burn Markstein length (mm).
$Re_{T,\ flame}$: Turbulent flame Reynolds number, $Re_{T,flame} = (u'/S_L)(r/\delta)$.
Da: Damköhler number, $Da = (u'/S_L)^{-1}(l_l/\delta)$..
$Re_{T,\ flow}$: Turbulent Reynolds number, $Re_{T,flow} = (u'/S_L)(l_l/\delta)$.
$S_{T,c=0.5}$: Turbulent burning velocity relating to $.S_{T,c=0.5} = \left(\frac{\langle r\rangle_{c=0.1}}{\langle r\rangle_{c=0.5}}\right)^2 \times S_T = (1.4)^2 \times S_T A$

Flammability

In preceding research [151], a re-examination of the chemical behaviors inherent in gas mixtures devoid of carbon compounds was conducted. Specifically, the focus centred on the intricate interplay of hydrogen and ammonia within an oxidizing environment. The exploration encompassed a meticulous analysis of various permutations involving fuels, oxidizers, and operational parameters. Leveraging a meticulously formulated and rigorously validated kinetic model, the comprehensive reactivity profile was methodically determined, and the thresholds of flammability were delineated.

This meticulous methodological approach, fortified with a robust set of tools for gauging the reactivity of lighter elements across diverse conditions, offers innovative avenues for architecting resilient and dependable processes within the realm of chemical production. Furthermore, it furnishes practical and implementable technological solutions aimed at establishing secure and sustainable energy supply chains.

The adopted methodology stands as a comprehensive and interdisciplinary framework, meticulously validating intricate models to facilitate a thorough characterization of reactivity and safety considerations throughout the entirety of a process's lifecycle. Consequently, these findings bear the promise of significantly augmenting processes and methodologies deployed across varied industrial domains. This model served as the computational basis for determining ternary mixtures as showcased in Fig. 10 and Fig. 11, calculating the lower and upper flammability limits alongside the equivalence boundaries for each specified case. For most of these cases no experimental data exists.

The described approach led to the LFL and UFL, respectively equal to 3.75 %v/v and 21.51 %v/v for pure CH_4. Compared to experimental data available in the current literature [156,157] these estimations are slightly conservative. This could be attributable to the assumption of perfectly adiabatic conditions posed for the numerical analysis. If compared with the results for hydrogen, the LFL differs significantly from the known [158] literature values, whereas the UFL can be predicted with sufficient accuracy. For ammonia, the lower limit is found to be closer to the actual literature value [71], whereas the upper limit is significantly overpredicted. Furthermore, it can be seen that the LFL of all mixtures only varies by a maximum of ten percent, which is mainly due to the proportion of NH_3. Whereas UFL also clearly depends on the H_2 content in the mixtures as shown in our previous work [159].

Applying these findings to high-temperature systems requires consideration of several aspects. As indicated in Table 1 and reflected in Figs. 10 and 11, stability limits for ammonia decrease with an increasing proportion in all mixtures. The ignition range diminishes, potentially leading to complications during the ignition process. Moreover, significant recirculation's and exhaust gas recirculation's are anticipated to prompt earlier flame detachment at the burner's surface. Within the oven itself, this scenario could increase the possibility of unburned fuels in peripheral areas if complete mixing cannot be guaranteed. Currently, only a few burner systems are available on the market that can operate using ammonia-hydrogen mixtures. However, for cases involving very high ammonia admixtures and for pure ammonia combustion, such systems are still largely confined to pilot-scale plants and are being attempted to be transferred to initial installations through sporadic research projects [9,160–162].

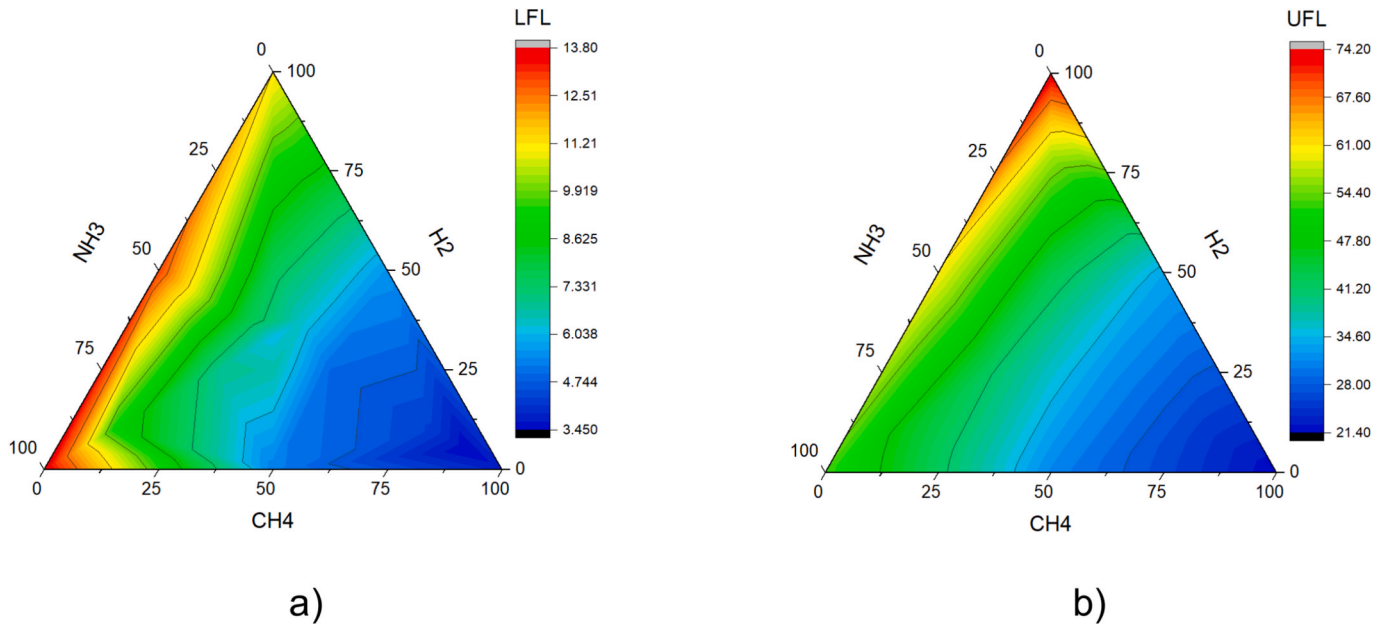

Fig. 10. Estimation of the flammability limits of CH_4:NH_3:H_2 mixtures for atmospheric conditions, a) lower flammability limit (LFL), b) upper flammability limit (UFL)

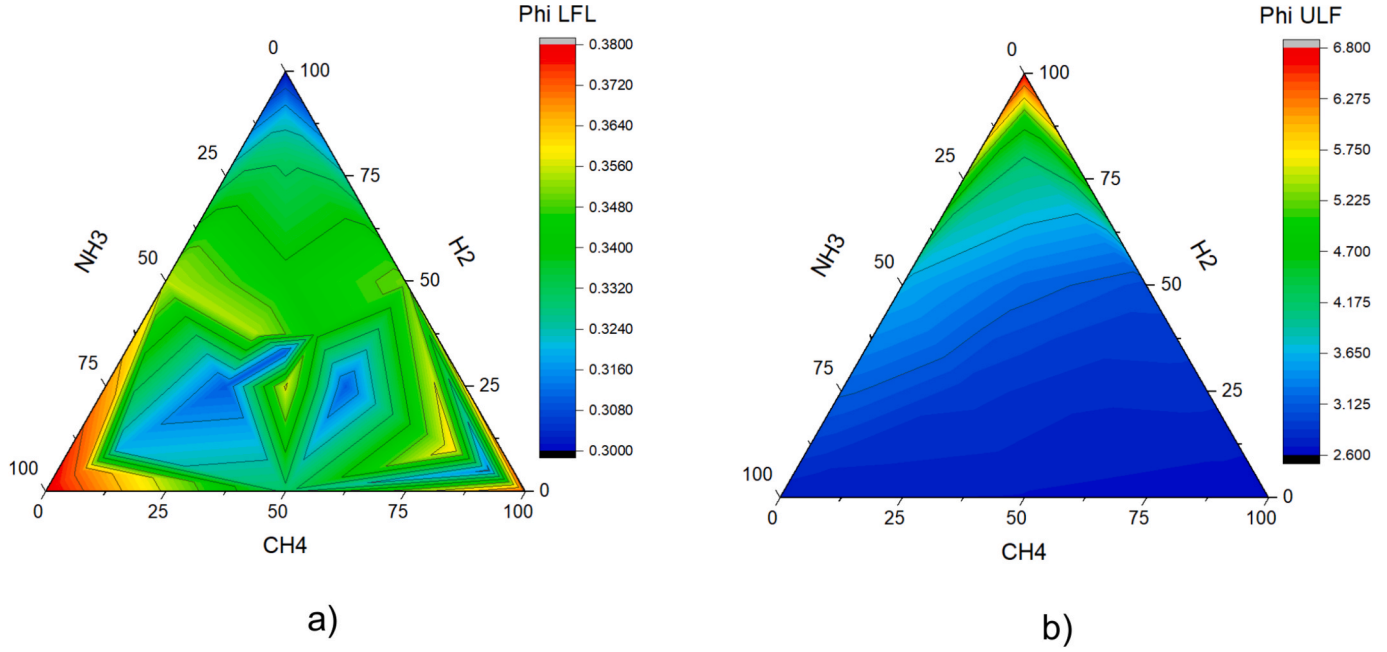

Fig. 11. Estimation of the flammability limits for the equivalence ratio of CH_4:NH_3:H_2 mixtures for atmospheric conditions, a) lower flammability limit (LFL), b) upper flammability limit (UFL)

Stability

Colson et al. [163] explored the stabilization mechanisms of an ammonia/methane non-premixed jet flame through local analysis. The addition of ammonia shifted the flame position towards the jet and downstream compared to a methane flame. This shift results from increased stoichiometric fraction and reduced mixture reactivity. Predicting the extremum point was found sufficient to anticipate flame position evolution. The transition from regimes I to II occurred at larger momentum ratio values with ammonia, indicating higher fuel jet velocities. Thermal interactions with the burner followed similar dynamics as previous work, but ammonia introduction drastically decreased burner temperature. As ammonia was introduced, the domain for flame stabilization gradually reduced due to lower reactivity and modified Z_{st} contours. This emphasizes the importance of considering laminar burning velocity variation and stoichiometric contours for predicting lift-off velocity. Alfazazi et al. [164] did stability investigations about the ammonia/hydrogen blends also in non-premixed flames in the context of pre-cracking. Measurements, performed at a fixed Reynolds Number (Re = 5500), utilized OH-PLIF and gas analyzers. Increasing NH_3 ratios led to shorter, broader flames with enhanced luminosity, while higher NH_3 concentrations caused flame extinction and re-ignition in the neck zone. Elevating H_2/N_2, at constant Re, induced a fuel-lean recirculation zone, shifting the reaction zone inward. While sustaining 100 % NH_3 was not achieved, similarities between F_{NH3_25} and pure H_2/

N_2 flames suggest potential for further optimization.

4. Diagnostic methods

In this chapter, measurement techniques that can be applied to ammonia flames are briefly summarized. Methods for flow measurement, control, and supply lines are well-established in chemical process engineering and could be adapted for use in thermal processing systems. For a comprehensive understanding of ammonia combustion, several quantities of interest have to be measured. These include local temperatures, species, flame speeds, flow fields, equivalence ratios, and heat release zones, to name just a few of them. Over the last decades, multiple diagnostic tools have been developed. and within the last years. have also been more frequently applied in the case of ammonia combustion. In the following, an overview of the recent developments will be provided. Most of these diagnostics are applied under controlled lab-scale conditions; however, indications towards more application-related cases will be highlighted.

In general, a distinction can be made between invasive and non-invasive methods. Invasive techniques are based on sampling and are often used to determine the combustion species involved. Here, Fourier-transform infrared spectroscopy (FTIR) [100], gas chromatography (GC) [165], or molecular beam mass spectrometry are among the most important techniques and provide detailed insights into the flame chemistry [166–168]. The sampling process can, however, strongly influence the combustion process, which is why care must be taken not to generate a sampling bias along the probe line.

Here, non-invasive techniques benefit from not disturbing the underlying process and additionally usually provide a much higher spatial and temporal resolution[169]. To measure species, typically spectroscopic techniques, either in the UV or the infrared, can be applied. The simplest form is emission spectroscopy, including capturing the spectrally resolved chemiluminescence signal of certain combustion intermediates [170]. Among them, NO is one of the most relevant species as it is directly related to NOx emissions, as one of the most important pollutants. NO has multiple characteristic emission peaks, which are strongest between 190 nm and 250 nm, as shown in the upcoming Fig. 18 and taken from [171]. With increasing wavelength in the flame spectrum, it is followed by OH with the strongest peak around 310 nm, but also visible transitions at lower wavelengths around 280 nm (the assignment of these peaks to NO in [171] is possibly erroneous). Additionally, species such as NH and NH_2 become prominent, which are typically of rather minor strength for conventional hydrocarbon fuels. The amber color of ammonia flame luminescence mainly stems from NH_2 and NO_2. The ratio of both signals additionally allows for a 2D determination of equivalence ratios [172]. In case of fuel mixtures with hydrocarbons, classical carbon species such as CH and C_2 become important but also rather minor species like CN may play an increasingly important role. Chemiluminescence-based methods were successfully applied in application conditions such as a spark-ignition engine [173]. In the infrared wavelength ranges, the combinations and overtones of rovibrational states of combustion products, such as water molecules, as the main combustion product, become dominant. However, these emission spectroscopic methods typically suffer from rather long acquisition times and typically result from a line-of-sight (LOS) detection setup. For faster measurements, absorption-based methods, either in the UV or the infrared, can be applied. The UV broadband absorption spectroscopy enables measurements of multiple species such as NO, OH, NH, and NH_3 [174]. The latter can also be measured in the infrared using a scanned laser absorption method [175,176]. The determination of temperatures using absorption bands of combustion products (such as water) is widely applied. In general, absorption-based methods are also imitated by their LOS nature, which can only be overcome by a coupling to tomography.

Among the most important optical diagnostics for ammonia combustion is laser-induced fluorescence (LIF) or planar laser-induced fluorescence (PLIF) [177,178], which enables the detection of species such as NO, OH, NH, and NH_3. The molecules are excited from their ground state, typically with a UV pulse, and the subsequent fluorescence signal is captured by a wavelength-filtered detector. With the targeted species, a transition from the reactants over intermediates to the post-reaction zone can be drawn, providing full process traceability and additional insights into flame structure or turbulence scales [105]. With the use of dedicated excitation strategies also LIF measurements of NH_2 become feasible [179]. Additionally, flame temperatures can be obtained typically using multiline NO LIF or OH LIF setups [180].

Raman spectroscopy is another in-situ tool that provides information about major species and temperature [181]. It can be applied for the detection of NO [182]. Most recently, it could also be shown to measure N_2O using Raman spectroscopy [183]. Quantification of this species is considered particularly relevant as it is a potent greenhouse gas and it is needed to further improve existing kinetic models. The major challenge related to Raman spectroscopy is its weak signal intensity compared to interfering signals such as fluorescence or flame luminescence. This can be overcome by applying rotational coherent Anti-Stokes Raman spectroscopy (RCARS), which provides species information on O_2 and N_2 and accurate temperatures [184].

Less frequently applied, yet showcased for ammonia combustion cases are techniques such as Laser Doppler Anemometry (LDA) for turbulence fields [79], Planar laser-induced photofragmentation fluorescence for ammonia slip [185], or Schlieren imaging for flame structure [186].

Although many of these methods have been used in laboratory and pilot plant scales, valuable insights can be gained for the direct development of burner systems. Some of these techniques should also be applicable in initial large-scale tests and could help identify potential emission sources and flame positions more accurately, thereby further improving the integration into thermal processing systems.

5. Chemical kinetic modeling

A chemical kinetic model is required to predict the combustion behaviour of any fuel. In combustion computational studies, they are also utilized not only to predict the global parameters like laminar flame speed and ignition delay time, but also to predict the emission behaviour of different fuels. A chemical kinetic model can provide valuable information that experiments cannot reach. For example, during the combustion of hydrocarbon fuels many intermediate species (e.g., OH, H, and O) are formed which are very hard to characterize experimentally, however, the kinetic model can provide the knowledge in this regard. It should also be noted that, robust and reliable chemical kinetic models are invaluable as they can be used in computational fluid dynamics (CFD) for designing engines, turbines, and furnaces. However, the reliability of the kinetic model is a major factor when choosing the mechanism for a CFD study. Kinetic models are generally built targeting certain combustion characteristics and operating regions as per one's desire. The comprehensive kinetic model is much more challenging to build as it needs to consider a wide array of experimental conditions and requires knowledge of fuel chemistry at a fundamental level. Regarding the ammonia combustion mechanism, yet not a single comprehensive kinetic model is reported in the literature, most of the reported mechanism is targeted for certain conditions only.

Studies on ammonia started as early as the 1960s [187,188] to understand the kinetics of flames containing ammonia. Later, several researchers conducted the experimental study over a wide range of compositions and conditions to gain more insight into the kinetics of ammonia-fuelled flames [189–191]. Miller and Bowman [192] proposed the first detailed reaction mechanism for ammonia oxidation based on ammonia combustion experiments from the literature. They compared their model predictions against the experimental data and showed a good performance of their model for ammonia combustion over a range of pressures, temperatures, and equivalence ratios. Over the years,

Miller's mechanism [192] has been correlated to a wide range of conditions in several ammonia and NO*x* studies [193–195]. In 2015, Mathieu et al. [196] were the first to conduct the shock tube experimental and modelling study of $NH_3/O_2/Ar$ mixture. The study of Mathieu et al. ranged over temperatures, 1560– 2455 K, pressures, 1.4, 11, and 30 atm and equivalence ratios, 0.5, 1.0, and 2.0 for mixtures of ammonia highly diluted in Ar (98–99 %). They compared their measurements against several models from the literature. They found that most of the models could not predict the ignition delay times with accuracy, and also found a wide discrepancy between the models. As ammonia started to get more attention as a future energy carrier, more models from different research groups followed. In 2018, Glarborg et al. [197] proposed a nitrogen chemistry for combustion modeling, which included NH3 as a fuel. In the same year, Shrestha et al. [198] also proposed a detailed reaction mechanism for ammonia and ammonia/hydrogen. The model was validated against a wide range of experimental conditions, which included laminar flame speed, ignition delay time, and speciation in a jet-stirred and flow reactor. Many kinetic models on NH_3 and NH3/H2 have been proposed afterward.

In 2005, Henshaw et al. [199] conducted an experimental study on NH_3-doped (1–4 %) methane premixed flame to measure the laminar burning velocity and NO emission. They found that the laminar burning velocity was decreased, and the NO formation was increased as the NH_3 concentration increased. In their study, they utilized the GRI (2000) mechanism to simulate their measurements. Regarding the NH_3/CH_4 mechanism, Tian et. al. [200] were the first to propose the NH_3/CH_4 kinetic model for NH_3/CH_4 combustion utilizing their experimental data obtained from $NH_3/CH_4/O_2/Ar$ burner stabilized premixed flame under low-pressure conditions. They measured the combustion intermediates and products in 11 premixed flames of different NH_3/CH_4 blends. The ammonia sub-set in their mechanism was adopted from the work of Skreiberg et al. [201]. The performance of this mechanism [200] was assessed by Hayakawa et al. [69] along with the mechanisms from Konnov [202], Lindstedt et al. [203], and Miller and Bowman [192] for ammonia/air laminar flame speed experimental data. None of these mechanisms could satisfactorily predict the laminar flame speed of ammonia/air blends. Same year, Mendiara and Glarborg [204] conducted an experimental study in a laminar flow reactor and developed a chemical kinetics model for NH3 oxidation for oxy-fuel combustion of CH_4/NH_3 with temperatures ranging from 973 to 1773 K under atmospheric pressure conditions. The kinetic mechanism employed was based on the Tian et. al. [200] and Skreiberg et al. [201] work. Likewise, the first auto-ignition timing investigation of NH3/CH4 blend was conducted by Dai et al. [205] utilizing the rapid compression machine. They also developed the mechanism to predict their experimental data. Their result showed that at $\phi = 0.5$, the ignition delay time of NH_3 was decreased by a factor of 5, while further increasing to 50 % only decreased by a factor of 6. This shows that as the CH_4 content in the fuel blend increases the sensitivity towards ignition delay time also decreases. Similar observations on NH_3 ignition delay time with other fuel blends where observed [206,207]. Currently several, models are proposed for NH_3/CH_4 on based on different experimental conditions.

It is well known to the combustion community that ammonia has low reactivity, which hinders its effective use in combustion devices such as engines and turbines. To overcome this limitation, several researchers have proposed to blend NH_3 with high reactive fuels such as H_2 [208–210], CH_4 [205,211], CH_3OH [212], C_2H_5OH, DME [207], and DEE [213]. To be in line with this study, we will limit our discussion to NH3, H2, and CH4 only. Hydrogen is considered to be one of the most reactive fuels; it has usually been used to promote the reactivity of hydrocarbon [65] and oxygenated hydrocarbon fuels [214,215]. As discussed above, currently, H_2 is also used to promote the reactivity of NH_3. Therefore, H_2 in this case is a reactivity promoter for NH_3 and CH_4; in contrast, CH_4 and H_2 both are reactivity enhancers for NH_3.

However, before we dive into the binary and tertiary blends of NH_3, H_2 and CH_4 it is worth looking at the NH_3 laminar flame speed. Laminar flame speed is one of the main combustion characteristics of the fuel. It is generally measured experimentally using various types of lab-scale combustion devices, commonly used are the heat flux burner, constant volume spherical combustion chamber, constant volume cylindrical combustion chamber, and Bunsen burner. From 2015 onwards large number of laminar flame speeds were reported in literature at different conditions. However, the majority of reported data are at standard pressure and temperature conditions. Experimental data at practical conditions are still limited. Recently, Chen et al. [216] measured the laminar flame speed of NH3/air and in N_2 diluted environment. They utilized the Bunsen approach based on flame cone angle to measure the laminar flame speed. To the authors knowledge, these are the first reported measurements in such a high preheating temperature; earlier measurements for NH3/air were up to 500 K [217]. The authors also measured the laminar flame speed at 298 K. Furthermore, the authors compared several recently published kinetic models against their experimental data. The authors found that most of the kinetic models were able to predict the laminar flame speed at standard pressure and temperature conditions. However, at elevated temperature conditions discrepancies between the models and the experimental data were more significant, as shown in Fig. 12. This clearly illustrates that more study is needed to develop a comprehensive kinetic model that can cover a wide range of conditions.

Now, we compare the laminar flame speed between different fuel blends. As observed in Fig. 7 at $\phi = 1.0$, 1 bar and 298 K, the laminar flame speed of H_2 (~230 cm/s) is highest, which is about a factor of ~ 31 and 6 compared to NH_3 and CH_4. However. CH_4 flame speed is only a factor of ~ 5 higher compared to NH_3. From this simple comparison one could aspect that H_2 will have more impact in promoting the reactivity of NH_3 compared to CH_4. To get more better insight into the binary and tertiary blend of these mixtures, we conducted the laminar flame speed simulation. The simulations were performed using the recent kinetic model developed by Shrestha et al. [218]. The results are shown in Fig. 13 for neat NH_3 and NH_3 95 % (a) and NH_3 90 % (b). It can be observed as expected the influence of H_2 is higher compared to CH_4 when comparing the binary mixture, for the tertiary mixture the impact is in between. For instance, the impact of mixing 5 % of H_2 and CH_4 only increased the flame speed by a factor of ~ 1.1 and ~ 1.15, and in the tertiary mixture flame speed was increased by a factor of ~ 1.12. For NH_3 90 % (Fig. 13a) modest increase is observed compared to NH_3 95 % (Fig. 13b). However, the interesting observation is that for NH_3/CH_4 blend the impact on the rich side ($\phi > 1.4$) was not seen to be significant compared to the lean side. In the case of NH_3/H_2, the laminar flame speed was elevated for all the equivalence ratios. For the NH_3/H_2 and $NH_3/CH_4/H_2$ blend, the flame speed at lean conditions was almost the same. Only observing the laminar flame speed in the tertiary blend, the chemistry is more controlled by the H_2 chemistry. However, one can observe the difference in laminar flame speed behaviour with NH_3/H_2 and NH_3/CH_4 binary fuel blends.

Unlike the laminar flame speed of NH_3/H_2 and NH_3/CH_4 blend, the reported ignition delay time for these blends is far less. To the authors knowledge, no ignition delay time of the tertiary blend of $NH_3/H_2/CH_4$ has been reported yet. As mentioned above, Mathieu et al. [196] reported the first NH3 ignition delay time measured in a shock tube. It was only in 2019 when the first RCM experiment on ignition delay time of NH_3 and NH_3/H_2 mixture was reported at intermediate temperature and high pressure by He et al. [219]. They conducted the study at 20, 40, and 60 bar, $\phi = 0.5 - 2.0$, and a temperature range, 950 to 1150 K. Their study showed that a higher H_2 mole fraction in the fuel mixture increases system reactivity. Furthermore, they observed that when the NH_3/H_2 fuel blend contains 20 % H_2, the fuel-rich mixtures exhibited the shortest ignition delay times, while for a blend having 1 % H_2, the equivalence ratio dependence was reversed. The mixture containing 5 % H_2 in fuel blend for $\phi = 1.0$ had the shortest ignition delay time. However, for neat NH_3, the leaner mixtures showed higher reactivity. Likewise, in the same year Pochet et al. [220] also performed the ignition delay time of NH_3

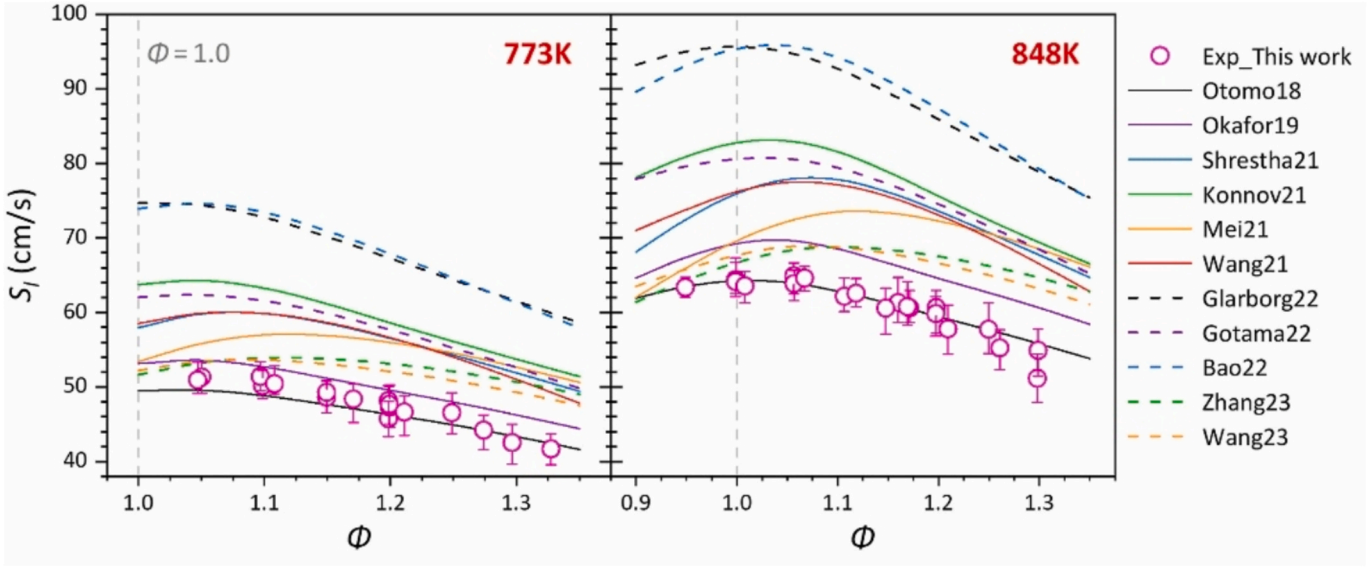

Fig. 12. Laminar flame speed of NH_3/air as a function of equivalence ratio at atmospheric pressure and inlet temperature of 773 K (left) and 848 K (right). Symbols are the experiment from Chen et al. [216], and lines are the model predictions. This figure is adopted from the work of Chen et al. [216]. For model reference, please see the reference cited therein.

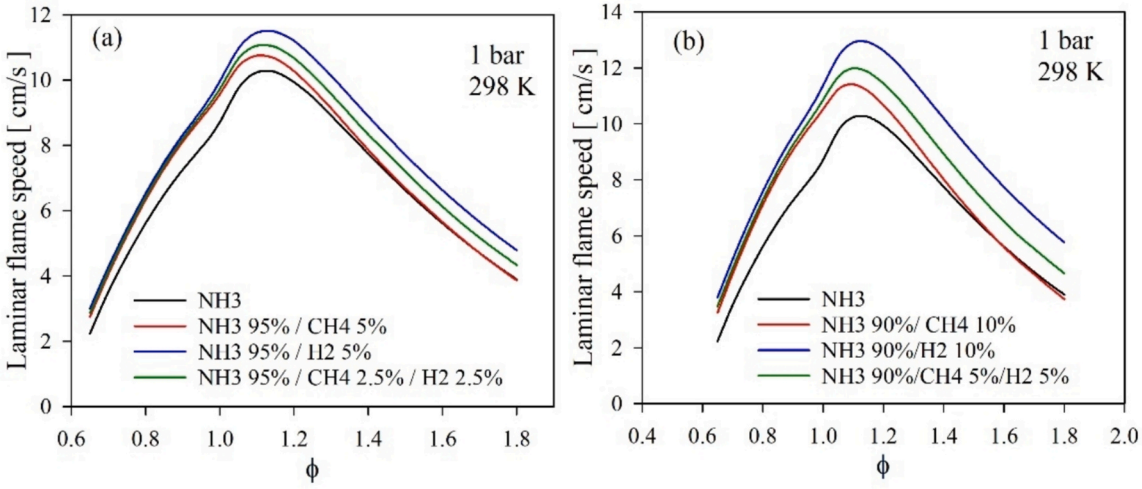

Fig. 13. Model-predicted laminar flame speed of NH3 and its blend with CH4 and H2. The percentage means the mole fraction of each component.

and NH_3/H_2 utilizing the rapid compression machine. Their study was focused on the lean conditions (ϕ = 0.2, 0.35, and 0.5). Based on their study [220], they suggested that, to have a reasonable promotion effect on NH_3, the H_2 fraction in fuel needs to be higher than 10 % (by volume). Both of study, He et al. [219] and Pochet et al. [220] utilized the available literature mechanism to perform the simulation. The former used 10 (see Fig. 14) while the later used 5 different mechanisms. Their study showed a significant discrepancy in the model predictions with each other, also none of the mechanisms were able to capture their measurements satisfactorily. Their study suggested more work is needed to improve the kinetic models. In subsequent years, many mechanisms were proposed, however, these mechanisms were able to predict the experimental data at standard conditions particularly laminar flame speed but still could not predict the low-temperature ignition delay time from RCM experiments. This again calls for the development of a robust and reliable kinetic model.

For the analysis purpose, we have conducted the simulation for NH_3, NH_3/H_2, NH_3/CH_4, and $NH_2/H_2/CH_4$ utilizing the Shrestha et al. [218] model, and the results are shown in Fig. 15. The simulation is conducted for ϕ = 1.0 and 20 bar, in a temperature range, 800 – 1500 K. In the binary and tertiary mixture, the NH_3 content in the fuel blend is maintained at 95 % (by mole). It can be observed in Fig. 15 that 5 % of H_2 and CH_4 can significantly decrease the ignition delay time of NH_3. As seen in Fig. 13, also the H_2 has a higher influence when compared between the binary blends only. For instance, at 1000 K, the ignition delay time of NH_3 was shortened by a factor of ~ 4.5 with H_2 while it was shorted by a factor of ~ 2.5 with CH_4. However, at a higher temperature of 1200 K, the H_2 and CH_4 shortened the ignition delay time by ~ 3.3 and 1.8, respectively. This suggests that at higher temperatures, the influence of H_2 and CH_4 is less compared to low temperatures. This is evident in Fig. 15. However, for the tertiary blend, the results are somewhat different, it can be observed that at low temperatures, the ignition delay time is closer to that with H_2, while at high temperatures it is closer to the fuel blend with CH_4. It should be noted that, unlike in binary blend, the fuel chemistry at the tertiary blend becomes more complex. As mentioned above, in a tertiary blend, H_2 is the promoter for both NH_3 and CH_4. Therefore, both fuel NH_3 and CH_4 will compete with the radical pools (e.g., OH, H, and O). However, with CH_4 in the system,

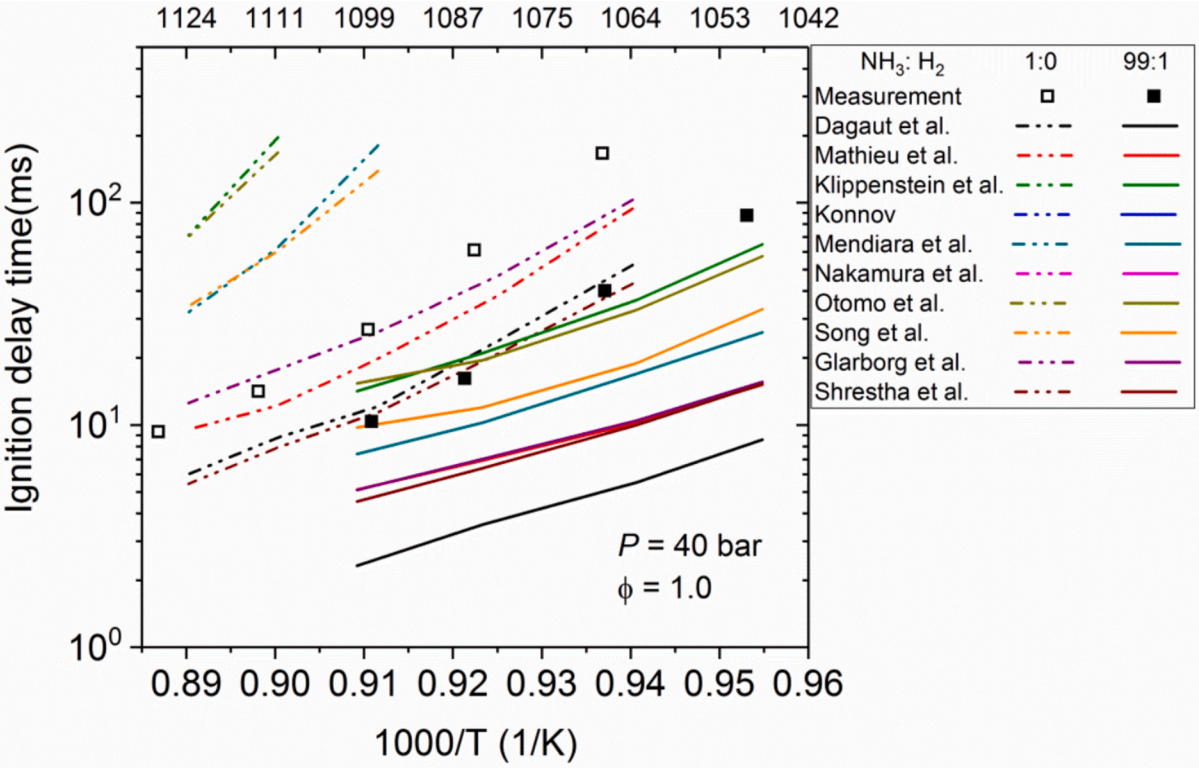

Fig. 14. Ignition delay time comparison between the experimental data (symbols) and model predictions (lines) for $\phi = 1.0$, NH_3 and NH_3/H_2 mixtures at 40 bar. Figure is adopted from He et al. [219], for model reference see references cited therein.

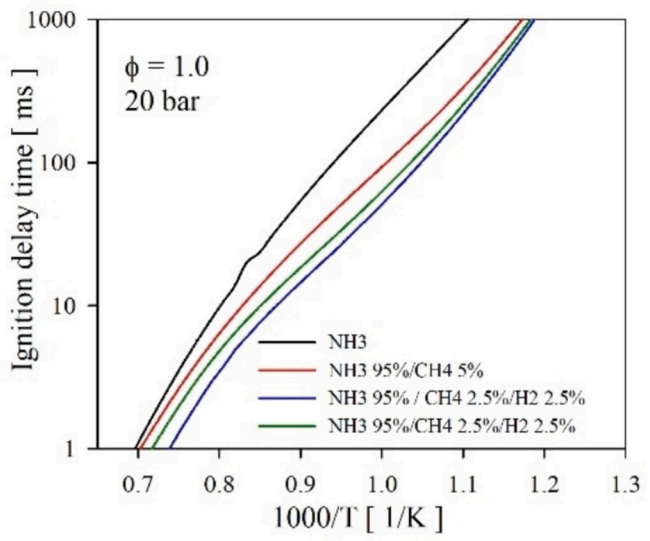

Fig. 15. Model-predicted ignition delay time of NH_3 and its blend with CH_4 and H_2 at $\phi = 1.0$ and 20 bar. The percentage means the mole fraction of each component.

there is also the interaction between the nitrogen and carbon chemistry. This was demonstrated by He et al. [212], who conducted the NH_3/CH_4 blend jet-stirred reactor study and measured the methylamine formation (CH_3NH_2). Their model suggests that the CH_3NH_2 is formed via the recombination reaction of CH_3 and NH_2 ($CH_3 + NH_2(+M) = CH_3NH_2$), which is consistent with the findings of Shrestha et al. [213]. We note here that, for any fuels, the H_2 mechanism is the core mechanism. The addition of interaction chemistry from carbon family makes it more complex. This is where the current kinetic models are currently struggling.

The main reason for the discrepancies observed between the kinetic model predictions (as seen in Fig. 12 and Fig. 14) is mainly due to the higher uncertainty in the rate constant of elementary reactions used in the models. Unlike in hydrocarbons, the elementary reactions within nitrogen chemistry are less explored. However, due to interest in ammonia researchers have recently started to explore some of the critical reactions in the NH_3 mechanism experimentally and theoretically. For instance, Marshall et al. [221] recently examined various reactions within the N_2H_2 system using CBS-APNO//M06-2X/ 6–311++G (2df,2p) level of theory. Their study differentiated between the *trans*- and *cis*- isomers of N_2H_2. Many of the kinetic model available in the literature only considers *trans* N_2H_2. N_2H_2 is an important intermediate during neat NH_3 combustion. The role of N_2H_2 is more dominant in rich conditions compared to lean conditions (see Shrestha et al. [208]). Therefore, proper consideration of their kinetics is important. Likewise, Klippenstein and Glarborg [222] recently explored the $NH_2 + HO_2$ reaction in its potential energy surface using a coupled cluster method with large basis sets. They suggested, three channels for $NH_2 + HO_2$ which are $NH_2 + HO_2 \rightarrow NH_3 + O_2$ (chain terminating), $NH_2 + HO_2 \rightarrow H_2NO + OH$ (chain branching) and $NH_2 + HO_2 \rightarrow HNO + H_2O$ (chain propagating). The authors employed the master equation to predict the pressure and temperature dependence of the $NH_2 + HO_2$ reaction. They found that reaction, $NH_2 + HO_2 \rightleftharpoons NH_3 + O_2$ is the dominant channel, with branching ratios of ~ 80 % at 500 K and ~ 72 % at 1500 K. Their values of the rate constants for $NH_2 + HO_2$ differed significantly from those used in the previous kinetic modeling studies. This reaction is very important at low temperatures conditions [223,224], which has a huge impact on the kinetic model.

Due to the global efforts in detailed reaction kinetics, significant progress has been made in recent years in improving the prediction of global combustion parameters. In particular, the prediction of emissions in large-scale plants plays a crucial role. The introduction of fuel nitrogen through ammonia presents major challenges for the simulation of

large-scale facilities. Therefore, a comprehensive, reliable and robust kinetic model is needed if ammonia is to be considered as the future energy carrier.

6. Emissions

One of the primary challenges hindering the widespread use of ammonia as a fuel is its tendency to produce fuel-derived nitrogen oxides (NOx). The formation of fuel NOx occurs when nitrogen chemically combines with the fuel, as is the case with ammonia (NH_3), giving rise to intermediate products like CN, HCN, HNO, NHi, and subsequent oxidation. Additionally, substantial amounts of thermal NOx can be generated under conditions of sufficiently high flame temperatures [225]. These nitrogen oxide emissions pose significant risks to both human health and the environment. They can impact the distribution of drinking water, contribute to eutrophication, and exacerbate respiratory illnesses if inhaled [226]. Nitrous oxide (N_2O), another potential by-product of ammonia combustion under specific operational conditions, exhibits a global warming potential 280 times that of CO_2 over a 20-year period [227]. Recent studies focusing on ammonia/hydrogen blends have reported that emissions of 240 ppm of N_2O have an approximately equivalent global warming impact to CO_2 emitted from a pure methane flame operating under dry low NOx scenarios. [228] It is therefore important to understand the kinetic mechanism of NO_x and N_2O formation and destruction pathways. Analysis of the detailed chemical pathways will help to understand the controlling mechanisms of these species. NO_x formation investigation in NH_3 fuelled combustion is not new, over the years, there have been many studies. As this review paper focuses on the industrial combustion system, we will mainly discuss high-temperature chemistry, which is the case of flames. In 1986, Bian et al. [229] investigated the ammonia-oxygen flame utilizing the Spalding-Botha burner. They measured the species profile of NH_3, O_2, H_2O, N_2, NO, and N_2O. In addition, they also measured some important radical species, H, OH, O, NH, and NH_2. They concluded that ammonia is predominantly consumed by OH radicals and by H-atoms to give NH_2 radicals. The NH_2 free radicals are consumed, by reacting with H and O H radicals, leading to the formation of NH radicals. The NH radicals produce the N_2 via the path forming nitric oxide. The NH radicals react with molecular oxygen to form nitric oxide.

In 1983, Chou et al. [230,231] investigated the rich $NH_3/O_2/N_2$ flame (ϕ = 1.28, 1.50 and 1.81) in a flat flame burner at atmospheric pressure conditions. Laser-induced fluorescence techniques (LIF) were used to measure relative concentration profiles of NO. Laser absorption measurements were made to derive an absolute concentration of NO in a lean $NH_3/O_2/N_2$ flame. It was found that in rich $NH_3/O_2/N_2$, flames NO concentrations decay more rapidly throughout the burnt gases than one would expect from the conventional mechanism of ammonia oxidation. They stated that reactions such as $NH_2 + NH_2$, and $NH + NH_2$, which ultimately yield N_2 are important in investigating rich flames.

Likewise, Bian et al. [232] and Vandooren [233] investigated the NH_3-doped H_2/O_2/Ar flames. Bian et al. studied lean and stoichiometric flames and highlighted that reactions $NH_2 + O = NO + H_2$ and $NH + O_2 = NO + OH$ are the main reactions for NO formation. Furthermore, they also stated $NH + NO = N_2O + H$ is the primary reaction for N_2O formation. In contrast, Vandooren studied rich flame and compared several reaction mechanisms with their experimental data. They concluded that the choice of the H_2/O_2 mechanism does not significantly influence the maximum concentration and the shapes of profiles of the major nitrogen-related species (NH_3, N_2, NO, N_2O). However, the concentration close to the burner is much more dependent. In 1994, Vandooren et al. [234] investigated the ammonia-nitric oxide flame. The study mainly highlighted the NO consumption reactions through the DeNOx process and evaluated the total rate constant and branching ratio of $NH_2 + NO = N_2 + H + OH$ / $NNH + OH$. One particular thing to notice in their study is that both reactions are chain propagating, while the current studies suggest that $NH_2 + NO$ has one path chain propagating, while the other channel is chain terminating [198,208,235]. Venizelos and co-workers [236–238] have made a similar contribution on NH_3 doped H_2 flames.

It was around 2010 when ammonia started being considered as a fuel for combustion applications. Duynslaegher et al. [168,239,240] studied the low-pressure NH_3 and NH_3/H_2 flames both experimentally and through modelling in their multiple study. In one of their study, they investigated the NH_3/H_2 flames where H_2 varied from 5 to 13 % in the fuel blend. Their results showed that as the H_2 concentration increased, the NH_3 consumption expedited. This is expected as the introduction of H_2 increases the key radical pools (OH, H, and O). This was also seen in other species as expected, were the early formation of NH_2, NO and N_2O was observed. For instance, NH_2 peak concentration did not change significantly however, the flame for 10 and 13 % H_2 shifted closer to the burner surface. Likewise, the maximum concentration of NO in the post flame was observed for 7 % H_2 fuel blend but not for 13 % However, the N_2O concentration in the flame increased as the H_2 concentration increased. As discussed above, NO and N_2O are both harmful, so finding the optimum fuel blend of NH_3/H_2 is crucial for minimum emissions. Their results indicate that the H_2 7 % or 10 % in fuel blend would be optimum. They also used the five different kinetic model available during that time to compare against their experimental data. Significant discrepancies between the model predictions were observed and none of the models could accurately capture the experimental data. This highlighted the requirement for improvement and update in the ammonia reaction mechanism. They highlighted that $H + NO_2 = NO + OH$ and $HNO + H = NO + H_2$ were the main reactions for NO monoxide formation. For N_2O, $NH + NO = N_2O + H$ and $N_2O + H = N_2 + OH$ were the main reaction for its formation and consumption. In 2016, Brackmann et al. [184] studied the structure of NH3/air flame (lean, stoichiometric, and rich conditions) utilizing the water-cooled stainless steel porous-plug burner. They obtained the OH, NH, and NO profiles by laser-induced fluorescence (LIF). To our knowledge, this was the first major study of a pure ammonia/air flame. They compared their experimental data against the four different reaction mechanisms available in the literature. It was observed that none of the models were able to predict the species profile accurately. The NO was under-predicted and over-predicted for lean and stoichiometric flames respectively, while for rich flames shift in flame position was observed along with the over-prediction. However, the peak concentration of OH was well captured by the models, though some discrepancies were seen in post-flame region. Likewise, for NH similar observation was observed as with NO. They identified different key reactions for their investigated flame species and optimized them in all of the used models. They were able to reduce the discrepancies between the models, however not successful in capturing all the measured species. This again highlighted the need for a closer look at the NH_3 reaction mechanism. We note here that by the time of Brackmann et al. study H_2 reaction mechanism was well established in the literature. Likewise, Osipova et al. [166] investigated the NH_3/O2/Ar and $NH_3/H_2/O_2$/Ar flame structure at atmospheric conditions using a molecular-beam mass spectrometric setup with soft electron-impact ionization. They measured stable species were NH_3, H_2, H_2O, N_2, and O_2, while intermediate species included NO and N_2O. They also used the four different kinetic models to compare against the experimental data. It was observed that in stoichiometric ammonia flame-stable species were well captured by models except H_2. The discrepancies were observed for NO and N_2O. Based on their study they suggested that H_2 in pure ammonia flame is mainly formed via $NH_2 \rightarrow NH \rightarrow N_2H_2 \rightarrow H_2$ pathway. The direct formation of H_2 is from $NH_2 + NH_2 = N_2H_2 + H_2$ while another pathway for H_2 formation is $NH_2 \rightarrow NH \rightarrow HNO \rightarrow H2$. It is interesting to observe the NO profiles in $NH_3/H_2/O_2$/Ar flame shown in Fig. 16 in lean and stoichiometric flame NO concentration rises along the height of the burner. After reaching the maximum it stabilzes is same level, while this is not the case with rich flame (Fig. 16 (c)). In rich flame, NO concentration rises and peaks to a maximum. After the maximum concentration is reached it again starts to

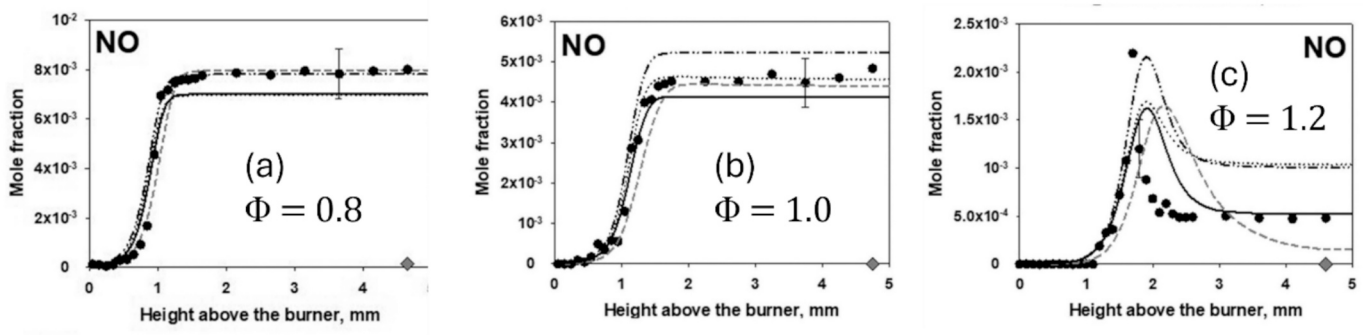

Fig. 16. NO mole fraction profile in $NH_3/H_2/O_2$/Ar flame at three different equivalence ratio. Figure adopted from Osipova et al. [166]. Symbols: experimental data [166], lines: kinetic model predictions. See [166] for sources of kinetic models.

decrease. This hints that the lean and stochiometric flame may be governed by same kinetics, while this may not be the case for rich flame. It is also worthy to note that as the equivalence ratio increases the NO concentration decreases.

In the subsequent year, Osipova et al. [167] again studied the NH_3/H_2 flame structure, however this time it was under elevated pressure conditions. This time they used eight different models from the literature to compare against the experimental data. The observation was similar to previous studies, they found that most of the models well predicted the stable species while discrepancies between models as well as with experimental data were observed for NO, NO_2 and N_2O. None of the tested models were able to predict these three species very well at the same time (see Fig. 17). It is interesting to observe in Fig. 17 that NO and N_2O both decrease as the equivalence ratio increases, while NO_2 concentration does not change significantly. It is also worth noting that the concentration of NO_2 is one order of magnitude less than NO and N_2O. Furthermore, it is interesting to observe in Fig. 18 that with an increase in pressure, the NO concentration decreases in all flames (lean, stoichiometric, and rich conditions). From these results, it can be identified that for NH_3/H_2 combustion, to control NOx and N_2O slightly rich flames would be appropriate. However, in very rich flames, NH_3 slip could occur as discussed above. Therefore, identifying the optimum conditions is crucial to utilize ammonia as a fuel in modern combustion devices.

For the methane/ammonia flame, Henshaw et al. [199] investigated the flame structure where NH_3 was used as a doping agent in atmospheric pressure conditions and a temperature of 363 K·NH_3 concentration was varied from 1 to 5 % in the fuel blend. It was found that as

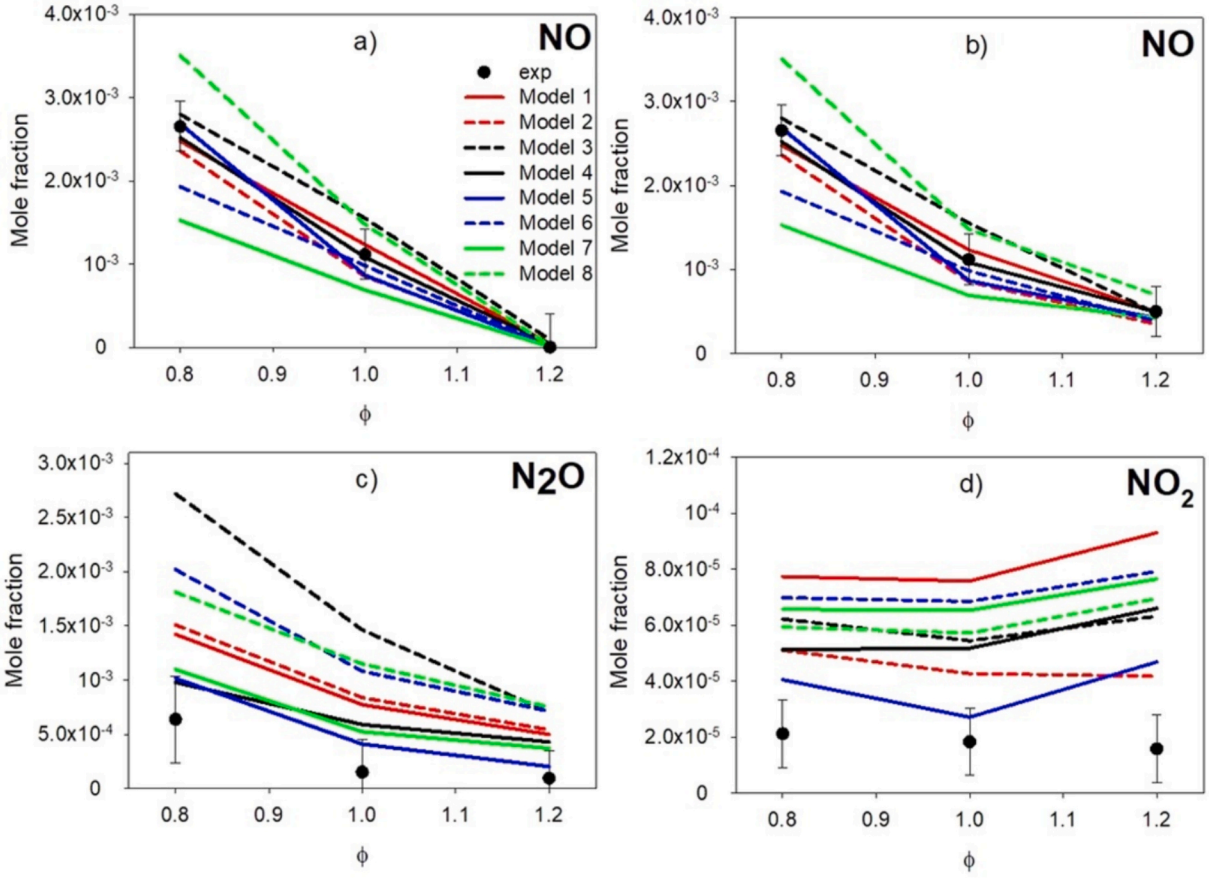

Fig. 17. Experimental and numerical values of NO concentration in post flame zone (a) and peak concentrations of NO (b), N_2O (c) and NO_2 (d) in $NH_3/H_2/O_2$/Ar flames vs φ at 6 atm. Figure adopted from Osipova et al. [167]. Symbols: experimental data, lines: model predictions.

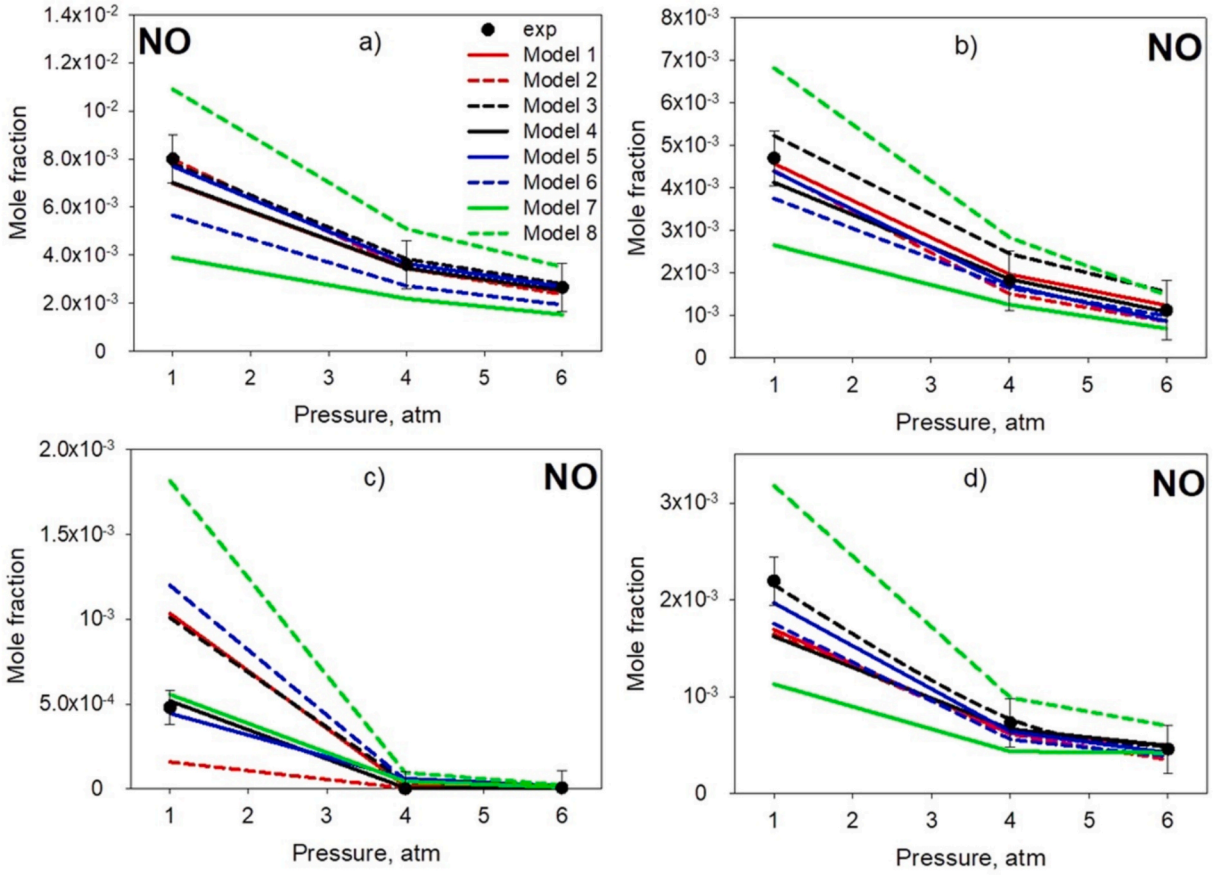

Fig. 18. Experimental and numerical values of NO concentration in post flame zone in lean (a), stoichiometric (b) and rich (c) $NH_3/H_2/O_2$/Ar flames, and NO peak concentration in rich (d) $NH_3/H_2/O_2$/Ar flame vs pressure. Figure adopted from Osipova et al. [167]. Symbols: experimental data, lines: model predictions.

the NH_3 concentration increases, the NO concentration in the flame increases. Further, increasing the NH_3 concentration decreased the adiabatic flame temperature, which in turn reduced the laminar flame speed. From this, it is clear that the NO forming in flame is steaming from fuel-bound nitrogen while thermal NO_x is associated with high temperature. The major study of NH_3/CH_4 flame structure was carried out by Tian et al. [200]. They investigated 11 premixed $NH_3/CH_4/O_2$/Ar flames at low pressure (4.0 kPa) and an equivalence ratio of 1.0 through experiment and modelling. The NH_3 concentration was varied from 0 to 100 % in the fuel blend. To model the flame, they compiled an NH_3/CH_4 reaction mechanism available from the literature. The compiled model well predicted the majority of stable species, however, H_2 was significantly underpredicted. The H_2O was also underpredicted in all the investigated flames. This clearly identified the room for improvement for the NH_3/CH_4 combustion mechanism. Their kinetic investigation suggested that the reactions, $H + O_2 = O + OH$, $NH_2 + O = HNO + H$, $NH_2 + NO = N_2 + H_2O$ and $NH + NO = N_2O + H$ play significant roles in NO and N_2 conversion. Later, NH_3-doped methane flame were investigated by other authors [241–243] where ammonia was not a measure fuel but used to understand the interaction kinetics between nitrogen and carbon family. Lamoureux et al. [243] found that in NH_3-doped flames, the NO concentration was twice as high as in a doped flame. In NH_3-doped flame, they also measured the HCN species, indicating the interaction between nitrogen and the carbon family. Rocha et al. [244] investigated the flame structure of a NH_3/CH_4/air flame. Laser-induced fluorescence techniques were utilized to study the premixed flame structures stabilized on a Bunsen burner. The NH_3 concentration was varied from 20 to 80 % in the fuel blend, with equivalence ratios ranging from 0.8–1.2, and pressure range 1–3 bar. They also conducted the Direct Numerical Simulation (DNS) study for the investigated flames. They used three different mechanisms from the literature, it was found that neither of the mechanisms was able to capture the experimental data for all the investigated flames. Their DNS results showed that with a higher ammonia ratio in the fuel blend, the NO reduction reaction $H + NO = HNO$ is enhanced. This reaction partly contributes to the decreasing NO emission with an increasing ammonia concentration in the fuel blend. Furthermore, at 3 bar and NH_3 molar ratio of 80 % in fuel blend, their analysis suggested that the two most important reactions that contribute to the formation of NO are $N_2O + H = NO + NH$ and $HNO + H = NO + H_2$. While HNO is found only in the premixed flame layer, N_2O can be found in both the premixed flame layer and the diffusion flame layer. Near the burner rim, these two layers are closer to each other; thus, the local formation rate of NO is higher than that in the downstream region as a result of the summation of the rates from these two reactions in the near burner region. Furthermore, reaction $N_2 + O = NO + N$ was also found to be important near the burner rim, where the concentration of O radicals is higher in the diffusion flame layer under fuel-rich conditions. This contributes further to the high NO concentration near the burner rim. Studies on NH_3 oxygenated fuel blends [207,213,245] have also suggested similar reaction pathways for NO formation and reduction.

Moreover, Woo et al. investigated non-premixed ammonia-methane flames, like those normally used in furnaces, analyzing the influential factors affecting NOx formation. Their findings demonstrated a consistent rise in NOx formation with increasing ammonia concentration, reaching maximum NOx emissions at an oxygen ratio of 0.7. These results underscored the dependency of the NOx formation process on the reacting flow structure [246]. In a recent study, methane/ammonia/hydrogen ternary blends were examined for the first time in a swirl burner under constant equivalence ratios of 1.2 at atmospheric

conditions. Minimal emissions of N_2O and NO_2 were observed for all fuel blends under rich conditions. Elevated NO emissions were noted with higher methane mixtures due to increased OH radical availability, while NO emissions decreased significantly with higher ammonia content due to enhanced availability of NH_2 radicals. Initially, NH_3 slip increased as methane content decreased, owing to reduced OH and H radical availability, but subsequently decreased again as hydrogen content increased. At this stage, hydrogen chemistry became dominant, ultimately leading to a substantial increase in ammonia slip as ammonia chemistry prevailed. [5] However, these findings do not yet provide a definitive generalization for industrial burners, as many of them typically operate with a slight excess of air. Systematic investigations for larger burner systems are currently scarce in the literature. Most measurements are available for premixed laboratory-scale flames, which in turn can be used to validate numerical results. This approach has been utilized, among others, by Shrestha et al. [198] to develop an ammonia mechanism specialized in predicting NOx and further extend it to non-premixed flames and NOx for hydrogen/ammonia mixtures [247]. Additionally, Da Rocha et al. [68] conducted a comparison of existing mechanisms with NOx implications and studied the behavior of H_2-NH_3 mixtures, see Fig. 16. It was observed that the maximum did not occur at one of the pure substances but at around 80 %, where most mechanisms converged. However, the absolute numerical values varied around 30 % for this point and up to a factor of 4 for pure ammonia. The selection of the mechanism is therefore crucial in predicting pollutant emissions.

Mashruk et al. [5] investigated the ternary blends of $CH_4/NH_3/H_2$ experimentally. The experiments were conducted in the tangential swirl burner, with a geometrical swirl of 1.08, at atmospheric pressure and an inlet temperature of 288 K. The burner was supplied with fully premixed mixtures of ammonia, methane, and hydrogen. Ammonia was varied from 0 to 100 %, and hydrogen was varied from 0 to 30 % (vol), and the rest was methane. Fig. 20 shows the Exhaust emissions for these blends. All the investigated cases show a relatively constant N_2O trend with increasing NH3 molar concentration. The NO_2 emissions are limited as discussed above. They suggested that unburned ammonia emissions and NO suffer considerable changes depending on the blends used. The high ammonia content in the fuel blend leads to high unburned ammonia concentrations. They found that ammonia emissions dropped for 30/50/20 $_{vol\%}$ and 20/55/25 $_{vol\%}$ for $CH_4/NH_3/H_2$ fuel blends. This was attributed to CH_4 and H_2 contents in the fuel blends, which eventually affect key radical species (H, O, and OH), which are responsible for ammonia oxidation. In some of the cases of a relatively high methane concentration, i.e., 20/55/25 (vol%) $CH_4/NH_3/H_2$, low unburned ammonia was observed, potentially as a consequence of the greater reactivity of such blends. It is also interesting to observe that at higher NH3 concentration, NO emissions are reduced. This might be due to the DeNOx effect, which happens via the reaction $NO + NH_2 \rightarrow N_2 + H_2O$ and other N_2-forming pathways [208,213,248,249].

While ammonia and hydrogen fuels are more environmentally friendly compared to fossil fuels due to the lack of CO_2/CO and UHC, their combustion still generates emissions necessitating meticulous handling. Hydrogen combustion may produce elevated levels of NO, while ammonia combustion can increase N_2O and NH_3 levels, as previously stated. Studies indicate that depending on the combustion efficiency and handling of ammonia, between 0.5 % and 5 % of nitrogen could escape as reactive compounds, significantly impacting climate change. [250] Ammonia can negatively affect natural ecosystems by contributing to soil acidification and threatening biodiversity. High concentrations of ammonia can be directly toxic to plants and lead to over-fertilization, which is particularly damaging to sensitive ecosystems such as peat bogs or meadows. These changes can have long-term consequences for biodiversity and the stability of these ecosystems. Advanced technologies for emission control, such as selective catalytic reduction (SCR) and lean-burn combustion, play a crucial role in alleviating these emissions and enhancing the environmental efficiency of furnaces. Numerous research studies have delved into the combustion mechanisms of ammonia and hydrogen fuels see the previous chapter and [9,251–253].

Ammonia slip, the unintentional release of unburned ammonia from combustion systems, poses a significant challenge in industrial ammonia combustion by reducing energy efficiency and introducing operational complications. When ammonia is not fully combusted, it escapes as an unused energy carrier, leading to increased fuel consumption and a deteriorated CO_2 balance [254]. Additionally, the slip can result in the formation of corrosive ammonium salts, such as ammonium bisulfate, which cause fouling of heat transfer surfaces and reduce the efficiency of exhaust heat recovery systems. To mitigate these effects, various engineering strategies have been developed and implemented, particularly

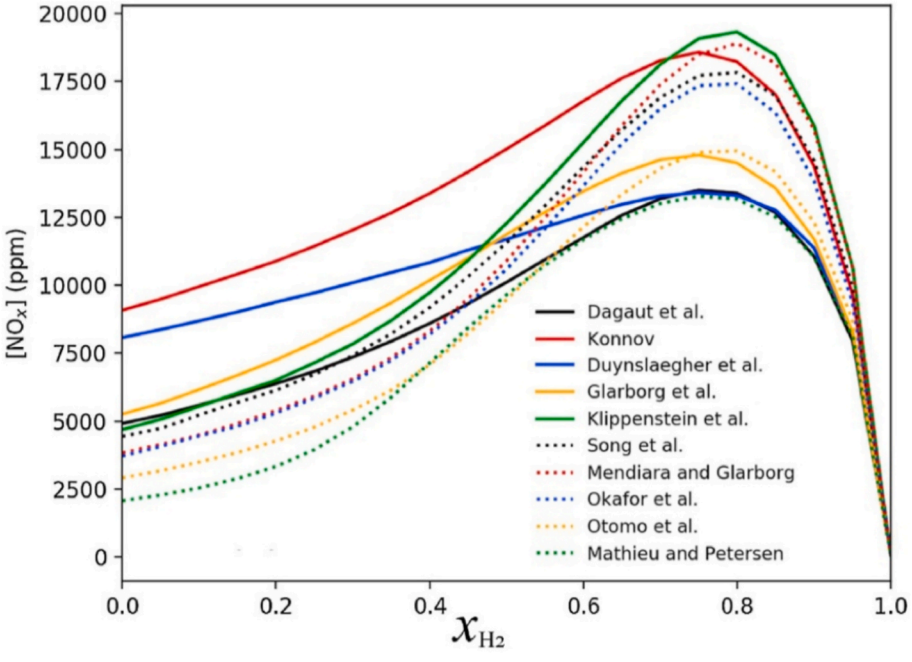

Fig. 19. NOx concentrations for stoichiometric NH_3/H_2/air mixtures as a function of the H_2 mole fraction in the fuel mixture at 1 bar and 298 K. Taken from [68]

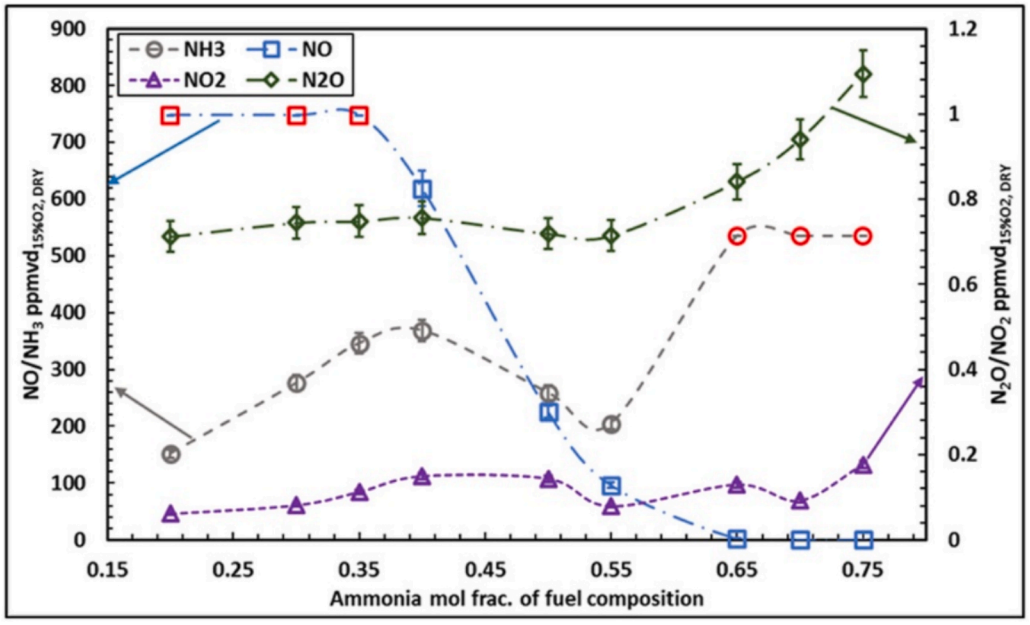

Fig. 20. NO2, N_2O, NH_3 and NO emissions at various ammonia mole fractions. Figure adopted from Mashruk et al. [5]. Symbols. experimental data.

in high-temperature industrial applications such as cement rotary kilns [9]. One key approach is combustion optimization. This includes precise control of the ammonia-air mixture using zone-specific injection systems equipped with real-time monitoring to ensure uniform distribution and complete combustion. Maintaining stable combustion chamber temperatures between 600 and 700 °C achieved, for example, through the use of heat recuperative systems like Swiss-roll burners helps to prevent ignition delays and flame quenching, both of which contribute to ammonia slip. Catalytic post-treatment represents a second critical strategy. Selective catalytic reduction (SCR) systems using titanium-vanadium catalysts are effective in simultaneously reducing NO_x emissions and oxidizing residual ammonia to nitrogen. For even lower slip levels, downstream ammonia slip catalysts (ASC), typically platinum-based, are employed to oxidize trace ammonia. However, these require exhaust gas temperatures above 300 °C to operate efficiently. Process control systems further enhance performance by dynamically adapting combustion parameters. The integration of NO_x sensors with machine learning algorithms allows for real-time adjustment of ammonia dosing in response to load changes. Additionally, exhaust gas recirculation (EGR), typically in the range of 30–40 %, promotes a more homogeneous fuel–air mixture and reduces localized hotspots that facilitate slip formation. Practical tests conducted in cement kilns have demonstrated that the combined implementation of these measures can reduce ammonia slip to below 2 ppm and increase overall system efficiency by 12–15 % [254]. The key to achieving these results lies in the intelligent integration of advanced sensor technology and adaptive control strategies capable of managing the complex interactions between ammonia combustion, NO_x formation, and heat transfer [9]. While ammonia is viewed as an environmentally friendly fuel, the potential environmental risks associated with the emission of other pollutants cannot be overlooked. Careful management and technological advancements are essential to minimize negative impacts on the climate and the environment. There is an urgent need for stringent regulations, measurement systems, and technical solutions to ensure that the benefits of ammonia as an energy carrier are not undermined by undesirable emissions.

7. Radiation effects

The characteristics of a flame's chemiluminescence, commonly known as its spontaneous emission, offer valuable insights into several essential attributes of the flame [255,256] For instance, a strong correlation exists between the intensity of chemiluminescence emitted by excited OH* and CH* radicals and the heat release rate in premixed hydrocarbon flames. [257] This particular attribute is frequently employed for heat release rate visualization using cameras or for determining flame transfer functions. [258] Fig. 17 shows a comparison of ammonia and methane flames in a swirl combustor. [100].

Fig. 18 illustrates the recorded chemiluminescence spectrum of stoichiometric methane-ammonia-air twin-flames with $X_{NH3} = 0.5$, alongside a strain rate of a = 150/s. Comparable spectra for equivalent flames were not found in existing literature. Besides OH*, CH*, and CO_2*, they found a notable contribution from excited radicals such as NO*, NH*, and CN* in the case of ammonia combustion. Evident contributions arise from distinct vibrational bands within the NO A-X electronic transition, spanning the 220–275 nm range. This is a wavelength range that is also partly detected with UV sensors. So that, besides methane and hydrogen, the usage of these sensors is also possible in ammonia flames and mixtures. In the UV and blue regions, spanning 200–457 nm, six excited radicals – NO*, OH*, NH*, CN*, CO_2*, and CH* – significantly contribute to the chemiluminescence of ammonia-methane-air flames. This intricate spectral complexity is advantageous for developing chemiluminescence-based sensors in combustion studies. While specific spectra for ammonia-methane flames were lacking, analogous contributions of excited radicals were documented in diverse flame conditions in other studies [259,260]. This highlights the diverse presence of excited radicals within chemiluminescence spectra across various flame types. Therefore, it will be possible to selectively investigate so of these species with bandpass filters or spectrometers to get more knowledge about the location of NH and CN radical production in industrial flames. This could lead to a sensor system for the detection of unburned components and help to avoid them.

Ryuichi et al. [261] set up a 10 kW experimental furnace to investigate radiative heat flux and radiation spectra during both ammonia fuel combustion and oxygen-enriched ammonia combustion in comparison to methane flames. The furnace spans a length of 1400 mm, with its inner wall enveloped in adiabatic material. Temperature profiles were measured with thermocouples, while additionally the heat flux and emission spectra emanating from the inner wall and the flame were detected at different positions. In an oxidizer with a 21 % O_2

concentration, the furnace's inner wall temperature experienced a decrease of approximately 200 K. Simultaneously, the maximum heat flux value under an ammonia non-premixed flame was about 22 % lower compared to that under the conditions of a methane/air non-premixed flame. In an oxidizer with a 30 % O_2 concentration, higher temperatures were achieved than those in the methane/air non-premixed condition, along with a 1.4 times greater intensity of total radiative heat flux, see Fig. 19.

8. Simulations for large-scale NH_3 combustion systems

In the past decade, numerous experimental and numerical studies have focused on ammonia combustion and its blends. Most research has been conducted at the lab scale to gain fundamental insights into combustion characteristics such as NOx formation, ignition delay times, flame length, and combustion efficiency. In the following section, the main characteristics of the studies are given; nevertheless, for detailed information regarding model formulations, assumptions, and validation strategies, the reader is referred to the respective primary literature. Many researchers use Computational Fluid Dynamics (CFD) to gain detailed spatially and if necessary, temporally resolved insights into the velocity, temperature and species distributions. This can help to better understand the interactions between the turbulence and chemical reactions. Fundamentally, one can differentiate between statistical turbulence models (RANS – Reynolds-Averaged Navier-Stokes) and temporally resolved turbulence models, such as Large Eddy Simulation (LES). Depending on the approach and the dimension of the problem (2D or 3D), the computational effort changes significantly, ranging from a few hours to multiple months. The reason for that is the principle of the models. RANS is only calculating averaged values, with the results being highly dependent on model parameters. In addition to that, no detailed statements can be made in regards to the turbulence-chemistry interactions. LES, on the other hand can give considerably more information, since a portion of the turbulence spectrum is directly resolved. This leads to a lesser dependency on model parameters but a higher computational cost when compared to RANS.

Füzesi et al. [262] investigated the combustion of three NH_3/CH_4 blends in a lab-scale atmospheric swirl flame burner using a RANS turbulence model combined with a Flamelet Generated Manifold (FGM) model. Validation against PIV/OH* chemiluminescence measurements showed good agreement between the experiment and CFD simulations, though NOx formation was underpredicted by a factor of two. Similarly, Alfazazi et al. [164] examined a lab-scale bluff body burner system for various CH_4/H_2 blends using the RANS approach and a Flamelet-based model. Preliminary LES studies provided insights into the mechanisms behind the formation of double OH layers. All the models were compared to a lab-scale experiment that used thermocouples for temperature measurements as well as OH-PLIF imaging.

Woo et al. [246] used a 2D CFD model with a detailed chemical reaction mechanism to study NOx emissions from a lab-scale coflow jet burner, considering both pure oxygen and oxygen/nitrogen mixtures as oxidizers. The NOx emission characteristics were well predicted across all configurations, aligning with trends in maximum NOx concentration within the flame. The composition of the exhaust gas was compared to values obtained by gas analysis. Bioche et al. [263] applied LES along with the thickened flame model to explore rich ammonia/hydrogen/air combustion in a lab-scale gas turbine burner (PRECCINSTA configuration). They analyzed various equivalence ratios and discovered that the trade-off between emissions shifts with the addition of hydrogen.

Bayramoğlu et al. [264] numerically examined blends of hydrogen, ammonia, and methane, focusing on Sandia Flame D with a 2D axisymmetric RANS model combined with species transport and a detailed reaction mechanism that showed acceptable agreement with experimental validation data. Their study highlighted limitations in the mixing of NH_3 with the fuel to prevent slower combustion, reduced adiabatic flame temperatures, and increased NOx production. Chaturvedi et al. [265] analyzed the characteristics of 70/30 NH_3/H_2 premixed combustion using CFD RANS models coupled with a FGM approach of an 8 kW test rig, which led to the development of a Chemical Reactor Network (CRN) to study NO formation pathways. The results were validated against experimental data including temperature measurements and gas composition.

Sun et al. [266] conducted a numerical investigation of a premixed NH_3/H_2/air swirling flame, analyzing NOx emission characteristics. Their 3D RANS, which also includes detailed chemistry, model demonstrated that increasing the hydrogen ratio significantly shortens the axial length of the premixed swirling flame and reduces unburnt NH_3, while NO formation increases, particularly at the flame edges and tips. The calculated results showed a good agreement when compared to PIV and temperature measurements. Chen et al. [52] discussed the impact of differential diffusion on H_2/NH_3 combustion. Using 2D direct numerical simulations (DNS) with detailed chemistry and species transport, they found that strong flame stretch and differential diffusion effects in H_2 pose significant challenges for combustor retrofitting, including potential misfire issues. DNS calculations by Wiseman et al. [267] examined the blow-out behavior of turbulent premixed $NH_3/H_2/N_2$-air and CH_4-air flames and compared them to OH-PLIF and OH chemiluminescence images.

In addition to single-flame configurations, Tu et al. [268] studied NH_3/CH_4 combustion in a lab-scale model combustor with and without air staging. Using a standard 3D RANS model, with detailed turbulence-chemistry interaction, they demonstrated stable combustion of pure NH_3 without sacrificing combustion efficiency, with a focus on the impact of air staging on NO emissions and combustion efficiency. In the experiments used for validation, exhaust gas was analyzed and flame images were taken.

Scaling up CFD modeling of NH_3 combustion for industrial applications presents significant challenges. Large Eddy Simulations are necessary to capture the turbulent mixing process and turbulence-chemistry interactions, but this requires considerable computational effort. Another major challenge is accurately modeling NOx formation, which differs significantly between NH_3 combustion and hydrocarbon or hydrogen combustion. While thermal NOx is dominant in hydrocarbon and hydrogen combustion, NH_3 combustion primarily involves fuel-bound nitrogen NOx. Integrating this mechanism into CFD by solving the associated transport equations increases the computational complexity, making this approach impractical for large-scale applications.

To address this, Romano et al. [269] developed a CRN based on preliminary RANS-CFD calculations using a FGM approach and applied it to an industrial gas turbine burner. Their study revealed higher NOx production rates for NH_3/CH_4 blends compared to H_2/CH_4 blends, and demonstrated that by incorporating a single calibration parameter from experiments, their numerical model accurately predicted NOx emissions.

Frank et al. [270] examined ammonia and hydrogen combustion in heavy-duty engines using a high-pressure dual-fuel combustion process. Their 3D RANS model with detailed chemistry, which was validated using a test engine with both flame luminosity and OH chemiluminescence measurements, showed that ammonia has a delayed ignition compared to hydrogen due to its lower flammability range, higher vaporization energy, and higher ignition temperature. The study suggested that increasing injection pressure or preheating ammonia, as well as adding more pilot diesel fuel, could improve the combustion process. Vigueras-Zuniga et al. [271] employed a 3D RANS model with a laminar flame concept to assess the effects of high pressure, high inlet temperatures, and higher power outputs in gas turbine systems fuelled by NH_3/H_2 blends. They focused on the combustion of a 70–30 mol% ammonia-hydrogen blend under rich conditions (equivalence ratio of $\phi = 1.2$) and compared their results against previous experiments.

9. Material components

In the development of combustors and other high-temperature components, the interplay between design, dimensions, and material selection hinges significantly upon the gas compositions, temperatures, flow rates, and stresses encountered within the combustion environment [59]. However, the limited literature on the suitability of current materials for ammonia-mixture-based combustion highlights the need for further research. In this context, valuable insights can be gained from the field of gas turbines, where intensive investigations into the material-fuel interaction behavior were conducted several years ago [272]. This need is underscored by the trend in Fig. 24, which illustrates the annual publications on ammonia, identified using the keywords "*Ammonia*" AND "*Hydrogen*" AND "*Combustion*" AND "*Gas Turbine*". This trend also stresses the need for increased focus on material compatibility to advance the application of ammonia as a fuel in high-temperature processes.

The distinct properties of ammonia-based blends present significant challenges compared to conventional hydrocarbon blends. These disparities create hurdles in adapting existing component designs and materials. Remarkable findings from a U.S. Army program highlighted the resilience of materials like Inconel 600 when exposed to high-temperature flows, with components such as nozzles, scrolls, or liners demonstrating remarkable resistance to the impact of these conditions. Other materials, such as Inconel X and 713C, also showed satisfactory resistance under similar conditions, though they are expensive [3]. Conversely, initial tests conducted by AIST revealed that ammonia use could deteriorate several materials due to hydrogen embrittlement, nitration, and susceptibility to acids (e.g., nitric acid) or bases (e.g., ammonium). However, thermal coatings based on zeolites and yttrium showed promise in mitigating these issues, although they are rarely used in high-temperature processes beside gas turbines. Preliminary results [273] suggest that these coatings offer higher resistance, protecting metal integrity during combustion operations that generate a spectrum of species from basic (e.g., $NH_4 +$) to acidic (e.g., HNO_3) environments. Nevertheless, further in-depth analyses are necessary to fully understand the material science behind these effects.

Recent research [58] examined the behavior of nickel-based alloys in premixed hydrogen/ammonia/air flames, revealing nearly five times higher hydrogen desorption from the metal compared to premixed methane/air flames. The critical significance lies in the interaction between metals and hydrogen in ammonia-based flames, stemming from fuel hydrogen or increased water vapor content. Hydrogen's ability to infiltrate the metal and alter its mechanical properties underscores its pivotal role. Extensive efforts have been dedicated to exploring the impact of hydrogen desorption on high-temperature materials, often utilizing cathodic hydrogen polarization at slightly elevated temperatures to accelerate the assessment of hydrogen concentrations. The conventional application of ammonia solutions (e.g., ammonium hydroxide) in boilers to elevate pH and curtail corrosion in diverse components is a widespread practice. The introduction of ammonia not only stabilizes pH but also reduces the dissolution of corrosive metal ions [274].

Ammonia demonstrates high corrosiveness towards copper, brass, zinc, nickel, and their alloys, particularly in the presence of water, and thus leads to a reduction of surface hardness [275]. This results in a characteristic greenish/blue color corrosion, as shown in Fig. 21. It is also corrosive towards certain plastics, and common gasket materials like Viton [276]. Impurities in liquid ammonia, such as air or carbon dioxide, can cause stress corrosion cracking of mild steel [277]. The chemical should not be mixed with bromine, chlorine, iodine, and hypochlorite [278] as ammonia is an alkaline reducing agent and reacts with acids (organic and inorganic), aldehydes, ketones, esters, phenols, cyanohydrins, halogens, and oxidizing agents [279], releasing poisonous gases and generating unstable reactions. These materials should be strictly avoided in any ammonia-based systems. Iron and steel,

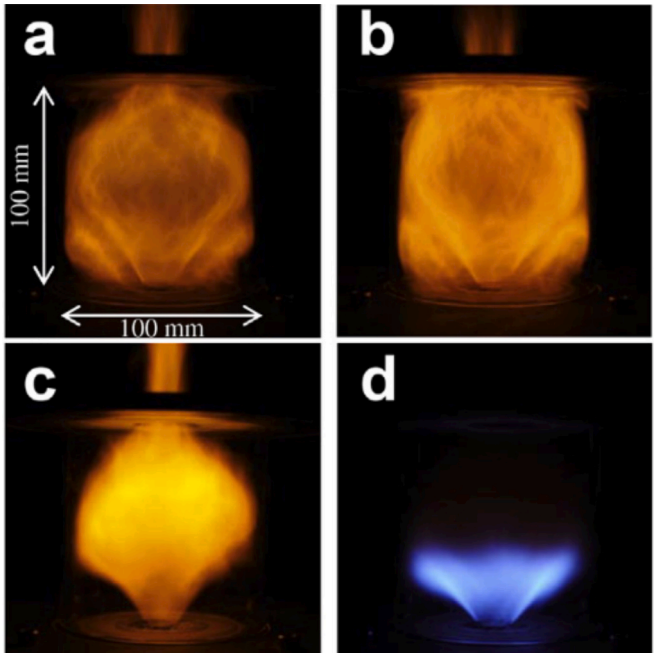

Fig. 21. Flames stabilized in the swirl burner with cylindrical liners, a, b, c, ammonia flames for different conditions, and d) methane flame. Taken from [100]

predominantly carbon steel and high-strength low-alloy steel, are the primary metals utilized in ammonia storage tanks, piping, and fittings.

Hot corrosion, a highly detrimental form of accelerated oxidation occurring in contaminated atmospheres [280], can be characterized into two types: type-I (high temperature) is within the range of 800–950 °C and type-II (low-temperature) occurs within the range of 600–800 °C [281]. Type-I hot corrosion occurs between the melting point of surface deposits and the vapor deposition dewpoint, causing corrosive damage to oxide layers. Type-II hot corrosion, on the other hand, arises from the formation of unstable complex mixed metal sulphate deposits. These deposits cause pitting or create uneven surfaces on the alloy, along with layers of corrosion products and additional deposits [280,281]. At high temperatures, such as those in ammonia combustion, hydrogen embrittlement and nitridation become significant concerns when using most steel grades. While carbon steel is generally less susceptible to hydrogen embrittlement compared to other steels, it can still suffer damage over time [282]. Adding elements like Cr, Ni, Mo, and V can inhibit these issues, possibly by stabilizing carbon and iron to prevent their conversion to hydrides and nitrides [20,283–286]. As a result, certain austenitic stainless steels, such as SS321, may be suitable for these conditions [287]. High Ni and Cr alloys have shown resistance to ammonia-related corrosion at elevated temperatures [20]. In addition, applying metal and metal oxide coatings to internal surfaces may enhance the corrosion resistance of cost-effective steel grades [283,287,288].

Anhydrous liquid ammonia, when exposed to temperatures as low as –33 °C, can induce stress corrosion cracking (SCC) in vessels made from carbon steel and high-strength low-alloy steel, particularly when oxygen is present [289]. This issue escalates with higher yield strength. Although SCC requires high stress levels usually not encountered during normal operation, residual welding stress levels together with applied stress can be enough to initiate SCC. Therefore, air, which contains oxygen, needs to be avoided completely in ammonia-containing systems [290]. Another interesting finding, supported by the Institute for Energy Technology in Norway, showed that water inhibits the formation and growth of SCC in ammonia tanks [291]. Therefore, it is recommended to add at least 0.1 % (weight) water to ammonia before transport [290].

Ammonia, in both its liquid and gaseous phase, is not particularly corrosive to ferrous materials since its pH fluctuates between 9.0 and 9.4. However, it is appropriate to emphasize that these materials passivate under alkaline conditions, as shown in Fig. 22. It has been a common practice to employ ammonia, which is highly soluble in water and forms an alkaline solution of ammonium hydroxide in boilers to increase pH, thus decreasing corrosion in these systems [292]. Ammonia, usually injected into the water-steam circuit increases pH, which usually tends to be around 7.0 to 7.6. Furthermore, solutions that include ammonia limit the dissolution of metal ions produced during corrosion, hence drastically decreasing the equilibrium potential concerning to the standard potential, changing thermodynamic conditions within the system [274]. However, there are cases where ammonia can be contaminated by other molecules. Should an ammonia tank be contaminated with HCl, the corrosion attack would be severe, leading to pitting of the material [293]. Ammonia can act as a protector for some steels while being detrimental to copper alloys. Furthermore, ammonia is not corrosive to carbon steels under atmospheric conditions, although its behavior can change with the addition of CO_2, H_2O, O_2, etc. (Fig. 23).

Given the need for heat (Figs. 24–26) in fuelling systems, crackers, or selective catalytic reduction (SCR), there's a necessity for heat exchangers that utilize engine cooling water and exhaust gas heat. These heat exchangers should be designed and operated in a manner that any ammonia leakage is directed into an intermediate substrate [56]. This precaution ensures that any potential ammonia does not pose a risk to the environment or the system's operation. Detection of ammonia should be a feature of any coolant utilized in sensitive industrial areas. Interestingly, diluted ammonia showcases varying corrosive behaviors depending on exposure conditions, transitioning from uniform corrosion to crack formation, stress-induced corrosion, and nitration. The role of temperature and pressure emerges as critical factors determining ammonia's impact on materials. Therefore, a thorough understanding of ammonia combustion's effects on materials is crucial for ensuring the integrity and safety of operational systems like furnaces, boilers, and gas turbines.

10. Furnace operation possibilities

As indicated earlier, drawbacks like low LBV and unstable flame significantly restrict the extensive use of ammonia as a fuel. Therefore, it's imperative to explore viable methods to enhance the reliability and environmental friendliness of ammonia combustion. Ongoing research encompasses techniques such as blending with hydrocarbon fuels, process intensification, and the development of pertinent combustion auxiliary technology.

However, regarding preheating, there are some discrepancies concerning the influence of temperature on NOx. Most studies have shown that thermal effects can lead to an increase in flame temperature and thermal NOx [171,296]. Nonetheless, an increase in efficiency also

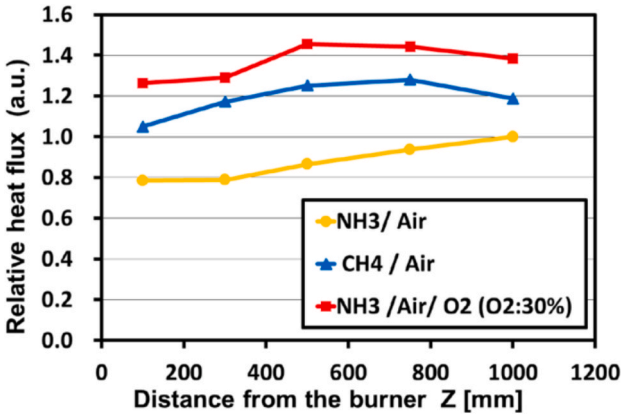

Fig. 23. Radiative heat flux distribution in an experimental furnace fired with a non-premixed flame (10kW), from [261]

resulted in a reduction of unburnt ammonia and NO_2 emissions. Alteration of pressure is not a common method in most furnaces; however, it can significantly impact NOx emissions. [252] Oxygen enrichment, as another approach to intensify combustion, mainly accelerates the laminar flame through thermal effects and the elevation of free radical concentrations such as NH_2, OH, and H. Various studies have shown that a 30 % oxygen concentration can bring the laminar burning velocity (LBV) to the same level as that of a 30 % hydrogen mixture combustion. In terms of emissions, NO production is encouraged due to the increase in HNO intermediates with rising oxygen content. This measure could potentially offer a viable option in the future due to increased oxygen production in decentralized electrolyzers, where post-treatment methods for NOx reduction could be employed. Although there have been few studies examining the impact of oxygen concentration on ammonia combustion, the development of relevant research will aid in optimizing the design of oxygen-enriched combustion [208] for future systems such as ammonia-coal and ammonia-methane, thereby expediting the process of ammonia application. [297].

Moreover, there exist possibilities for constructive modifications in burner design. This has, for example, been demonstrated with additively manufactured parts for non-premixed ammonia blend burners at a technical level, where a clear reduction in NOx emissions was achieved [298]. Further, this also includes the potential utilization of porous media burners to heighten the efficiency of ammonia combustion. When the flame is stabilized within a porous media burner, both solid conduction and radiation heat transfer mechanisms come into play. These mechanisms contribute to an elevation [299] in the temperature of the pre-mixed gas while concurrently minimizing heat loss. Additionally, a hybrid heating approach employing microwaves [300] or plasma-assisted combustion [301] could present a viable means to

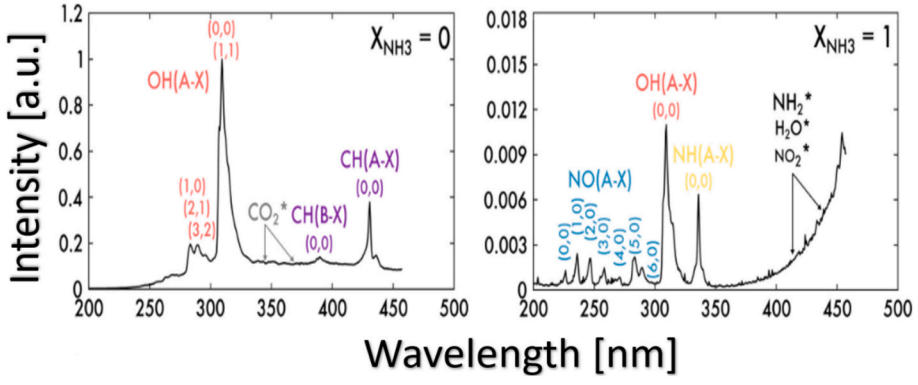

Fig. 22. Chemiluminescence spectrum of stoichiometric twin-flames for $X_{NH3} = 0$ (pure methane) and (c) $X_{NH3} = 1$ (pure ammonia). Taken from [171]

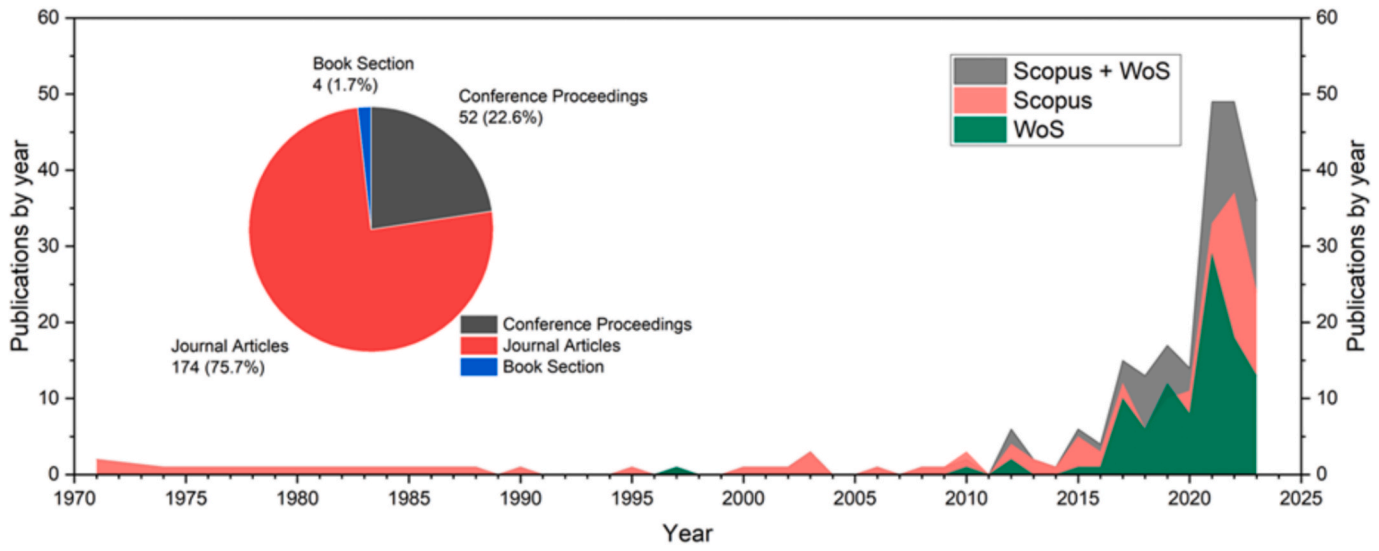

Fig. 24. Annual publications on ammonia-hydrogen gas turbines. Data was collected from Scopus and Web of Science (WoS) databases as of August 2024.

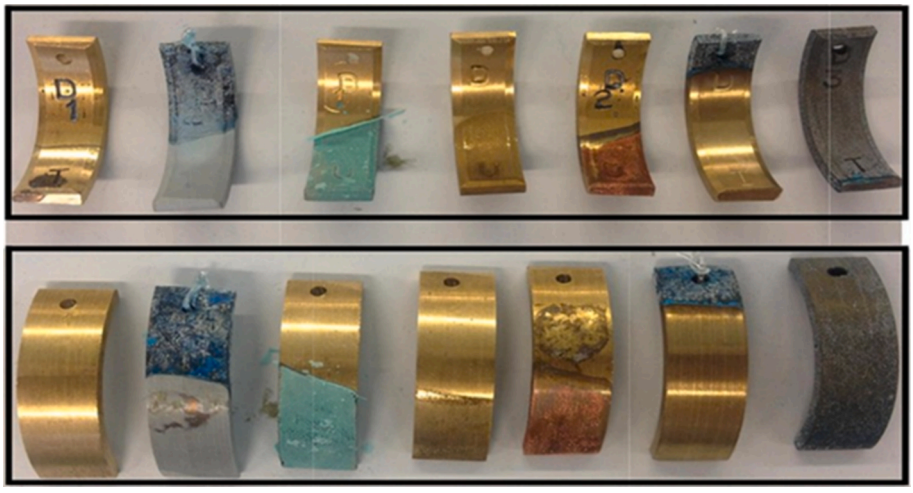

Fig. 25. Brass samples exposed to different levels (pH) of ammonia concentration [294].

amplify the reactivity of these relatively inert flames. The integration of such technology in ammonia combustion is anticipated to offset the instability observed in ammonia combustion and alleviate the issue of high NOx emissions. Finally, catalytic ammonia combustion [302] is recognized as a promising technique due to its potential to lower NOx emissions and achieve superior combustion efficiency at reduced operating temperatures. Studies have revealed a correlation between the efficiency of ammonia combustion and the bond energy of metal–oxygen within metal oxides. Nevertheless, empirical evidence to validate the feasibility of implementing catalytic ammonia combustion in practical applications remains insufficient.

Promising combustion technologies, encompassing porous media, plasma-assisted, and catalytic combustion, not only have the capacity to enhance combustion stability but also exhibit the potential to curtail the emission of pollutants. However, rigorous examination is imperative to assess the enduring stability and reliability of porous media during prolonged operational periods. The application of these methodologies within large-scale industrial facilities is likely to require substantial time for implementation but should be considered as an eventual objective.

Currently, several projects attempt to demonstrate the use of green ammonia as a substitute for fossil fuels in large power and heating facilities worldwide. Japan, through its recent NEDO program (New Energy and Industrial Technology Development Organization) allocated ~$450 M USD for the technological development and implementation of ammonia as an energy vector. Over the projects that are currently being evaluated, JERA – Japan's power utility company- joined forces with IHI, a Japanese equipment manufacturer, for the replacement of some of their coal burners with ammonia. The move seeks to replace up to 100 % coal with ammonia by the end of the decade, with results that have demonstrated the replacement of up to 20 % ammonia successfully in a large boiler unit in their facilities [303]. The research has shown the improved thermal characteristics of these units, as ammonia gas improves some of the combustion reactions whilst also mitigating carbon emissions in the same percentage of the ammonia replaced in the combustion chambers. Along those lines, JERA is searching for international suppliers capable of securing up to 500,000 tons/year of ammonia for their facility at Hekinan power plant.

Similarly, Mitsubishi Power announced the development of 100 % ammonia-fed boilers for industrial heat applications. The initiative comes in hand with the announcement of the first gas turbine running on pure ammonia. Finally, all these works seek to have an impact in Asia through collaboration agreements that will ensure that ammonia-based technologies from Japan are implemented for carbon reduction in the region. Evidence of these agreements is the MoU signed between IHI,

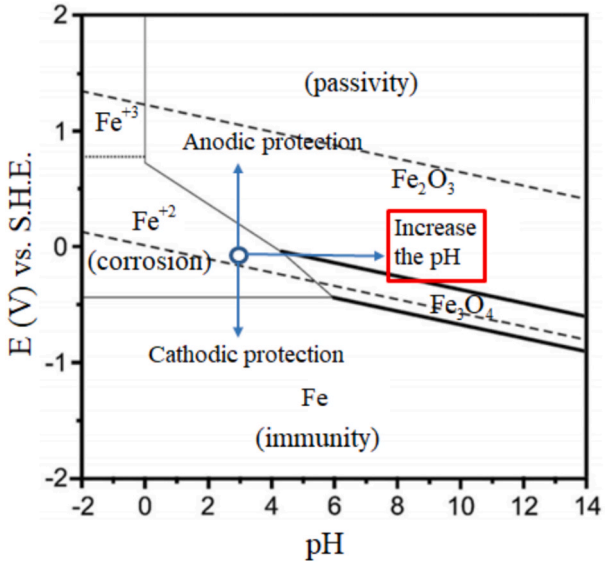

Fig. 26. Pourbaix diagram. Passive conditions that iron can reach with pH increase. Reproduced from [295].

Kowa and Adani Power to perform feasibility studies of ammonia-coal co-firing at the Mundra power plant in Gujarat, India. From 20 % ammonia, the study will seek to reach up to 100 % ammonia in the process burners [304].

Advanced Asian economies are currently working towards the development of ammonia systems capable of substituting large coal requirements in large furnace applications. South Korea recently announced that 2.1 % of total electricity generation would be conducted by hydrogen and ammonia by 2030, increasing to 7.1 % by 2036 [305,306]. Most of this fuel would be ammonia imports coming from third countries with large renewable capacity. Works taking place in Japan and other countries have demonstrated that ammonia can be burned directly, hence making the chemical their preferred option for thermal power and industrial boilers. In 2021, the Ministry of Industry, Trade and Energy (MOTIE) launched a promotion team for power generation demonstration purposes using hydrogen/ammonia. The team includes Korea Electric and Power Corporation (KEPCO), five public power generation companies and private companies related to the value chains of hydrogen/ammonia provision. The initiative has been joined by cement and steel producers [307] Major Korean boilermakers and chemical companies as well as research institutes and universities, are engaged in this project and are conducting preliminary studies for two years. Successive to the project, in 2023, MOTIE has funded a 5-year demonstration project aiming at 20 % ammonia co-firing to four commercial-scale power plants: two boilers including Shin Boryeong power plant, and two units, including Samcheok power plant. After the demonstration project, the 20 % co-firing will be extended to the other 24 coal-power generation units [307]. After successful commercial operation of 20 % co-firing, higher co-firing rates are planned after expected combustion system modifications.

China has recently jumped on the train of ammonia energy. In January 2022, the Chinese government took a significant step towards promoting the development of new energy storage [308]. Notably, ammonia was included as an energy storage medium for the first time. Later that year, the Ministry of Science and Technology (MOST) and National Natural Science Foundation (NSFC) announced at least three major national R&D projects to investigate the fundamentals of ammonia combustion and to develop ammonia co-combustion technology with coal and natural gas.

In terms of smaller units, considerable work has taken place in Japan and places like the UK. FloGas, one of the major propane suppliers in Northern Europe, has joined efforts with Cardiff University to develop a 1 MW unit firing ammonia/hydrogen, hence replacing propane for heating applications in the food and farming industries. The works have demonstrated the versatility of ammonia/hydrogen blending at medium power ratios, with the potential of large NOx abatement whilst also decarbonising steam production for these sectors. Numerical modelling combined with experimental studies will deliver a practical solution for a farming site to show, for the first time, the use of the molecule to deliver clean power for these energy-intensive processes. Hydrogen, obtained from the partial cracking of ammonia, will serve to improve combustion features whilst also increasing power ratios in compact units. The work promises to support the net-zero agenda of the UK and other places in Europe [309].

Finally, it is important to note that these developments and technological achievements are not only meant to be single cases in the vast universe of the energy transition agenda. Recently, the International Standards Organization, ISO, concluded the writing of the first proposal for a Technical Standard for the development, testing and acceptance of ammonia-fired facilities > 100 MW power [310]. The initiative, led by IHI, brings experts from all corners of the globe to agree on parameters, nomenclatures, definitions, and objectives required to achieve international consensus and create the standard that will support the large, practical transition of ammonia as a fuel in these facilities. The move creates the foundations for further progress in the regulatory and legal areas for the use of ammonia at a global scale, hence showing that ammonia fuel will be part of the future.

11. Summary and conclusion

In conclusion, ammonia combustion presents both significant potential and considerable challenges for its adoption as a sustainable fuel source in the global effort to decarbonize energy systems. As a carbon-free hydrogen carrier with relatively high energy density and an already established production and distribution infrastructure, ammonia represents a promising alternative to conventional fossil fuels, particularly in hard-to-abate sectors such as heavy industry and maritime transport. However, the practical deployment of ammonia in combustion-based systems faces several technical barriers. These include its inherently low laminar burning velocity (LBV), pronounced flame instability, and the formation of high levels of nitrogen oxides (NOx) under standard combustion conditions. Recent advances, such as blending ammonia with hydrocarbons or hydrogen, preheating, and the use of combustion auxiliaries, have shown potential to mitigate these issues by improving flame stability, ignition behavior, and overall combustion efficiency. Nevertheless, further research is required, particularly under the high-temperature and high-pressure conditions typical of industrial applications, to validate and optimize these methods. To bridge the gap between laboratory research and real-world implementation, a phased integration strategy is proposed. This would begin with ammonia co-firing in existing combustion systems, leveraging current infrastructure to gradually reduce carbon emissions, and ultimately transition toward fully dedicated ammonia-fueled technologies. Such a transformation demands a comprehensive approach: burner designs must be modified or retrofitted to accommodate ammonia's unique combustion characteristics, effective NOx mitigation strategies such as staged combustion or exhaust after-treatment must be employed, and strict safety protocols for handling and storage must be developed and enforced. In parallel, the complexity of nitrogen chemistry in ammonia combustion and the inconsistencies between current kinetic models and experimental results underscore the urgent need for more accurate, validated modeling tools. Furthermore, while ammonia combustion does not emit CO_2 directly, it still produces pollutants such as NOx and nitrous oxide (N_2O), which are potent greenhouse gases and contributors to air pollution. The implementation of advanced emission control technologies, such as selective catalytic reduction (SCR) and lean-burn combustion, is therefore critical to minimizing environmental impact. The development of efficient, cost-effective solutions for

emission reduction remains a key requirement for the widespread acceptance of ammonia as a clean fuel. Material compatibility also presents important challenges. Corrosion, embrittlement, and nitration of components in ammonia-fueled systems are particularly problematic under high-temperature conditions or in the presence of impurities. Encouragingly, recent research has identified mitigation strategies, including the use of corrosion-resistant alloys, protective coatings, and the controlled addition of water to ammonia to reduce material degradation. Innovations in combustion technologies, such as porous media burners, plasma-assisted ignition, and catalytic combustion, are also emerging as promising pathways to improve ammonia combustion efficiency, stability, and emissions performance. These technological developments will be essential to unlock the full potential of ammonia as a practical energy carrier. On the global stage, countries such as Japan, South Korea, and China are at the forefront of ammonia-based power generation and co-firing projects. Their active investment in ammonia infrastructure and pilot-scale implementation highlights the growing momentum behind ammonia as part of a broader low-carbon energy strategy. Additionally, the increasing availability of green ammonia, produced using renewable energy sources, and international cooperation on the development of technical standards, are important enablers for scaling up ammonia combustion technologies worldwide.

Ultimately, while considerable challenges remain, ammonia holds great promise as a carbon-free fuel capable of contributing significantly to the decarbonization of high-temperature industrial processes. Continued research, technological innovation, and cross-sector collaboration will be essential to fully realize its role in a sustainable, low-carbon energy future.

CRediT authorship contribution statement

Sven Eckart: Writing – review & editing, Writing – original draft, Visualization, Project administration, Methodology, Investigation, Data curation, Conceptualization. **Ernesto Salzano:** Writing – review & editing, Supervision. **Andreas Richter:** Writing – original draft, Data curation. **Mohammad Alnajideen:** Writing – original draft, Data curation. **Agustin Valera Medina:** Writing – original draft, Supervision, Data curation. **Krishna Prasad Shrestha:** Writing – original draft, Supervision, Data curation. **Ahmed Yasiry:** Writing – original draft, Data curation. **Wang Jinhua:** Supervision. **Florian Bauer:** Writing – original draft, Data curation. **Chunkan Yu:** Writing – original draft, Data curation. **Hartmut Krause:** Writing – review & editing, Supervision, Project administration. **Gianmaria Pio:** Writing – review & editing, Writing – original draft, Project administration, Data curation, Conceptualization.

Declaration of competing interest

The authors declare that they have no known competing financial interests or personal relationships that could have appeared to influence the work reported in this paper.

Acknowledgements

S.E. and E.S.s work was supported by the European Union under the Horizon Europe project CESAR (Centre of Excellence for Safety Research, GA No 101186946). Cardiff University authors gratefully acknowledge the support from the EPSRC through the projects OceanREFuel—Ocean Renewable Energy Fuels (EP/W005018/1), MariNH3 (EP/W016656/1), and Storage of Ammonia For Energy (SAFE)—AGT Pilot (EP/T009314/1).

Data availability

No data was used for the research described in the article.

References

[1] Valera-Medina A, Amer-Hatem F, Azad AK, Dedoussi IC, de Joannon M, Fernandes RX, et al. Review on Ammonia as a potential fuel: from Synthesis to Economics. Energy Fuels 2021;35:6964–7029.
[2] Dimitriou P, Javaid R. A review of ammonia as a compression ignition engine fuel. Int J Hydrogen Energy 2020. https://doi.org/10.1016/j.ijhydene.2019.12.209.
[3] Valera-Medina A, Xiao H, Owen-Jones M, David W, Bowen PJ. Ammonia for power. Prog Energy Combust Sci 2018;69:63–102.
[4] S. Mashruk, Kovaleva, Marina: Zitouni, Seif-Eddine, P. Brequigny, C. Rouselle, A. Valera-Medina, Ammonia/Hydrogen/Methane Characteristic Profiles for Atmospheric Combustion Applications, International Conference on Applied Energy (2021).
[5] Mashruk S, Vigueras-Zuniga MO, Tejeda-del-Cueto ME, Xiao H, Yu C, Maas U, et al. Combustion features of CH4/NH3/H2 ternary blends. Int J Hydrogen Energy 2022;47:30315–27.
[6] Pio G, Barba D, Palma V, Salzano E. A Numerical Study on the effect of Temperature and Composition on the Flammability of Methane–Hydrogen Sulfide Mixtures. Combust Sci Technol 2019;191:1541–57.
[7] Chai WS, Bao Y, Jin P, Tang G, Zhou L. A review on ammonia, ammonia-hydrogen and ammonia-methane fuels. Renew Sustain Energy Rev 2021;147:111254.
[8] Wang D, Lee M, Suzuki Y. Nitriding Effects of Ammonia Flames on Iron-based Metal Walls. J Ammonia Energ 2023;1. https://doi.org/10.18573/jae.8.
[9] Valera-Medina A, Banares-Alcantara R, editors. Techno-economic challenges of green ammonia as an energy vector. London, Oxford, San Diego, Cambridge, MA: Elsevier Academic Press; 2021.
[10] International Cement Review, Heidelberg Materials investigates ammonia as hydrogen carrier, 2024, https://www.cemnet.com/News/story/176590/heidelberg-materials-investigates-ammonia-as-hydrogen-carrier.html, accessed 30 July 2025.
[11] G.C. David Perilli, Global Cement (19 March 2025).
[12] M. Zhu, Revolutionising the cement industry with ammonia, 2025, https://www.cranfield.ac.uk/press/news-2024/revolutionizing-the-cement-industry-with-ammonia, accessed 30 July 2025.
[13] Y. Ma, J.W. Bae, S.-H. Kim, Matic Jovičević-Klug, K. Li, D. Vogel, D. Ponge, M. Rohwerder, D.R. Baptiste Gault, Reducing Iron Oxide with Ammonia: A Sustainable Path to Green Steel, 2023, https://ammoniaenergy.org/articles/new-rd-ammonia-as-a-green-steel-enabler/, accessed 30 July 2025.
[14] Ciccarelli G, Jackson D, Verreault J. Flammability limits of NH3–H2–N2–air mixtures at elevated initial temperatures. Combust Flame 2006;144:53–63.
[15] Randall DJ, Tsui TKN. Ammonia toxicity in fish. Mar Pollut Bull 2002;45:17–23.
[16] Liu P, Chen B, Bennett A, Pitsch H, Roberts WL. Probing the influence of hydrogen cyanide on PAH chemistry. Proc Combust Inst 2023;39:1139–46.
[17] Lu G, Song Y, Li S, Liang X, Zhang F, Wang K. Influence of ethene and propene on fuel reactivity and cyanides formation in ammonia combustion kinetics. Fuel 2024;368:131635.
[18] R.P. Padappayil, J. Borger, StatPearls: Ammonia Toxicity, Treasure Island (FL), 2024.
[19] Sutton I. Process Risk and Reliability Management. Elsevier 2015:580–601.
[20] M. Davies, in: S.D. Cramer, B.S. Covino (Eds.), Corrosion: Environments and Industries, ASM International, 2006, pp. 727–735.
[21] Cozzani V, Salzano E. Threshold values for domino effects caused by blast wave interaction with process equipment. J Loss Prev Process Ind 2004;17:437–47.
[22] Yu C, Valera-Medina A. A Comprehensive Numerical Study on the Inhibition effect of Ammonia on Various (Un)strained Premixed Stoichiometric Hydrogen/Air Flame Systems. Energy Fuels 2024. https://doi.org/10.1021/acs.energyfuels.4c04052.
[23] Zanobetti F, Pio G, Jafarzadeh S, Ortiz MM, Cozzani V. Inherent safety of clean fuels for maritime transport. Process Saf Environ Prot 2023;174:1044–55.
[24] Al-Breiki M, Bicer Y. Comparative life cycle assessment of sustainable energy carriers including production, storage, overseas transport and utilization. J Clean Prod 2021;279. https://doi.org/10.1016/j.jclepro.2020.123481.
[25] Zanobetti F, Pio G, Jafarzadeh S, Muñoz Ortiz M, Cozzani V. Decarbonization of maritime transport: Sustainability assessment of alternative power systems. Journal of Cleaner Production 417 2023. https://doi.org/10.1016/j.jclepro.2023.137989.
[26] Na'inna AM, Phylaktou HN, Andrews GE. Explosion flame acceleration over obstacles: effects of separation distance for a range of scales. Process Saf Environ Prot 2017;107:309–16.
[27] Duong PA, Ryu BR, Song MK, van Nguyen H, Nam D, Kang H. Safety Assessment of the Ammonia Bunkering Process in the Maritime Sector: a Review. Energies 2023;16. https://doi.org/10.3390/en16104019.
[28] Luan X, Zhang B, Short M, Chen T. Calibration and sensitivity analysis of under-expanded hydrogen jet CFD simulation based on surrogate modeling. J Loss Prev Process Ind 2025;94:105535.
[29] Venetsanos AG. Homogeneous non-equilibrium two-phase choked flow modeling. Int J Hydrogen Energy 2018;43:22715–26.
[30] Carboni M, Pio G, Mocellin P, Pilo F, Vianello C, Russo P, et al. Experimental and numerical characterization of hydrogen jet fires. Int J Hydrogen Energy 2022;47:21883–96.
[31] S. Mannan, Lees' loss prevention in the process industries: hazard identification, assessment and control. Vol 1, 4th ed., Butterworth Heinemann, 2012.
[32] Pio G, Carboni M, Salzano E. Realistic aviation fuel chemistry in computational fluid dynamics. Fuel 2019;254. https://doi.org/10.1016/j.fuel.2019.115676.

[33] de Liso BA, Pio G, Salzano E. Fire behaviour of liquid solvents for energy storage applications. Process Saf Environ Prot 2024;188:726–34.
[34] de Liso BA, Pio G, Salzano E. Experimental and advanced numerical characterization of toluene fires. Fuel 2025;397:135448.
[35] C. van den Bosch, R. Weterings, Methods for calculation of physical effects, CPR 14E (1996).
[36] Elishav O, Mosevitzky Lis B, Miller EM, Arent DJ, Valera-Medina A, Grinberg Dana A, et al. Progress and prospective of Nitrogen-based Alternative Fuels. Chem Rev 2020;120:5352–436.
[37] Mastellone ML, Ponte M, Arena U. Design of mitigation systems for indoor and outdoor ammonia releases. J Loss Prev Process Ind 2003;16:93–101.
[38] Buchlin J-M. Mitigation of industrial hazards by water spray curtains. J Loss Prev Process Ind 2017;50:91–100.
[39] Fan H, Xu X, Abdussamie N, Chen P-S-L, Harris A. Comparative study of LNG, liquid hydrogen, and liquid ammonia post-release evaporation and dispersion during bunkering. Int J Hydrogen Energy 2024;65:526–39.
[40] Crowl DA, Louvar JF. Chemical process safety: Fundamentals with applications. 3rd ed. Upper Saddle River, NJ: Prentice Hall; 2014.
[41] Vidal M, Rogers WJ, Holste JC, Mannan MS. A review of estimation methods for flash points and flammability limits. Process Saf Prog 2004;23:47–55.
[42] Egolfopoulos FN, Hansen N, Ju Y, Kohse-Höinghaus K, Law CK, Qi F. Advances and challenges in laminar flame experiments and implications for combustion chemistry. Prog Energy Combust Sci 2014;43:36–67.
[43] Pio G, Dong X, Salzano E, Green WH. Automatically generated model for light alkene combustion. Combust Flame 2022;241:112080.
[44] Lu T, Law CK. Toward accommodating realistic fuel chemistry in large-scale computations. Prog Energy Combust Sci 2009;35:192–215.
[45] NTSB/PAB-07/02 National Transportation Safety Board, DCA05-MP001 Anhydrous Ammonia Pipeline Rupture Near Kingman, Pipeline Accident Brief (2004).
[46] Edith Ismene Nicolaou, https://medium.com/@edie_nicol/green-patrol-a-leading-russian-environmental-organization-recently-reported-on-an-ammonia-leak-2ec21fb2e874), 2015.
[47] G. Smith, A Hazard Assessment of Ammonia as a Fuel (2013).
[48] S. Ito, S. Kato, T. Saito, T. Fujimori, H. Kobayashi, Development of ammonia/natural gas dual fuel gas turbine combustor (2016).
[49] Valera-Medina A, Marsh R, Runyon J, Pugh D, Beasley P, Hughes T, et al. Ammonia–methane combustion in tangential swirl burners for gas turbine power generation. Appl Energy 2017;185:1362–71.
[50] Chen L, Wang C, Wang W. Effect of ammonia co-firing on heat transfer, safety, and economy of coal-fired boilers. Fuel 2023;334:126649.
[51] Valera-Medina A, Morris S, Runyon J, Pugh DG, Marsh R, Beasley P, et al. Ammonia, methane and Hydrogen for Gas Turbines. Energy Procedia 2015;75:118–23.
[52] Chen X, Guivarch T, Lulic H, Hasse C, Chen Z, Ferraro F, et al. Evaluation of hydrogen/ammonia substitute fuel mixtures for methane: effect of differential diffusion. Int J Hydrogen Energy 2024;69:1056–68.
[53] Kekul O, Ilbas M, Karyeyen S. Hydrogen concentration effects on a swirl-stabilized non-premixed burner using ammonia. Int J Hydrogen Energy 2024;52:1288–305.
[54] Mazzotta L, Lamioni R, D'Alessio F, Meloni R, Morris S, Goktepe B, et al. Modeling Ammonia-Hydrogen-Air Combustion and Emission Characteristics of a Generic Swirl Burner. J Eng Gas Turbines Power 2024;146. https://doi.org/10.1115/1.4064807.
[55] Sato D, Davies J, Mazzotta L, Mashruk S, Valera-Medina A, Kurose R. Effects of Reynolds number and ammonia fraction on combustion characteristics of premixed ammonia-hydrogen-air swirling flames. Proc Combust Inst 2024;40:105283.
[56] Valera-Medina A, Vigueras-Zuniga MO, Shi H, Mashruk S, Alnajideen M, Alnasif A, et al. Ammonia combustion in furnaces: a review. Int J Hydrogen Energy 2024;49:1597–618.
[57] D. Wang, M. Lee, Y. Suzuki, Nitriding Effects of Ammonia Flames on Iron-based Metal Walls, jae 1 (2023), doi:10.18573/jae.8.
[58] Kovaleva M, Dziedzic D, Mashruk S, Evans S, Valera-Medina A, Galindo-Nava E, et al. Volume 7: Industrial and Cogeneration; Manufacturing Materials and Metallurgy; Microturbines, Turbochargers, and Small Turbomachines; Oil & Gas Applications. Am Soc Mech Eng 2022.
[59] Alnaeli M, Alnajideen M, Navaratne R, Shi H, Czyzewski P, Wang P, et al. High-temperature materials for complex components in ammonia/hydrogen gas turbines: a critical review. Energies 2023;16:6973.
[60] Üstün CE, Eckart S, Valera-Medina A, Paykani A. Data-driven prediction of laminar burning velocity for ternary ammonia/hydrogen/methane/air premixed flames. Fuel 2024;368:131581.
[61] Szanthoffer AG, Papp M, Turányi T. Identification of well-parameterised reaction steps in detailed combustion mechanisms – a case study of ammonia/air flames. Fuel 2025;380:132938.
[62] Szanthoffer AG, Zsély IG, Kawka L, Papp M, Turányi T. Testing of NH3/H2 and NH3/syngas combustion mechanisms using a large amount of experimental data. Appl Energy Combust Sci 2023;14:100127.
[63] Berwal P, Khandelwal B, Kumar S. Effect of ammonia addition on laminar burning velocity of CH_4/H_2 premixed flames at high pressure and temperature conditions. Int J Hydrogen Energy 2023. https://doi.org/10.1016/j.ijhydene.2023.06.326.
[64] Eckart S, Zsély IG, Krause H, Turányi T. Effect of the variation of oxygen concentration on the laminar burning velocities of hydrogen-enriched methane flames. Int J Hydrogen Energy 2023. https://doi.org/10.1016/j.fuel.2023.128964.
[65] Eckart S, Pizzuti L, Fritsche C, Krause H. Experimental study and proposed power correlation for laminar burning velocity of hydrogen-diluted methane with respect to pressure and temperature variation. Int J Hydrogen Energy 2022:6334–48.
[66] Drost S, Eckart S, Yu C, Schießl R, Krause H, Maas U. Numerical and experimental investigations of CH_4/H_2 mixtures: ignition delay times, laminar burning velocity and extinction limits. Energies 2023;16:2621.
[67] Eckart S, Prieler R, Hochenauer C, Krause H. Application and comparison of multiple machine learning techniques for the calculation of laminar burning velocity for hydrogen-methane mixtures. Therm Sci Eng Prog 2022;32:101306.
[68] Da Rocha RC, Costa M, Bai X-S. Chemical kinetic modelling of ammonia/hydrogen/air ignition, premixed flame propagation and NO emission. Fuel 2019;246:24–33.
[69] Hayakawa A, Goto T, Mimoto R, Arakawa Y, Kudo T, Kobayashi H. Laminar burning velocity and Markstein length of ammonia/air premixed flames at various pressures. Fuel 2015;159:98–106.
[70] Takizawa K, Takahashi A, Tokuhashi K, Kondo S, Sekiya A. Burning velocity measurements of nitrogen-containing compounds. J Hazard Mater 2008;155:144–52.
[71] Pfahl U, Ross M, Shepherd J, Pasamehmetoglu K, Unal C. Flammability limits, ignition energy, and flame speeds in H_2–CH_4–NH3–N2O–O2–N2 mixtures. Combust Flame 2000;123:140–58.
[72] Law CK. Combustion physics. 1st ed. Cambridge: Cambridge University Press; 2010.
[73] Peters N. The turbulent burning velocity for large-scale and small-scale turbulence. J Fluid Mech 1999;384:107–32.
[74] Andrews GE, Bradley D, Lwakabamba SB. Turbulence and turbulent flame propagation—A critical appraisal. Combust Flame 1975;24:285–304.
[75] Abdel-Gayed RG, D B. A two-eddy theory of premixed turbulent flame propagation. Phil Trans R Soc Lond A 1981;301:1–25.
[76] Bradley D. How fast can we burn? Symp (Int) Combust 1992;24:247–62.
[77] Zitouni S, Bréquigny P, Mounaïm-Rousselle C. Turbulent partially cracked ammonia/air premixed spherical flames. Fuel Commun 2024;20:100126.
[78] Du Wang C, Ji Z, Wang S, Wang T, Zhang JY. Measurement of oxy-ammonia laminar burning velocity at normal and elevated temperatures. Fuel 2020;279:118425.
[79] Fan Q, Liu X, Xu L, Subash AA, Brackmann C, Aldén M, et al. Flame structure and burning velocity of ammonia/air turbulent premixed flames at high Karlovitz number conditions. Combust Flame 2022;238:111943.
[80] Dai H, Wang J, Cai X, Su S, Zhao H, Huang Z. Measurement and scaling of turbulent burning velocity of ammonia/methane/air propagating spherical flames at elevated pressure. Combust Flame 2022;242:112183.
[81] Wang S, Elbaz AM, Wang G, Wang Z, Roberts WL. Turbulent flame speed of NH_3/CH_4/H_2/H_2O/air-mixtures: effects of elevated pressure and Lewis number. Combust Flame 2023;247:112488.
[82] Bradley D, Lawes M, Liu K, Woolley R. The quenching of premixed turbulent flames of iso-octane, methane and hydrogen at high pressures. Proc Combust Inst 2007;31:1393–400.
[83] Lawes M, Ormsby MP, Sheppard CG, Woolley R. The turbulent burning velocity of iso-octane/air mixtures. Combust Flame 2012;159:1949–59.
[84] Sick V, Hartman MR, Arpaci VS, Anderson RW. Turbulent scales in a fan-stirred combustion bomb. Combust Flame 2001;127:2119–23.
[85] Weiß M, Zarzalis N, Suntz R. Experimental study of Markstein number effects on laminar flamelet velocity in turbulent premixed flames. Combust Flame 2008;154:671–91.
[86] Galmiche B, Mazellier N, Halter F, Foucher F. Turbulence characterization of a high-pressure high-temperature fan-stirred combustion vessel using LDV, PIV and TR-PIV measurements. Exp Fluids 2014;55:1636.
[87] Xu S, Huang S, Huang R, Wei W, Cheng X, Ma Y, et al. Estimation of turbulence characteristics from PIV in a high-pressure fan-stirred constant volume combustion chamber. Appl Therm Eng 2017;110:346–55.
[88] Zhao H, Li G, Wang J, Huang Z. Experimental study of H_2/air turbulent expanding flames over wide equivalence ratios: effects of molecular transport. Fuel 2023;341:127652.
[89] Fairweather M, Ormsby MP, Sheppard CGW, Woolley R. Turbulent burning rates of methane and methane–hydrogen mixtures. Combust Flame 2009;156:780–90.
[90] Mandilas C, Ormsby MP, Sheppard CGW, Woolley R. Effects of hydrogen addition on laminar and turbulent premixed methane and iso-octane–air flames. Proc Combust Inst 2007;31:1443–50.
[91] Ichikawa A, Naito Y, Hayakawa A, Kudo T, Kobayashi H. Burning velocity and flame structure of CH_4/NH_3/air turbulent premixed flames at high pressure. Int J Hydrogen Energy 2019;44:6991–9.
[92] Karpov V, Lipatnikov A, Imont V. A test of an engineering model of premixed turbulent combustion. Symp (Int) Combust 1996;26:249–57.
[93] Bradley D, Lawes M, Mansour MS. Correlation of turbulent burning velocities of ethanol–air, measured in a fan-stirred bomb up to 1.2MPa. Combust Flame 2011;158:123–38.
[94] Wu MS, Kwon S, Driscoll JF, Faeth GM. Turbulent premixed hydrogen/air flames at high Reynolds numbers. Combust Sci Technol 1990;73:327–50.
[95] Chaudhuri S, Wu F, Law CK. Scaling of turbulent flame speed for expanding flames with Markstein diffusion considerations. Phys Rev E Stat Nonlin Soft Matter Phys 2013;88:33005.

[96] Zhao H, Wang J, Cai X, Dai H, Bian Z, Huang Z. Flame structure, turbulent burning velocity and its unified scaling for lean syngas/air turbulent expanding flames. Int J Hydrogen Energy 2021;46:25699–711.
[97] Kitagawa T, Nakahara T, Maruyama K, Kado K, Hayakawa A, Kobayashi S. Turbulent burning velocity of hydrogen–air premixed propagating flames at elevated pressures. Int J Hydrogen Energy 2008;33:5842–9.
[98] Goulier J, Comandini A, Halter F, Chaumeix N. Experimental study on turbulent expanding flames of lean hydrogen/air mixtures. Proc Combust Inst 2017;36:2823–32.
[99] Ichimura R, Hadi K, Hashimoto N, Hayakawa A, Kobayashi H, Fujita O. Extinction limits of an ammonia/air flame propagating in a turbulent field. Fuel 2019;246:178–86.
[100] Hayakawa A, Arakawa Y, Mimoto R, Somarathne KD, Kunkuma A, Kudo T, et al. Experimental investigation of stabilization and emission characteristics of ammonia/air premixed flames in a swirl combustor. Int J Hydrogen Energy 2017;42:14010–8.
[101] Somarathne KD, Kunkuma Amila A, Hayakawa HK. Numerical investigation on the combustion characteristics of turbulent premixed ammonia/air flames stabilized by a swirl burner. J Fluid Sci Technol 2016;11:JFST0026-JFST0026.
[102] Xia Y, Hashimoto G, Hadi K, Hashimoto N, Hayakawa A, Kobayashi H, et al. Turbulent burning velocity of ammonia/oxygen/nitrogen premixed flame in O_2-enriched air condition. Fuel 2020;268:117383.
[103] Wang S, Elbaz AM, Wang Z, Roberts WL. The effect of oxygen content on the turbulent flame speed of ammonia/oxygen/nitrogen expanding flames under elevated pressures. Combust Flame 2021;232:111521.
[104] Hashimoto G, Hadi K, Xia Y, Hamid A, Hashimoto N, Hayakawa A, et al. Turbulent flame propagation limits of ammonia/methane/air premixed mixture in a constant volume vessel. Proc Combust Inst 2021;38:5171–80.
[105] Xu L, Fan Q, Liu X, Cai X, Subash AA, Brackmann C, et al. Flame/turbulence interaction in ammonia/air premixed flames at high karlovitz numbers. Proc Combust Inst 2023;39:2289–98.
[106] K.D.K. Somarathne, H. Yamashita, S. Colson, E. Okafor, A. Hayakawa, T. Kudo, H. Kobayashi (Eds.), Liquid Ammonia Spray Combustion and Emission Characteristics with Gaseous Hydrogen/air Co-firing, 13th Asia-Pacific Conference on Combustion 2021 ADNEC, 2021.
[107] Somarathne KD, Kunkuma Amila EC, Okafor A, Hayakawa T, Kudo O, Kurata N, et al. Emission characteristics of turbulent non-premixed ammonia/air and methane/air swirl flames through a rich-lean combustor under various wall thermal boundary conditions at high pressure. Combust Flame 2019;210:247–61.
[108] Yamashita H, Hayakawa A, Oku K, Colson S, Reibel G, Chen Y, et al. Visualization of liquid ammonia spray using 2p-SLIPI and comparison of liquid ammonia spray and gaseous ammonia combustion in a swirl combustor at atmospheric pressure. Fuel 2024;371:131833.
[109] Shy SS, Liu CC, Lin JY, Chen LL, Lipatnikov AN, Yang SI. Correlations of high-pressure lean methane and syngas turbulent burning velocities: effects of turbulent Reynolds, Damköhler, and Karlovitz numbers. Proc Combust Inst 2015;35:1509–16.
[110] Chiu C-W, Dong Y-C, Shy SS. High-pressure hydrogen/carbon monoxide syngas turbulent burning velocities measured at constant turbulent Reynolds numbers. Int J Hydrogen Energy 2012;37:10935–46.
[111] Liu C-C, Shy SS, Peng M-W, Chiu C-W, Dong Y-C. High-pressure burning velocities measurements for centrally-ignited premixed methane/air flames interacting with intense near-isotropic turbulence at constant Reynolds numbers. Combust Flame 2012;159:2608–19.
[112] Shy SS, Liu CC, Shih WT. Ignition transition in turbulent premixed combustion. Combust Flame 2010;157:341–50.
[113] P.D. Ronney, in: J. Buckmaster, T. Takeno (Eds.), Springer, 1995, pp. 1–22.
[114] Zimont VL. Theory of turbulent combustion of a homogeneous fuel mixture at high reynolds numbers, Combust Explos. Shock Waves 1979;15:305–11.
[115] Tamadonfar P, Gülder ÖL. Effects of mixture composition and turbulence intensity on flame front structure and burning velocities of premixed turbulent hydrocarbon/air Bunsen flames. Combust Flame 2015;162:4417–41.
[116] Kobayashi H, Seyama K, Hagiwara H, Ogami Y. Burning velocity correlation of methane/air turbulent premixed flames at high pressure and high temperature. Proc Combust Inst 2005;30:827–34.
[117] Kobayashi H, Kawabata Y, Maruta K. Experimental study on general correlation of turbulent burning velocity at high pressure. Symp (Int) Combust 1998;27:941–8.
[118] Chaudhuri S, Wu F, Zhu D, Law CK. Flame speed and Self-Similar Propagation of Expanding Turbulent Premixed Flames. Phys Rev Lett 2012;108:44503.
[119] Nguyen MT, Yu DW, Shy SS. General correlations of high pressure turbulent burning velocities with the consideration of Lewis number effect. Proc Combust Inst 2019;37:2391–8.
[120] Driscoll J. Turbulent premixed combustion: Flamelet structure and its effect on turbulent burning velocities. Prog Energy Combust Sci 2008;34:91–134.
[121] Lipatnikov AN, Chomiak J. Molecular transport effects on turbulent flame propagation and structure. Prog Energy Combust Sci 2005;31:1–73.
[122] Bradley D, Lau AKC, Lawes M, Smith FT. Flame stretch rate as a determinant of turbulent burning velocity. Philos Trans Phys Sci Eng 1992;338:359–87.
[123] Wang Z, Zhou B, Yu S, Brackmann C, Li Z, Richter M, et al. Structure and burning velocity of turbulent premixed methane/air jet flames in thin-reaction zone and distributed reaction zone regimes. Proc Combust Inst 2019;37:2537–44.
[124] Ávila CD, Cardona S, Abdullah M, Younes M, Jamal A, Guiberti TF, et al. Experimental assessment of the performance of a commercial micro gas turbine fueled by ammonia-methane blends. Appl Energy Combust Sci 2023;13:100104.
[125] Kurata O, Iki N, Matsunuma T, Inoue T, Tsujimura T, Furutani H, et al. Performances and emission characteristics of NH3–air and NH3CH4–air combustion gas-turbine power generations. Proc Combust Inst 2017;36:3351–9.
[126] Kurata O, Iki N, Inoue T, Matsunuma T, Tsujimura T, Furutani H, et al. Development of a wide range-operable, rich-lean low-NOx combustor for NH3 fuel gas-turbine power generation. Proc Combust Inst 2019;37:4587–95.
[127] Kobayashi H, Tamura T, Maruta K, Niioka T, Williams FA. Burning velocity of turbulent premixed flames in a high-pressure environment. Symp (Int) Combust 1996;26:389–96.
[128] Ichikawa Y, Otawara Y, Kobayashi H, Ogami Y, Kudo T, Okuyama M, et al. Flame structure and radiation characteristics of $CO/H_2/CO_2$/air turbulent premixed flames at high pressure. Proc Combust Inst 2011;33:1543–50.
[129] Kobayashi H, Otawara Y, Wang J, Matsuno F, Ogami Y, Okuyama M, et al. Turbulent premixed flame characteristics of a CO/H2/O2 mixture highly diluted with CO2 in a high-pressure environment. Proc Combust Inst 2013;34:1437–45.
[130] Dai H, Wang J, Cai X, Su S, Zhao H, Huang Z. Lewis number effects on laminar and turbulent expanding flames of NH_3/H_2/air mixtures at elevated pressures. Proc Combust Inst 2023;39:1689–97.
[131] Wang S, Elbaz AM, Arab OZ, Roberts WL. Turbulent flame speed measurement of NH3/H2/air and CH4/air flames and a numerical case study of NO emission in a constant volume combustion chamber (C.V.C.C.). Fuel 2023;332:126152.
[132] Cai X, Fan Q, Bai X-S, Wang J, Zhang M, Huang Z, et al. Turbulent burning velocity and its related statistics of ammonia-hydrogen-air jet flames at high Karlovitz number: effect of differential diffusion. Proc Combust Inst 2023;39:4215–26.
[133] Yang W, Ranga Dinesh K, Luo KH, Thevenin D. Direct numerical simulation of turbulent premixed ammonia and ammonia-hydrogen combustion under engine-relevant conditions. Int J Hydrogen Energy 2022;47:11083–100.
[134] Yu R, Lipatnikov AN. DNS study of dependence of bulk consumption velocity in a constant-density reacting flow on turbulence and mixture characteristics. Phys Fluids 1994;29(2017):65116.
[135] Chi C, Han W, Thévenin D. Effects of molecular diffusion modeling on turbulent premixed NH_3/H_2/air flames. Proc Combust Inst 2023;39:2259–68.
[136] Tang H, Yang C, Wang G, Krishna Y, Guiberti TF, Roberts WL, et al. Scalar structure in turbulent non-premixed $NH_3/H_2/N_2$ jet flames at elevated pressure using Raman spectroscopy. Combust Flame 2022;244:112292.
[137] Tang H, Yang C, Krishna Y, Wang G, Roberts WL, Guiberti TF, et al. Differential diffusion effects in the near field of non-premixed NH3/H2/N2-air jet flames at elevated pressure. Exp Therm Fluid Sci 2023;149:111020.
[138] Wang G, Tang H, Yang C, Magnotti G, Roberts WL, Guiberti TF. Quantitative laser-induced fluorescence of NO in ammonia-hydrogen-nitrogen turbulent jet flames at elevated pressure. Proc Combust Inst 2023;39:1465–74.
[139] Valera-Medina A, Pugh DG, Marsh P, Bulat G, Bowen P. Preliminary study on lean premixed combustion of ammonia-hydrogen for swirling gas turbine combustors. Int J Hydrogen Energy 2017;42:24495–503.
[140] Valera-Medina A, Gutesa M, Xiao H, Pugh D, Giles A, Goktepe B, et al. Premixed ammonia/hydrogen swirl combustion under rich fuel conditions for gas turbines operation. Int J Hydrogen Energy 2019;44:8615–26.
[141] Katoch A, Guiberti TF, de Campos DV, Lacoste DA. Dual-fuel, dual-swirl burner for the mitigation of thermoacoustic instabilities in turbulent ammonia-hydrogen flames. Combust Flame 2022;246:112392.
[142] Zitouni S, Brequigny P, Mounaïm-Rousselle C. Turbulent flame speed and morphology of pure ammonia flames and blends with methane or hydrogen. Proc Combust Inst 2023;39:2269–78.
[143] Lhuillier C, Brequigny P, Contino F, Mounaïm-Rousselle C. Experimental investigation on ammonia combustion behavior in a spark-ignition engine by means of laminar and turbulent expanding flames. Proc Combust Inst 2021;38:5859–68.
[144] Lipatnikov AN, Chomiak J. Turbulent flame speed and thickness: phenomenology, evaluation, and application in multi-dimensional simulations. Prog Energy Combust Sci 2002;28:1–74.
[145] Lipatnikov AN, Chomiak J. Effects of premixed flames on turbulence and turbulent scalar transport. Prog Energy Combust Sci 2010;36:1–102.
[146] Chaudhuri S, Akkerman V, Law CK. Spectral formulation of turbulent flame speed with consideration of hydrodynamic instability. Phys Rev E Stat Nonlin Soft Matter Phys 2011;84:26322.
[147] Kobayashi H, Kawazoe H. Flame instability effects on the smallest wrinkling scale and burning velocity of high-pressure turbulent premixed flames. Proc Combust Inst 2000;28:375–82.
[148] Jiang LJ, Shy SS, Li WY, Huang HM, Nguyen MT. High-temperature, high-pressure burning velocities of expanding turbulent premixed flames and their comparison with Bunsen-type flames. Combust Flame 2016;172:173–82.
[149] Venkateswaran P, Marshall A, Shin DH, Noble D, Seitzman J, Lieuwen T. Measurements and analysis of turbulent consumption speeds of H_2/CO mixtures. Combust Flame 2011;158:1602–14.
[150] Dai H, Wang J, Su S, Su L, Cai X, Huang Z. Turbulent burning velocity of hydrogen/n-heptane/air propagating spherical flames: effects of hydrogen content. Combust Flame 2024;260:113248.
[151] Pio G, Eckart S, Richter A, Krause H, Salzano E. Detailed kinetic analysis of synthetic fuels containing ammonia. Fuel 2024;362:130747.
[152] Poinsot T, Veynante D, Candel S. Diagrams of premixed turbulent combustion based on direct simulation. Symp (Int) Combust 1991;23:613–9.
[153] Cai X, Wang J, Bian Z, Zhao H, Zhang M, Huang Z. Self-similar propagation and turbulent burning velocity of CH_4/H_2/air expanding flames: effect of Lewis number. Combust Flame 2020;212:1–12.

[154] Bowers J, Durant E, Ranjan R. Effects of pressure and characteristic scales on the structural and statistical features of methane/air turbulent premixed flames. Flow Turbul Combust 2024. https://doi.org/10.1007/s10494-024-00550-6.
[155] Fan Q, Liu X, Cai X, Brackmann C, Alden M, Bai X-S, et al. Structure and scalar correlation of ammonia/air turbulent premixed flames in the distributed reaction zone regime. Combust Flame 2022;241:112090.
[156] S. Eckart, G. Pio, T. Zirwes, F. Zhang, E. Salzano, H. Krause, H. Bockhorn, Impact of carbon dioxide and nitrogen addition on the global structure of hydrogen flames, Fuel- In Press (2022) 126929.
[157] Zlochower IA, Green GM. The limiting oxygen concentration and flammability limits of gases and gas mixtures. J Loss Prev Process Ind 2009;22:499–505.
[158] Karim GA, Wierzba I, Boon S. The lean flammability limits in air of methane, hydrogen and carbon monoxide at low temperatures. Cryogenics (Guildf) 1984; 24:305–8.
[159] Gianmaria P, Sven E, Ernesto S, Hartmut K. Kinetic parameters for safety of hydrogen-containing mixtures. Chem Eng Trans 2022;90:475–80.
[160] Tamura M, Gotou T, Ishii H, Riechelmann D. Experimental investigation of ammonia combustion in a bench scale 1.2 MW-thermal pulverised coal firing furnace. Appl Energy 2020;277:115580.
[161] Ishihara S, Zhang J, Ito T. Numerical calculation with detailed chemistry of effect of ammonia co-firing on NO emissions in a coal-fired boiler. Fuel 2020;266: 116924.
[162] Y. Hagihara, Y. Yamamoto, M. Numata, T. Matsuda, in: K. Aika, H. Kobayashi (Eds.), CO2 free ammonia as an energy carrier: Japan's insights, Springer, Singapore, 2023, pp. 641–651.
[163] Colson S, Kuhni M, Hayakawa A, Kobayashi H, Galizzi C, Escudié D. Stabilization mechanisms of an ammonia/methane non-premixed jet flame up to liftoff. Combust Flame 2021;234:111657.
[164] Alfazazi A, Elbaz AM, Li J, Abdelwahid S, Im HG, Dally B. Characteristics of ammonia-hydrogen nonpremixed bluff-body-stabilized flames. Combust Flame 2023;258:113066.
[165] Alfazazi A, Es-sebbar E, Kumar S, Abdelwahid S, Asiri AH, Zhao W, et al. Effects of ammonia in-situ partial cracking on the structure of bluff-body non-premixed flames. Proc Combust Inst 2024;40:105697.
[166] Osipova KN, Korobeinichev OP, Shmakov AG. Chemical structure and laminar burning velocity of atmospheric pressure premixed ammonia/hydrogen flames. Int J Hydrogen Energy 2021;46:39942–54.
[167] Osipova KN, Sarathy SM, Korobeinichev OP, Shmakov AG. Chemical structure of premixed ammonia/hydrogen flames at elevated pressures. Combust Flame 2022; 246:112419.
[168] Duynslaegher C, Jeanmart H, Vandooren J. Flame structure studies of premixed ammonia/hydrogen/oxygen/argon flames: Experimental and numerical investigation. Proc Combust Inst 2009;32:1277–84.
[169] Aldén M. Spatially and temporally resolved laser/optical diagnostics of combustion processes: from fundamentals to practical applications. Proc Combust Inst 2023;39:1185–228.
[170] Sun J, Bao Y, Ravelid J, Nilsson S, Konnov AA, Ehn A. Application of emission spectroscopy in plasma-assisted NH_3/air combustion using nanosecond pulsed discharge. Combust Flame 2024;263:113400.
[171] Zhu X, Khateeb AA, Roberts WL, Guiberti TF. Chemiluminescence signature of premixed ammonia-methane-air flames. Combust Flame 2021;231:111508.
[172] Weng W, Aldén M, Li Z. Visible chemiluminescence of ammonia premixed flames and its application for flame diagnostics. Proc Combust Inst 2023;39:4327–34.
[173] Sun J, Tang Q, Wen M, Huang L, Liu H, Yao M. Combustion characteristics and flame development of ammonia in an optical spark-ignition engine. Fuel 2024; 375:132601.
[174] Yang X, Peng Z, Ding Y, Du Y. Spatially resolved broadband absorption spectroscopy measurements of temperature and multiple species (NH, OH, NO, and NH 3) in atmospheric-pressure premixed ammonia/methane/air flames. Fuel 2023;332:126073.
[175] Alturaifi SA, Mathieu O, Petersen EL. A shock-tube study of NH_3 and NH_3/H_2 oxidation using laser absorption of NH_3 and H_2O. Proc Combust Inst 2023;39: 233–41.
[176] S. Clees, T.M. Rault, M. Figueroa-Labastida, S.C. Barnes, Ferris, Alison M., Hansen, Ronald K., 13th U.S. National Combustion MeetingAt: College Station, TX.
[177] Gu W, Liu X, Wang Z, Zheng H. Applications of PLIF in fundamental research on turbulent combustion of hydrogen and hydrogen hybrid fuels: a brief review. Int J Hydrogen Energy 2024;78:1240–74.
[178] Wang G, Wang S, Guiberti TF. Simultaneous planar laser-induced fluorescence measurement of reactant NH_3, radical NH, and pollutant NO in ammonia-hydrogen flames using a single dye laser. Combust Flame 2023;256:112981.
[179] Tang H, Ezendeeva D, Magnotti G. Simultaneous measurements of NH_2 and major species and temperature with a novel excitation scheme in ammonia combustion at atmospheric pressure. Combust Flame 2023;250:112639.
[180] Baba NE, Desgroux P, Lamoureux N. OH and NO profiles in premixed $NH_3/O_2/N_2$ low-pressure flames measured by calibrated-LIF: Comparison with modeling. Proc Combust Inst 2024;40:105498.
[181] Tang H, Yang C, Wang G, Guiberti TF, Magnotti G. Raman spectroscopy for quantitative measurements of temperature and major species in high-pressure non-premixed NH3/H2/N2 counterflow flames. Combust Flame 2022;237: 111840.
[182] Zubairova A, Kim H, Aldén M, Brackmann C. Fluorescence-free quantitative measurements of nitric oxide and major species in an ammonia/air flame with Raman spectroscopy. Proc Combust Inst 2023;39:1317–24.
[183] Lill J, Stark M, Schultheis R, Weinmann A, Dreizler A, Geyer D. Towards non-intrusive, quantitative N_2O Raman measurements in ammonia flames. Proc Combust Inst 2024;40:105458.
[184] Brackmann C, Alekseev VA, Zhou B, Nordström E, Bengtsson P-E, Li Z, et al. Structure of premixed ammonia + air flames at atmospheric pressure: Laser diagnostics and kinetic modeling. Combust Flame 2016;163:370–81.
[185] Weng W, Brackmann C, Aldén M, Li Z. Planar laser-induced photofragmentation fluorescence for quantitative ammonia imaging in combustion environments. Combust Flame 2022;235:111687.
[186] Wei D, Fang H, Hu L, Rong Y, Zhou H. Effect of acoustic excitation on the combustion and emission characteristics of methane-ammonia-air swirling flame. Fuel 2023;352:129117.
[187] Fenimore CP, Jones GW. Oxidation of ammonia in flames. J Phys Chem 1961;65: 298–303.
[188] Maclean DI, Wagner HG. The structure of the reaction zones of ammonia-oxygen and hydrazine-decomposition flames. Symp (Int) Combust 1967;11:871–8.
[189] Fisher CJ. A study of rich ammonia/oxygen/nitrogen flames. Combust Flame 1977;30:143–9.
[190] Miller JA, Smooke MD, Green RM, Kee RJ. Kinetic modeling of the oxidation of ammonia in flames. Combust Sci Technol 1983;34:149–76.
[191] Dasch CJ, Blint RJ. A mechanistic and experimental study of ammonia flames. Combust Sci Technol 1984;41:223–44.
[192] Miller JA, Bowman CT. Mechanism and modeling of nitrogen chemistry in combustion. Prog Energy Combust Sci 1989;15:287–338.
[193] Lee JH, Kim JH, Park JH, Kwon OC. Studies on properties of laminar premixed hydrogen-added ammonia/air flames for hydrogen production. Int J Hydrogen Energy 2010;35:1054–64.
[194] Lee JH, Lee SI, Kwon OC. Effects of ammonia substitution on hydrogen/air flame propagation and emissions. Int J Hydrogen Energy 2010;35:11332–41.
[195] Um DH, Joo JM, Lee S, Kwon OC. Combustion stability limits and NOx emissions of nonpremixed ammonia-substituted hydrogen-air flames. Int J Hydrogen Energy 2013;38:14854–65.
[196] Mathieu O, Petersen EL. Experimental and modeling study on the high-temperature oxidation of Ammonia and related NOx chemistry. Combust Flame 2015;162:554–70.
[197] Glarborg P, Miller JA, Ruscic B, Klippenstein SJ. Modeling nitrogen chemistry in combustion. Prog Energy Combust Sci 2018;67:31–68.
[198] Shrestha KP, Seidel L, Zeuch T, Mauss F. Detailed kinetic mechanism for the oxidation of ammonia including the formation and reduction of nitrogen oxides. Energy Fuels 2018;32:10202–17.
[199] Henshaw PF, D'Andrea T, Mann KR, Ting DS. Premixed ammonia-methane-air combustion. Combust Sci Technol 2005;177:2151–70.
[200] Tian Z, Li Y, Zhang L, Glarborg P, Qi F. An experimental and kinetic modeling study of premixed $NH_3/CH_4/O_2$/Ar flames at low pressure. Combust Flame 2009; 156:1413–26.
[201] Skreiberg Ø, Kilpinen P, Glarborg P. Ammonia chemistry below 1400 K under fuel-rich conditions in a flow reactor. Combust Flame 2004;136:501–18.
[202] Konnov AA. Implementation of the NCN pathway of prompt-NO formation in the detailed reaction mechanism. Combust Flame 2009;156:2093–105.
[203] Lindstedt RP, Lockwood FC, Selim MA. Detailed kinetic modelling of chemistry and temperature effects on ammonia oxidation. Combust Sci Technol 1994;99: 253–76.
[204] Mendiara T, Glarborg P. Ammonia chemistry in oxy-fuel combustion of methane. Combust Flame 2009;156:1937–49.
[205] Dai L, Gersen S, Glarborg P, Mokhov A, Levinsky H. Autoignition studies of NH3/ CH4 mixtures at high pressure. Combust Flame 2020;218:19–26.
[206] Issayev G, Giri BR, Elbaz AM, Shrestha KP, Mauss F, Roberts WL, et al. Combustion behavior of ammonia blended with diethyl ether. Proc Combust Inst 2021;38:499–506.
[207] Issayev G, Giri BR, Elbaz AM, Shrestha KP, Mauss F, Roberts WL, et al. Ignition delay time and laminar flame speed measurements of ammonia blended with dimethyl ether: a promising low carbon fuel blend. Renew Energy 2022;181: 1353–70.
[208] Shrestha KP, Lhuillier C, Barbosa AA, Brequigny P, Contino F, Mounaïm-Rousselle C, et al. An experimental and modeling study of ammonia with enriched oxygen content and ammonia/hydrogen laminar flame speed at elevated pressure and temperature. Proc Combust Inst 2021;38:2163–74.
[209] Lhuillier C, Brequigny P, Lamoureux N, Contino F, Mounaïm-Rousselle C. Experimental investigation on laminar burning velocities of ammonia/hydrogen/ air mixtures at elevated temperatures. Fuel 2020;263:116653.
[210] Sabia P, Manna MV, Ragucci R, de Joannon M. Mutual inhibition effect of hydrogen and ammonia in oxidation processes and the role of ammonia as "strong" collider in third-molecular reactions. Int J Hydrogen Energy 2020;45: 32113–27.
[211] Manna MV, Ragucci R, de Joannon M, Sabia P. The interaction between NH_3 and CH_4 oxidation chemistry: a comprehensive study through combustion regimes and thermokinetic instabilities. Fuel 2024;371:131868.
[212] He X, Li M, Shu B, Fernandes R, Moshammer K. Exploring the effect of Different Reactivity Promoters on the Oxidation of Ammonia in a Jet-Stirred Reactor. J Phys Chem A 2023;127:1923–40.
[213] Shrestha KP, Giri BR, Elbaz AM, Issayev G, Roberts WL, Seidel L, et al. A detailed chemical insights into the kinetics of diethyl ether enhancing ammonia combustion and the importance of NOx recycling mechanism. Fuel Commun 2022;10:100051.

[214] Velamati RK, Mohammad A, Eckart S, Veetil JE. Ignition and cool flame interactions of DME/H_2/air blends in a micro-channel with a wall temperature gradient. Int J Thermofluids 2024;24:100891.
[215] Eckart S, Benaissa S, Alsulami RA, Juhany KA, Krause H, Mohammad A. Laminar burning velocity, emissions, and flame structure of dimethyl ether-hydrogen air mixtures. Int J Hydrogen Energy 2023;48:35771–85.
[216] Ai Y, Zhou Z, Chen Z, Kong W. Laminar flame speed and Markstein length of syngas at normal and elevated pressures and temperatures. Fuel 2014;137:339–45.
[217] Kanoshima R, Hayakawa A, Kudo T, Okafor EC, Colson S, Ichikawa A, et al. Effects of initial mixture temperature and pressure on laminar burning velocity and Markstein length of ammonia/air premixed laminar flames. Fuel 2022;310:122149.
[218] Shrestha KP, Giri BR, Pelé R, Aljohani K, Brequigny P, Mauss F, et al. A comprehensive chemical kinetic modeling and experimental study of NH_3-methanol/ethanol combustion towards net-zero CO_2. Combust Flame 2024.
[219] He X, Shu B, Nascimento D, Moshammer K, Costa M, Fernandes RX. Auto-ignition kinetics of ammonia and ammonia/hydrogen mixtures at intermediate temperatures and high pressures. Combust Flame 2019;206:189–200.
[220] Pochet M, Dias V, Moreau B, Foucher F, Jeanmart H, Contino F. Experimental and numerical study, under LTC conditions, of ammonia ignition delay with and without hydrogen addition. Proc Combust Inst 2019;37:621–9.
[221] Marshall P, Rawling G, Glarborg P. New reactions of diazene and related species for modelling combustion of amine fuels. Mol Phys 2021;119:e1979674.
[222] Klippenstein SJ, Glarborg P. Theoretical kinetics predictions for NH2 + HO2. Combust Flame 2022;236:111787.
[223] Dai L, Gersen S, Glarborg P, Levinsky H, Mokhov A. Experimental and numerical analysis of the autoignition behavior of NH3 and NH3/H2 mixtures at high pressure. Combust Flame 2020;215:134–44.
[224] Liao W, Wang Y, Chu Z, Tao C, Yang B. Chemical insights into the two-stage ignition behavior of NH3/H2 mixtures in an RCM. Combust Flame 2023;256:112985.
[225] Mashruk S, Kovaleva M, Alnasif A, Chong CT, Hayakawa A, Okafor EC, et al. Nitrogen oxide emissions analyses in ammonia/hydrogen/air premixed swirling flames. Energy 2022;260:125183.
[226] D. Price, R. Birnbaum, R. Batiuk, M. McCullough, R. Smith, PB-98-104631/XAB; EPA-452/R-97/002, Nitrogen oxides: Impacts on public health and the environment, PB-98-104631/XAB; EPA-452/R-97/002.
[227] C. Costa, M. Wironen, K. Racette, E.K. Wollenberg, Global Warming Potential* (GWP*): Understanding the implications for mitigating methane emissions in agriculture, CGIAR Research Program on Climate Change, Agriculture and Food Security, 2021.
[228] Mashruk S, Xiao H, Valera-Medina A. Rich-Quench-Lean model comparison for the clean use of humidified ammonia/hydrogen combustion systems. Int J Hydrogen Energy 2021;46:4472–84.
[229] Bian J, Vandooren J, van Tiggelen PJ. Experimental study of the structure of an ammonia-oxygen flame. Symp (Int) Combust 1988;21:953–63.
[230] Chou MS, Dean AM, Stern D. Laser absorption measurements of OH, NH, and NH2 in NH3/O2 flames: Determination of an oscillator strength for NH2. J Chem Phys 1982;76:5334–40.
[231] Chou M-S, Dean AM, Stern D. Laser induced fluorescence and absorption measurements of NO in NH3/O2 and CH4/air flames. J Chem Phys 1983;78:5962–70.
[232] Bian J, Vandooren J, van Tiggelen PJ. Experimental study of the formation of nitrous and nitric oxides in H2−O2−Ar flames seeded with NO and/or NH3. Symp (Int) Combust 1991;23:379–86.
[233] Vandooren J. Comparison of the Experimental Structure of an Ammonia Seeded Rich-Hydrogen-Oxygen-Argon Flame with the calculated Ones along Several Reaction Mechanisms. Combust Sci Technol 1992;84:335–44.
[234] Vandooren J, Bian J, van Tiggelen PJ. Comparison of experimental and calculated structures of an ammonia nitric oxide flame. Importance of the NH_2 + NO reaction. Combust Flame 1994;98:402–10.
[235] Eckart S, Shrestha KP, Giri BR, Fang Q, Chen C, Li W, et al. Chemical insights into ethyl acetate flames from experiment and kinetic modeling: Laminar burning velocity, speciation and NO emission. Proc Combust Inst 2024;40:105487.
[236] Ravikrishna RV, Sahu AB. Advances in understanding combustion phenomena using non-premixed and partially premixed counterflow flames: a review. Int J Spray Combust Dynam 2018;10:38–71.
[237] Venizelos DT, Sausa RC. Detailed chemical kinetics studies of an NH3/N2O/Ar flame by laser-induced fluorescence, mass spectrometry, and modeling. Proc Combust Inst 2000;28:2411–8.
[238] Shmakov AG, Korobeinichev OP, Rybitskaya IV, Chernov AA, Knyazkov DA, Bolshova TA, et al. Formation and consumption of NO in H_2+O_2+N_2 flames doped with NO or NH_3 at atmospheric pressure. Combust Flame 2010;157:556–65.
[239] Duynslaegher C, Contino F, Vandooren J, Jeanmart H. Modeling of ammonia combustion at low pressure. Combust Flame 2012;159:2799–805.
[240] Duynslaegher C, Jeanmart H, Vandooren J. Ammonia combustion at elevated pressure and temperature conditions. Fuel 2010;89:3540–5.
[241] Brackmann C, Nilsson EJ, Nauclér JD, Aldén M, Konnov AA. Formation of NO and NH in NH_3-doped CH_4 + N_2 + O_2 flame: Experiments and modelling. Combust Flame 2018;194:278–84.
[242] Samu V, Varga T, Rahinov I, Cheskis S, Turányi T. Determination of rate parameters based on NH_2 concentration profiles measured in ammonia-doped methane–air flames. Fuel 2018;212:679–83.
[243] Lamoureux N, Marschallek-Watroba K, Desgroux P, Pauwels J-F, Sylla MD, Gasnot L. Measurements and modelling of nitrogen species in CH_4/O_2/N_2 flames doped with NO, NH_3, or NH_3+NO. Combust Flame 2017;176:48–59.
[244] Rocha RC, Zhong S, Xu L, Bai X-S, Costa M, Cai X, et al. Structure and Laminar Flame speed of an Ammonia/Methane/Air Premixed Flame under Varying pressure and Equivalence Ratio. Energy Fuel 2021;35:7179–92.
[245] Shrestha KP, Giri BR, Pelé R, Aljohani K, Brequigny P, Mauss F, et al. A comprehensive chemical kinetic modeling and experimental study of NH3−methanol/ethanol combustion towards net-zero CO2 emissions. Combust Flame 2025;274:113954.
[246] Woo M, Choi BC, Ghoniem AF. Experimental and numerical studies on NOx emission characteristics in laminar non-premixed jet flames of ammonia-containing methane fuel with oxygen/nitrogen oxidizer. Energy 2016;114:961–72.
[247] Thomas DE, Shrestha KP, Mauss F, Northrop WF. Extinction and NO formation of ammonia-hydrogen and air non-premixed counterflow flames. Proc Combust Inst 2023;39:1803–12.
[248] Shrestha KP, Eckart S, Drost S, Fritsche C, Schießl R, Seidel L, et al. A comprehensive kinetic modeling of oxymethylene ethers (OMEn, n=1–3) oxidation - laminar flame speed and ignition delay time measurements. Combust Flame 2022;246:112426.
[249] Manna MV, Sabia P, Shrestha KP, Seidel L, Ragucci R, Mauss F, et al. NH3NO interaction at low-temperatures: an experimental and modeling study. Proc Combust Inst 2023;39:775–84.
[250] A. Wong, S.D. Selin, C. Eastham, C. Mounaïm-Rouselle, Zhang C., Allroggen F., Environmental Research Letters.
[251] Wang S, Wang Z, Elbaz AM, Han X, He Y, Costa M, et al. Experimental study and kinetic analysis of the laminar burning velocity of NH3/syngas/air, NH3/CO/air and NH3/H2/air premixed flames at elevated pressures. Combust Flame 2020;221:270–87.
[252] Okafor EC, Somarathne KKA, Hayakawa A, Kudo T, Kurata O, Iki N, et al. Towards the development of an efficient low-NOx ammonia combustor for a micro gas turbine. Proc Combust Inst 2019;37:4597–606.
[253] Sorrentino G, Sabia P, Bozza P, Ragucci R, de Joannon M. Low-NOx conversion of pure ammonia in a cyclonic burner under locally diluted and preheated conditions. Appl Energy 2019;254:113676.
[254] B. Sun, X. Kang, Y. Wang, Combustion characteristics of ammonia–air in a heat-recirculating Swiss-roll burner, Phys. Fluids (1994) 36 (2024), doi:10.1063/5.0233685.
[255] Docquier N, Candel S. Combustion control and sensors: a review. Prog Energy Combust Sci 2002;28:107–50.
[256] Guethe F, Guyot D, Singla G, Noiray N, Schuermans B. Chemiluminescence as diagnostic tool in the development of gas turbines. Appl Phys B 2012;107:619–36.
[257] Hardalupas Y, Orain M. Local measurements of the time-dependent heat release rate and equivalence ratio using chemiluminescent emission from a flame. Combust Flame 2004;139:188–207.
[258] Palies P, Durox D, Schuller T, Candel S. The combined dynamics of swirler and turbulent premixed swirling flames. Combust Flame 2010;157:1698–717.
[259] Leipertz A, Obertacke R, Wintrich F. Industrial combustion control using UV emission tomography. Symp (Int) Combust 1996;26:2869–75.
[260] Fan LS, Xie ZQ, Park JB, He XN, Zhou YS, Jiang L, et al. Synthesis of nitrogen-doped diamond films using vibrational excitation of ammonia molecules in laser-assisted combustion flames. J Laser Appl 2012;24. https://doi.org/10.2351/1.3685299.
[261] Ryuichi M, Ryohei O, et al. NH3/ N2/ O2Non-Premixed Flame in a 10 kW Experimental Furnace – Characteristics of Radiative Heat transfer. NH3 Fuel Conference 2017 (2017)..
[262] Füzesi D, Wang S, Józsa V, Chong CT. Ammonia-methane combustion in a swirl burner: Experimental analysis and numerical modeling with Flamelet Generated Manifold model. Fuel 2023;341:127403.
[263] Bioche K, Bricteux L, Bertolino A, Parente A, Blondeau J. Large Eddy simulation of rich ammonia/hydrogen/air combustion in a gas turbine burner. Int J Hydrogen Energy 2021;46:39548–62.
[264] Bayramoğlu K, Bahlekeh A, Masera K. Numerical investigation of the hydrogen, ammonia and methane fuel blends on the combustion emissions and performance. Int J Hydrogen Energy 2023;48:39586–98.
[265] Chaturvedi S, Santhosh R, Mashruk S, Yadav R, Valera-Medina A. Prediction of NOx emissions and pathways in premixed ammonia-hydrogen-air combustion using CFD-CRN methodology. J Energy Inst 2023;111:101406.
[266] Sun Y, Cai T, Shahsavari M, Sun D, Sun X, Zhao D, et al. RANS simulations on combustion and emission characteristics of a premixed NH3/H2 swirling flame with reduced chemical kinetic model. Chin J Aeronaut 2021;34:17–27.
[267] Wiseman S, Rieth M, Gruber A, Dawson JR, Chen JH. A comparison of the blow-out behavior of turbulent premixed ammonia/hydrogen/nitrogen-air and methane–air flames. Proc Combust Inst 2021;38:2869–76.
[268] Tu Y, Zhang H, Guiberti TF, Avila Jimenez CD, Liu H, Roberts WL. Experimental and numerical study of combustion and emission characteristics of NH3/CH4/air premixed swirling flames with air-staging in a model combustor. Appl Energy 2024;367:123370.
[269] Romano C, Cerutti M, Babazzi G, Miris L, Lamioni R, Galletti C, et al. Ammonia blends for gas-turbines: Preliminary test and CFD-CRN modelling. Proc Combust Inst 2024;40:105494.
[270] Frankl S, Gleis S, Karmann S, Prager M, Wachtmeister G. Investigation of ammonia and hydrogen as CO2-free fuels for heavy duty engines using a high pressure dual fuel combustion process. Int J Engine Res 2021;22:3196–208.

[271] Vigueras-Zuniga M-O, Tejeda-del-Cueto M-E, Vasquez-Santacruz J-A, Herrera-May A-L, Valera-Medina A. Numerical predictions of a Swirl Combustor using complex Chemistry Fueled with Ammonia/Hydrogen Blends. Energies 2020;13:288.
[272] Mustafa L, Ślefarski R, Jankowski R, Alnajideen M, Eckart S. Modeling the Thermodynamics of Oxygen-Enriched Combustion in a GE LM6000 Gas Turbine using CH4/NH3 and CH4/H2. Energies 2025;18:3221.
[273] Kurata O, Norihiko I, Inoue T, Fujitani T, Fan Y, Matsunuma T, et al. in: 19AIChE: annual meeting. FL: Orlando; 2019.
[274] Pedeferri P. Corrosion Science and Engineering. Cham: Springer International Publishing; 2018.
[275] Wang D, Xing Y, Lee M, Suzuki Y. Effects of wall temperature and water vapor on the nitriding of stainless steel induced by ammonia flames. Proc Combust Inst 2024;40:105562.
[276] Sariola L. Safe use of ammonia as ICE fuel. Vaasa: Masterarbeit; 2020.
[277] Health and Safety Executive, Corrosion / selection of materials, https://www.hse.gov.uk/comah/sragtech/techmeasmaterial.htm, accessed 25 September 2024.
[278] Graco, Chemical Compatibility Guide, 2013, https://www.graco.com/content/dam/graco/ipd/literature/misc/chemical-compatibility-guide/Graco_ChemCompGuideEN-B.pdf, accessed 26 September 2024.
[279] Valera-Medina A, Banares-Alcantara R. Techno-economic challenges of green ammonia as energy vector. London, United Kingdom: Academic Press; 2021.
[280] Stringer J. High-temperature corrosion of superalloys. Mater Sci Technol 1987;3:482–93.
[281] M. Müller, in: K. Hack (Ed.), SGTE Casebook: Thermodynamics at Work (Woodhead Publishing in materials), Woodhead Publishing, 2008, pp. 239–247.
[282] Xu K. Gaseous Hydrogen Embrittlement of Materials in Energy Technologies. Elsevier 2012:526–61.
[283] Dwivedi SK, Vishwakarma M. Hydrogen embrittlement in different materials: a review. Int J Hydrogen Energy 2018;43:21603–16.
[284] S.J. Kim, E.H. Hwang, J.S. Park, S.M. Ryu, D.W. Yun, H.G. Seong, Inhibiting hydrogen embrittlement in ultra-strong steels for automotive applications by Ni-alloying, npj Mater Degrad 3 (2019), doi:10.1038/s41529-019-0074-5.
[285] J. Lee, T. Lee, D.-J. Mun, C.M. Bae, C.S. Lee, Comparative study on the effects of Cr, V, and Mo carbides for hydrogen-embrittlement resistance of tempered martensitic steel, Scientific reports 9 (2019) 5219.
[286] Lee J, Lee T, Kwon YJ, Mun D-J, Yoo J-Y, Lee CS. Role of Mo/V carbides in hydrogen embrittlement of tempered martensitic steel. Corros Rev 2015;33:433–41.
[287] Kim H-J, Jeon S-H, Yang W-S, Yoo B-G, Chung Y-D, Ha H-Y, et al. Effects of titanium content on hydrogen embrittlement susceptibility of hot-stamped boron steels. J Alloy Compd 2018;735:2067–80.
[288] de Sanctis O, Gómez L, Pellegri N, Durán A. Behaviour in hot ammonia atmosphere of SiO2-coated stainless steels produced by a sol-gel procedure. Surf Coat Technol 1995;70:251–5.
[289] Cramer SD, Covino BS, editors. Corrosion: Environments and Industries. ASM International; 2006.
[290] EFMA, Guidance for Transporting Ammonia by Rail, 2007, https://www.fertilizerseurope.com/wp-content/uploads/2019/08/Guidance_for_transporting_ammonia_in_rail_4.pdf, accessed 26 September 2024.
[291] Lunde L, Nyborg R. The effect of oxygen and water on stress corrosion cracking of mild steel in liquid and vaporous ammonia. Plant/Oper Prog 1987;6:11–6.
[292] Schorr M. Corrosion control in ammonia plants. Nitrogen 1994:44–7.
[293] Alec Groysman, Physicochemical Behavior of Engineering Materials in Ammonia and its Derivatives, 2017, http://eurocorr.efcweb.org/2018/abstracts/7/101877.pdf, accessed 26 September 2024.
[294] Davalos-Monteiro R. Observations of corrosion product formation and stress corrosion cracking on brass samples exposed to ammonia environments. Mat Res 2019;22. https://doi.org/10.1590/1980-5373-MR-2018-0077.
[295] Perry SC, Gateman SM, Stephens LI, Lacasse R, Schulz R, Mauzeroll J. Pourbaix Diagrams as a simple Route to first Principles Corrosion simulation. J Electrochem Soc 2019;166:C3186–92.
[296] Chen Y, Zhang B, Su Y, Sui C, Zhang J. Effect and mechanism of combustion enhancement and emission reduction for non-premixed pure ammonia combustion based on fuel preheating. Fuel 2022;308:122017.
[297] Li J, Huang H, Kobayashi N, He Z, Osaka Y, Zeng T. Numerical study on effect of oxygen content in combustion air on ammonia combustion. Energy 2015;93:2053–68.
[298] Biebl M, Leicher J, Giese A, Wieland C. A comprehensive study of non-premixed combustion of ammonia and its blends: Flame stability and emission reduction. Fuel 2025;386:134501. https://doi.org/10.1016/j.fuel.2025.134501.
[299] Su S-S, Hwang S-J, Lai W-H. On a porous medium combustor for hydrogen flame stabilization and operation. Int J Hydrogen Energy 2014;39:21307–16.
[300] Eckart S, Dasari SA, Collins E, Behrend R, Urbina J, Krause H. Effects of microwaves on burning velocity, UV–VIS-spectra, and exhaust gas composition of premixed propane flames. Flow Turbulence Combust 2023;110:629–48.
[301] Ju Y, Lefkowitz JK, Reuter CB, Won SH, Yang X, Yang S, et al. Plasma assisted low temperature combustion. Plasma Chem Plasma Process 2016;36:85–105.
[302] Hinokuma S, Matsuki S, Kawabata Y, Shimanoe H, Kiritoshi S, Machida M. Copper oxides supported on aluminum oxide borates for catalytic ammonia combustion. J Phys Chem C Nanomater Interfaces 2016;120:24734–42.
[303] Obayashi Y. JERA ends ammonia co-firing trial at coal power station with positive results. Reuters 2024.
[304] J. Atchison, Trailing ammonia-coal co-firing in India, ammoniaenergy.org (2022).
[305] Zeng Y, Kweon J, Kim G-M, Jeon C-H. Carbon-free power generation strategy in South Korea: CFD simulation for ammonia injection strategies through boiler burner configurations in tangentially fired boiler. Energy 2024;309:133076.
[306] Julian Atchison, South Korea sets targets for hydrogen & ammonia power generation, 2021, https://ammoniaenergy.org/articles/south-korea-sets-targets-for-hydrogen-ammonia-power-generation/.
[307] K. Kang, J. Lee, Korea forms ambitious public-private green ammonia alliance, 2021, https://www.kedglobal.com/hydrogen-economy/newsView/ked202107160003.
[308] J. Ji, in: News and Information for Chemical Engineers, pp. 408–419.
[309] Ammonia as a low Carbon Fuel, https://amburn.co.uk, accessed 24 October 2024.
[310] International Standards Organization, ISO/DTS 21343: Oil and gas industries including lower carbon energy — Fuel ammonia —Requirements and guidance for boilers for power generation, 2024, https://www.iso.org/standard/86727.html, accessed 24 October 2024.